Spectral Cross-calibration of the Konus-Wind, the Suzaku/WAM, and the Swift/BAT Data using Gamma-Ray Bursts

Takanori SAKAMOTO,[1,2,3] Valentin PAL'SHIN,[4] Kazutaka YAMAOKA,[5] Masanori OHNO,[6] Goro SATO,[6] Rafail APTEKAR, [4] Scott S. BARTHELMY,[3] Wayne H. BAUMGARTNER,[1,2,3] Jay R. CUMMINGS,[1,2,3] Edward E. FENIMORE,[7] Dmitry FREDERIKS, [4] Neil GEHRELS,[3] Sergey GOLENETSKII, [4] Hans A. KRIMM,[1,8,3] Craig B. MARKWARDT,[1,9,3] Kaori ONDA,[12] David M. PALMER,[7] Ann M. PARSONS,[3] Michael STAMATIKOS, [10,3] Satoshi SUGITA, [13] Makoto TASHIRO, [12] Jack TUELLER,[3] and Tilan N. UKWATTA,[11,3]

[1] *Center for Research and Exploration in Space Science and Technology (CRESST), NASA Goddard Space Flight Center, Greenbelt, MD 20771, U.S.A.*

Taka.Sakamoto@nasa.gov

[2] *Joint Center for Astrophysics, University of Maryland, Baltimore County, 1000 Hilltop Circle, Baltimore, MD 21250, U.S.A.*

[3] *NASA Goddard Space Flight Center, Greenbelt, MD 20771, U.S.A.*

[4] *Ioffe Physico-Technical Institute, Laboratory for Experimental Astrophysics, 26 Polytekhnicheskaya, St Petersburg 194021, Russian Federation*

[5] *Department of Physics and Mathematics, Aoyama Gakuin University, 5-10-1 Fuchinobe, Chuo-ku, Sagamihara, Kanagawa 252-5258*

[6] *Institute of Space and Astronautical Science (ISAS/JAXA), 3-1-1 Yoshinodai, Sagamihara, Kanagawa 229-8510*

[7] *Los Alamos National Laboratory, P.O. Box 1663, Los Alamos, NM 87545, U.S.A.*

[8] *Universities Space Research Association, 10211 Wincopin Circle, Suite 500, Columbia, MD 21044-3432, U.S.A.*

[9] *Department of Astronomy, University of Maryland, College Park, MD 20742, U.S.A.*

[10] *Oak Ridge Associated Universities, P.O. Box 117, Oak Ridge, TN 37831-0117, U.S.A.*

[11] *Center for Nuclear Studies, Department of Physics, George Washington University, Washington, DC 20052, U.S.A.*

[12] *Department of Physics, Saitama University, 255 Shimo-Okubo, Sakura, Saitama 338-8570*

[13] *coTopia Science Institute, Nagoya University, Furo-cho, chikusa, Nagoya 464-8603*

Abstract

1

We report on the spectral cross-calibration results of the *Konus-Wind*, the *Suzaku*/WAM, and the *Swift*/BAT instruments using simultaneously observed gamma-ray bursts (GRBs). This is the first attempt to use simultaneously observed GRBs as a spectral calibration source to understand systematic problems among the instruments. Based on these joint spectral fits, we find that 1) although a constant factor (a normalization factor) agrees within 20% among the instruments, the BAT constant factor shows a systematically smaller value by 10-20% compared to that of *Konus-Wind*, 2) there is a systematic trend that the low-energy photon index becomes steeper by 0.1-0.2 and E_{peak} becomes systematically higher by 10-20% when including the BAT data in the joint fits, and 3) the high-energy photon index agrees within 0.2 among the instruments. Our results show that cross-calibration based on joint spectral analysis is an important step to understanding the instrumental effects which could be affecting the scientific results from the GRB prompt emission data.

Key words: gamma rays: observations

1. Introduction

Precise measurements of prompt emission spectra of Gamma-Ray Bursts (GRBs) is essential for understanding the physics of relativistic shocks. For instance, the peak energy in the observed prompt GRB νF_ν spectrum (E_{peak}) is believed to correspond to the critical energy of synchrotron radiation from accelerated electrons with a minimum Lorentz factor (e.g. Sari et al. 1998). The burst bolometric fluence, which requires an accurate measurement of the broadband spectrum to calculate, reflects the total radiated energy in the prompt emission phase. Moreover, the power-law photon index below E_{peak} can be used for testing whether the origin of the emission is indeed synchrotron (e.g. Preece et al. 1998). Similarly, the power-law photon index above E_{peak} should inform us about the power-law index, p, of electrons ($N(\gamma_e) \propto \gamma_e^{-p}$) in the framework of the synchrotron shock model (e.g. Sari et al. 1998; Kaneko et al. 2006).

Additionally, several empirical relationships based on E_{peak} have been proposed. They are A) the correlation between E_{peak} in the GRB rest frame ($E_{\text{peak}}^{\text{src}}$) and the isotropic radiated energy (E_{iso}), the so called the $E_{\text{peak}}^{\text{src}}$-$E_{\text{iso}}$ (Amati) relation (Amati et al. 2002; Amati 2006), B) the correlation between the $E_{\text{peak}}^{\text{src}}$ energy and the collimation-corrected energy (E_γ), the so called $E_{\text{peak}}^{\text{src}}$-$E_\gamma$ (Ghirlanda) relation (Ghirlanda et al. 2004), C) the correlation between $E_{\text{peak}}^{\text{src}}$, E_{iso}, and the achromatic break time in the afterglow light curve (t_{jet}) (Liang & Zhang 2005), D) the relationship between $E_{\text{peak}}^{\text{src}}$ and the isotropic peak luminosity ($L_{\text{iso}}^{\text{peak}}$), the so called the $E_{\text{peak}}^{\text{src}}$- $L_{\text{iso}}^{\text{peak}}$ (Yonetoku) relation (Yonetoku et al. 2004), and E) the correlation between $L_{\text{iso}}^{\text{peak}}$, $E_{\text{peak}}^{\text{src}}$, and the time scale of the brightest 45 per cent of the background subtracted counts in the light curve of the prompt emission (Firmani et al. 2006; Rossi et al. 2008). However, there is much discussion whether these empirical relationships reflect the fundamental physics of GRBs

or are due to instrumental effects (e.g. Cabrera et al. 2006; Butler et al. 2007; Sato et al. 2007; Ghirlanda et al. 2007). The measurements of the broad-band GRB spectra by multiple GRB instruments is a necessary step to understand instrumental effect on these empirical relations.

Swift (Gehrels et al. 2004) is providing more details for understanding GRBs (e.g. Zhang 2007). However, because of the narrow energy band of the Burst Alert Telescope (BAT; 15-150 keV; Barthelmy et al. 2005) on board *Swift*, very limited information about the spectrum of the prompt emission is available from the BAT data alone. The Wide-band All-sky Monitor (WAM; 50-5000 keV; Yamaoka et al. 2009) which is the active shield of the Hard X-ray detector (HXD; Takahashi et al. 2007; Kokubun et al. 2007) aboard *Suzaku* (Mitsuda et al. 2007) has also been detecting *Swift* GRBs. The WAM has very large effective area from 300 keV to 5 MeV (400 cm^2 even at 1 MeV), where BAT has no sensitivity. The $Konus-Wind$ instrument (Aptekar et al. 1995), which has been on-orbit since 1994 collecting spectral and temporal data from GRBs, has also been detecting *Swift* GRBs and providing information about the spectral properties of *Swift* GRBs using its broad-band energy coverage (10-10,000 keV).

In this paper, we report on the cross-calibration effort of the energy response for *Konus-Wind* (hereafter KW), *Suzaku*/WAM (hereafter WAM), and *Swift*/BAT (hereafter BAT), using simultaneously observed GRBs. Each instrument has its own pros and cons for the calibration of its energy response. For instance, the BAT uses the Crab nebula as a standard source to calibrate its energy response using its imaging capability. On the other hand, there is an uncertainty in the energy response for a source which has a hard spectrum, such as a GRB, due to the lack of a known steady bright hard X-ray source with a similar spectrum as GRBs. The γ-ray instruments without an imaging capability such as WAM require the Earth occultation technique to collect a special set of the data to calibrate their energy response using a steady source like the Crab.[1] However, their instruments have a much simpler energy response compared to that of an imaging detector such as the BAT. This work allows us to compensate the weak points in the spectral calibration of each instrument by combining the data, and to understand the systematic uncertainty of the energy response when using GRBs as the spectral calibration sources. The paper is organized in the following manner. In §2, we describe the instrumentation of KW, WAM and BAT. In §3, we summarize the GRB samples used in this cross-calibration work and the methods of analyzing the data of each instrument. We show the results in §4. Our conclusions are summarized in §5. The quoted errors in this work are at the 90% confidence level, unless otherwise stated.

---

[1] Since the Wind spacecraft is at distances of 1-7 light-seconds from Earth, it is not possible to use the Earth occultation techniques to collect the data of a steady source.

2. Instruments

2.1. Konus-Wind

The KW is a gamma-ray spectrometer designed to study temporal and spectral characteristics of gamma-ray bursts, solar flares, SGR bursts, and other transient phenomena in a wide energy range from 10 keV to 10 MeV. It consists of two identical omnidirectional NaI(Tl) detectors (S1 and S2) one of which points toward the south ecliptic pole thereby observing the south ecliptic hemisphere (S1), and the other observes the north ecliptic hemisphere (S2). Each detector has an effective area of ~80–160 cm^2 depending on the photon energy and incident angle. In interplanetary space far outside the Earth's magnetosphere, the KW has the advantages over Earth-orbiting GRB monitors of continuous coverage, uninterrupted by Earth occultation, and a steady background, undistorted by passages through the Earth's trapped radiation.

The instrument operates in two modes: waiting and triggered. In the triggered mode 64 spectra are measured in two partially overlapping energy ranges with nominal bounds 10–750 keV (PHA1) and 0.2–10 MeV (PHA2). Each range has 63 channels. The first four spectra are obtained with a fixed accumulation time of 64 ms. For the subsequent 52 spectra, the adaptation system determines the accumulation times which can vary from 0.256 to 8.192 s. The last 8 spectra are obtained in 8.192 s each. As a result the minimum duration of spectral measurements is 79.104 s, and the maximum, 491.776 s. Due to the degradation of the photomultiplier tubes, the overall energy range has shifted to ~20 keV – 14 MeV at the present time. Further details can be found in Aptekar et al. (1995).

The instrument calibration is described in Terekhov et al. (1998). The detector response matrix (DRM), which is a function only of the burst angle relative to the instrument axis, is computed using the GEANT4 package (Agostinelli et al. 2003). The last version of DRM contains responses for 225 photon energies between 5 keV and 16 MeV on a quasi-logarithmic scale for incident angles between 0° and 90° with a step of 5°. The energy scale is calibrated in-flight using 1460 keV line of ^{40}K and the 511 keV annihilation line (see the background spectrum shown in Figure 1).

The KW has been detecting GRBs in the triggered mode at a rate of ~125 per year. It has detected 100 triggered GRBs simultaneously with Swift-BAT with an average rate of 20 bursts per year.

2.2. Suzaku/WAM

The WAM is a large and thick BGO active shield for the *Suzaku* HXD. The WAM consists of four perpendicular walls, references as WAM 0 to 3, each with a geometrical area of ~ 800cm^2. The nominal energy range is 50-5000 keV, but depends on the gain of the photomultipliers. The field of view is about half of the sky. Since the *Suzaku* launch on July 10,

2005, the WAM has been working nominally and has been detecting GRBs at a rate of 140 per year including both triggered and un-triggered events. The coincident rate with the KW and the BAT triggers is ~70 and ~14 per year, respectively.

There are two kinds of the WAM data for GRB analysis: transient (TRN) data and burst (BST) data. The BST data will be available only when the GRB trigger is produced by an on-board trigger system. The TRN data has 1 s time resolution and 55 energy channels for any time, while the BST data, for 64 seconds (from 8 s before to 56 s after a GRB trigger), has both 1/64 s time resolution and 4 energy channels, and 1/2 s time resolution and 55 channels. The WAM is inside the spacecraft, hence, incident gamma-rays suffer from heavy absorption due to other satellite materials. Therefore, the WAM response is very complex, and heavily dependent on incident angles. We have constructed a *Suzaku* mass model using GEANT4 (Agostinelli et al. 2003) and verified the Monte Carlo simulation results by comparison between the pre-launch calibration data and the experimental data taken during in-flight calibrations for certain directions.

In the in-flight calibration, we calibrate the gain drift of the detectors after every SAA passage using the 511 keV annihilation line (Yamaoka et al. 2009). For the energy response, the Crab spectrum obtained by the earth occultation technique is used to verify the energy response. Figure 2 shows the examples of the Crab spectra. We found that the WAM Crab spectrum is well fit by the single power-law model with a photon index of ~2.1. The energy flux in the 100-500 keV band is $\sim 1 \times 10^{-8}$ erg cm^{-2} s^{-1}. This is roughly consistent with the value reported by other gamma-ray instruments (e.g. Sizun et al. 2004). However, in this Crab calibration, it is difficult to calibrate the energy response above several hundreds of keV for various incident directions. This is because the exposure time of the Crab data for a certain direction by this technique is strongly limited by the fact how long the satellite can keep the same attitude (typically a day). Therefore, a GRB would be a suitable source to calibrate the energy response for various incident angles, and also, up to a higher energy range than the Crab. You can find a detailed description of the Crab calibration and the earth occultation technique of the WAM data in Kira et al. (2009).

2.3. *Swift/BAT*

The BAT is a highly sensitive (the effective area including the mask modulation is $\sim$ 1,400 cm^2 at 50 keV on-axis), large field of view (FOV) (2.2 sr for > 10% coded FOV), coded-aperture telescope that detects and localizes GRBs in real time. The BAT detector plane is composed of 32,768 pieces of CdZnTe (CZT: $4 \times 4 \times 2$ mm), and the coded-aperture mask is composed of $\sim$ 52,000 lead tiles ($5 \times 5 \times 1$ mm) with a 1 m separation between mask and detector plane. The energy range is 14–150 keV for imaging or mask-weighting, which is a technique to subtract the background based on the modulation resulting from the coded mask, with a non-coded response up to 350 keV. Further detailed descriptions, references and the in-orbit

calibration status of the BAT can be found in the BAT1 GRB catalog (Sakamoto et al. 2008).

The important update on the spectral calibration of the BAT since the BAT1 GRB catalog has been published is the understanding of the problem in the energy response above 100 keV. The BAT team investigated the ground calibration data more deeply and found that the mobility-lifetime products of electrons and holes ($\mu\tau$) which determine the characteristics of an individual CZT detector (Sato et al. 2005; Suzuki et al. 2005) have to be 1.7 larger than those originally determined. After updating the $\mu\tau$ values, the BAT team confirmed that the adjustment which we were applying to reproduce the canonical Crab spectrum[2] above 100 keV is no longer needed. Therefore, the BAT team reduces the systematic error above 100 keV to a flat 4% (previously, the systematic error was 4% at 100 keV, and then increased to 12% at 150 keV; see Figure 2 of Sakamoto et al. 2008). The Crab data and the GRB data have been re-analyzed using the updated energy response and applying the new systematic error vector. The spectral shape and the flux agree within the systematic uncertainties, which are mainly due to the off-axis response, to previous results (within $\sim$5% in the photon index and within $\sim$10% in the flux from the canonical Crab spectrum). These changes in the energy response and the systematic error are available to the public (CALDB 20081026).

Another important update is related to the gain change of the detectors. The BAT team has recognized shifts of peak energies in spectra from the on-board ^{241}Am tagged source towards lower energies. An analysis of four years of on-board ^{241}Am spectra shows the shift is about 2.5 keV for the 59.5 keV peak. The BAT team also noticed that the Crab data on January 21-23, 2009 shows a systematically steeper photon index of 0.05 and also a lower flux of about 5% comparing to previous years. Motivated by these results, the BAT team has developed new calibration files to store the information (coefficients to convert from PHA channel to energy) to correct this gain change as a function of time. After applying the new gain correction, the scatter of the 59.5 keV line energy is $\sim$0.1 keV over the four-year period. Furthermore, no systematic trends in the photon index and the flux have been seen in the Crab data on 2009 by applying this new gain correction. The BAT team is planning to provide new calibration files every 6 months to correct for additional gain drifts as they may occur.[3]

The results of the Crab spectral analysis based on these latest in-orbit calibrations are presented at Sakamoto et al. (2010). We have used the updated energy response and the systematic error, and also the spectral file applying the new gain correction for this cross-calibration work.

---

[2]   The Crab canonical spectral parameters in the BAT energy range are -2.15 for the photon index and 2.11×10^{-8} ergs cm^{-2} s^{-1} for the flux in the 15-150 keV band.

[3]   The calibration files will be available to the public in 2010 or early 2011.

3.   Analysis

We have selected 14 GRBs which were simultaneously detected by all three instruments, and also have enough statistics to perform spectral analysis. We extracted 36 spectra to do the joint analysis. Table 1 shows the GRB samples in this work and the trigger time of each instrument in UTC in the form of $YYYY/MM/DD\ hh:mm:ss.sss$ where $YYYY$ is year, MM is month, DD is day of month, hh is hour, mm is minute, and $ss.sss$ is second with three decimals. Table 2 shows the GRB position in the sky from the BAT data (Sakamoto et al. 2008) and the incident angles of GRBs for each instrument in the unit of degrees. In Table 3 and 4, we summarize the energy fluence and the 1-s peak energy flux measured by KW, WAM and BAT for those samples. Table 5 shows the spectral time intervals in the start time from the trigger time, t_{start} and the stop time from the trigger time, t_{stop} in the unit of seconds (the trigger time of each instrument is shown in Table 1). Since the KW spectral data are binned by the flight software in a time variable manner, we adjusted the BAT and the WAM spectral intervals to that of the KW. To determine the same time region with the KW spectrum, we calculated the arrival time difference of the GRB photons from the spacecraft to the Earth center (Time of flight; ToF) for each instrument. The ToFs of each instrument are shown in the last three columns of Table 5 in the unit of seconds.

During the process of finding the spectral time interval, we tried to select at least one region for each burst where the $Swift$ spacecraft is not slewing. Since the current BAT energy response generator, `batdrmgen`, performs its calculations for a fixed single incident angle, it is necessary to do the joint spectral fits for a time interval when the BAT data are not affected by a spacecraft slew. For the time intervals which include the spacecraft slew in the BAT data, we used the averaged energy response. The procedure for creating the averaged BAT energy response is as followings: We created the energy response for every 5 s period taking into account the position of the GRB in detector coordinates. And then, we weighted these energy responses by the 5 s count rates and created the averaged energy response. The spectral intervals which contain the spacecraft slew in the BAT data are indicated by the superscript "S" in the 2nd column of Table 5.

The joint spectral fits are performed by `xspec` (ver. 11.3.2). The spectrum was fitted by a simple power-law (PL) model,

$$f(E) = K_{100}^{\mathrm{PL}} \left(\frac{E}{100\,\mathrm{keV}} \right)^{\alpha^{\mathrm{PL}}} \tag{1}$$

where α^{PL} is the power-law photon index and K_{100}^{PL} is the normalization at 100 keV in units of photons cm^{-2} s^{-1} keV^{-1}, by a cutoff power-law (CPL) model,

$$f(E) = K_{100}^{\mathrm{CPL}} \left(\frac{E}{100\,\mathrm{keV}} \right)^{\alpha^{\mathrm{CPL}}} \exp \left(\frac{-E\left(2 + \alpha^{\mathrm{CPL}}\right)}{E_{\mathrm{peak}}} \right) \tag{2}$$

where α^{CPL} is the power-law photon index, E_{peak} is the peak energy in the $\nu \mathrm{F}_\nu$ spectrum and

7

K_{100}^{CPL} is the normalization at 100 keV in units of photons cm^{-2} s^{-1} keV^{-1}, and by the Band function (Band et al. 1993),

$$f(E) = \begin{cases} K_1 \left(\frac{E}{100\,\mathrm{keV}}\right)^{\alpha} \exp\left(\frac{-E\,(2+\alpha)}{E_{\mathrm{peak}}}\right) & E < \left(\frac{(\alpha-\beta)E_{\mathrm{peak}}}{(2+\alpha)}\right) \\ K_1 \left(\frac{(\alpha-\beta)E_{\mathrm{peak}}}{(2+\alpha)100\,\mathrm{keV}}\right)^{\alpha-\beta} \left(\frac{E}{100\,\mathrm{keV}}\right)^{\beta} & E \geq \left(\frac{(\alpha-\beta)E_{\mathrm{peak}}}{(2+\alpha)}\right) \end{cases} \tag{3}$$

where α is the low-energy photon index, β is the high-energy photon index, E_{peak} is the peak energy in the $\nu \mathrm{F}_{\nu}$ spectrum and K_1 is the normalization at 100 keV in units of photons cm^{-2} s^{-1} keV^{-1}. We multiply the model by the constant factor to understand the calibration uncertainties among the instruments. The constant factor for the KW data is fixed to 1, and the constant factors of the BAT and the WAM are kept as free parameters. However, we fix the BAT constant factor to 1, and keep the WAM constant factor as a free parameter in the case of the BAT and WAM joint fit. Other spectral parameters such as photon indices, E_{peak} and a normalization are the same for all instruments. If a GRB has been observed by two WAM detectors, we used both data in the joint fit analysis. We call WAM$_{SP1}$ and WAM$_{SP2}$ for each detector throughout the paper. The actual detector ID number of WAM$_{SP1}$ and WAM$_{SP2}$ are summarized in Table 2.

3.1. KW data analysis

The KW data are processed using standard KW analysis tools, which convert the spectral data collected on-board from the internal format to PHA-files in FITS format suitable for analysis in `xspec`. The dead time correction has been applied. For the given incident angle, the DRM is calculated by linear interpolation of the DRMs for the nearest angles. Since the KW background is very stable, we use an average spectrum over a $\sim$100–300 s long interval after the burst as the background spectrum.

3.2. WAM data analysis

The *Suzaku* WAM data were analyzed using HEADAS version 6.6.2. Spectral accumulations were carried out by `hxdmkwamspec` and `hxdmkbstspec` for the TRN data and BST data, respectively. The deadtime was corrected. For two bright bursts: GRB 061007 and GRB 080328, we added 5 % systematic errors to the energy channels lower than 400 keV, taking into account the ADC digitization errors. The instrumental background varies with time, even during GRB time intervals, hence we used a model background which interpolates the best-fit 4th-order polynomial function of the data in each 500 s before and after the time intervals. The energy response was calculated by the latest response generator (version 1.9) based on the incident angles shown in Table 2. It cannot reproduce the low energy spectrum for energies less than 120 keV, corresponding to the 3 lowest energy channels. Thus, the fitting energy range was limited above $\sim$120 keV.

3.3. BAT data analysis

We used HEAsoft 6.5 and the latest CALDB for the BAT data processing. The BAT event-by-event data, which have a time resolution of 98 μsec (Palmer et al. 2005), are used in the analysis. Since all of the GRBs in our sample have not been exceeding 2.6×10^6 s^{-1} in the raw count-rate, the deadtime effect is negligible in the BAT data (see Palmer et al. 2005 for the details about the deadtime effect in the BAT data). The spectral file (PHA file) is created with `batbinevt` specifying the time interval (tstart and tstop options). The tool `batphasyserr` is used to apply the systematic error into the PHA files. We run `batdrmgen` to create the energy response file. We exclude the BAT data of the Reg2 and the Reg12 of GRB 051008 and the whole intervals of GRB 060124 from the cross-calibration work because the event-by-event data are not available for these intervals. Except for these intervals, the event-by-event data are available to create the spectrum. Therefore, it is possible to choose exactly the same time interval selected by other missions for the BAT spectrum using event-by-event data.

4. Results

Figures 3-5 show the light curves of the KW, the WAM and the BAT instruments. The vertical lines on the figures correspond to the intervals from which we extract the spectra to perform the joint fits. Figure 6-7 show examples of the KW (black), the WAM$_{SP1}$ (green), the WAM$_{SP2}$ (blue) and the BAT (red) observed spectra along with the best fit model as solid lines and the residuals from the best fit model in the bottom panel. The top label of each figure describes the GRB name and the interval of the fit. The best fit model is shown at the left top of the figure. As shown in Figure 8, the distribution of the reduced χ^2 of the KW fit and all the joint fits based on the best fit model is centered around 1. The systematically smaller reduced χ^2 seen in the inclusion of the BAT data is due to apply a large systematic error in the BAT spectral data. The linear fit to the data (a linear coefficient and an offset) between the best fit parameter obtained by the joint fit and the KW fit (results of Fig 9, 10, 12, 13, 14, 15, 16, and 17) are shown in Table 6 for a CPL and in Table 7 for the Band function. The spectral parameters and the fluxes of each spectral interval and instruments are presented in Table 8-79. We report the instrument which fixes the constant factor to 1 for calculating the flux in the last column of the flux tables. We are not reporting the spectral parameters of the model which does not constrain the parameters (e.g. parameters of the Band function fit based on the BAT data alone.)

4.1. KW and BAT joint fit

Figure 9 and 10 summarize the relationship between the best fit spectral parameters from the joint KW-BAT fit and the fit made by the KW data alone, and between the constant factor of BAT and the spectral parameters. The results based on a CPL model and the Band function are shown in Figure 9 and in Figure 10 respectively. The BAT spectra which are not

affected by the spacecraft slew are shown in blue in the figures. As seen in the figures, there is no systematic trend between the spectral data affected by the spacecraft slew and not affected by the spacecraft slew. Therefore, we concluded that there is no systematic problem in using the BAT spectra data during the slew using our weighted energy response.

Most of the photon indices based on the joint fits agree with the KW best fits values within the uncertainties. However, we do see a systematic trend that the joint fit photon indices are systematically steeper (smaller values) than in the KW fit. This systematic difference in the indices is 0.1 steeper for a CPL fit and 0.2 steeper for the Band function fit on average as seen in Table 6 and 7. Overall E_{peak} agrees between the joint fit and the KW fit. Although it is not well constrained, the high energy photon index β of the Band function fit agrees between the joint fits and the KW fit. The most noticeable systematic difference in the joint fits is the systematically smaller constant factor for the BAT data. The BAT constant factor is $\sim$12% smaller than that of the KW. As can be seen in the bottom panels of Figure 9 and 10, there is no systematic trend between the 12% smaller BAT constant factor and the best fit photon indices, E_{peak}, or the best fit spectral model. Since this trend has been seen for the most of the combination of joint fits using the BAT data as we describe in the following sections, we believe that this trend of the constant factor in the BAT data is intrinsic to the BAT energy response.

To investigate the consistency in the spectral parameters especially α and E_{peak} derived from the BAT data alone we select the fitting results which show the difference in chi-squared between a PL and a CPL fit to be greater than 6 ($\Delta\chi^2 = \chi^2_{\mathrm{PL}} - \chi^2_{\mathrm{CPL}} > 6$) in the BAT fit. This is the same $\Delta\chi^2$ criterion used in the BAT1 catalog (Sakamoto et al. 2008). As demonstrated in Sakamoto et al. (2009), the BAT spectrum alone can determine E_{peak} if the observed spectrum has a sufficiently high signal-to-noise ratio and also E_{peak} is located inside the BAT energy range. The left and right panels of Figure 11 show α and E_{peak} derived by the KW-BAT joint fit versus the BAT fit in a CPL model. We do see a similar trend with the KW-BAT and the KW fit of $\sim$0.1-0.2 steeper α and $\sim$10% higher E_{peak} on average between the KW-BAT and the BAT fits. However, most of the α and E_{peak} values derived from the BAT data alone are consistent within the errors with the KW-BAT joint fit values. We note that there is one spectrum, GRB 051008 Reg1, which show $E_{\mathrm{peak}} \sim$800 keV in the KW-BAT joint fit (same as in the KW fit and in the KW-WAM-BAT fit), but E_{peak} of the spectrum is $\sim$200 keV in the BAT fit. Since E_{peak} of this spectrum is around $\sim$800 keV in the different combination of joint fits, we believe that E_{peak} of these spectra are greater than 200 keV. Therefore, we should use caution if E_{peak} derived by the BAT data alone is near the upper boundary of the effective BAT energy range of $\sim$150 keV. We also note that the values derived with the BAT spectrum alone are consistent with those derived with BAT-KW joint fit, only when the fit is done with a CPL model and E_{peak} can be determined.

4.2. KW and WAM joint fit

Figure 12 and 13 summarize the joint fit results of the KW and the WAM data. The parameters α and E_{peak} in both the CPL fit and the Band fit are consistent between the joint fit and the KW fit. The difference in α is well less than 0.1 on average for both a CPL fit and the Band fit. Furthermore, according to a linear fit of parameters between the KW-WAM fit and the KW fit, the difference is relatively small: 6% in E_{peak} for both the CPL fit and the Band fit on average. The high energy photon index β of the Band function is also consistent. The systematically small constant factor $\sim$0.2 of GRB 051221A is due to the four times larger time interval in the WAM data (see Table 5). Also note that the WAM$_{SP2}$ constant factor (WAM detector ID 3) of GRB 060105 is in the range of 2-3. This is due to the large uncertainty of the energy response at the extreme off-axis incident angle[4] ($\theta = 5.7°$).

4.3. BAT and WAM joint fit

Figure 14 and 15 summarize the joint fit results of the BAT and the WAM data. The general trend in α and E_{peak}, which we mentioned in section 4.1 (the KW- BAT joint fit) is clearly seen in this joint fit. The joint fit α are 0.2-0.3 steeper on average in the joint fit than in the KW fit for both the CPL model and the Band function. Moreover, the joint fit E_{peak} is systematically higher by 11% for the CPL fit and 14% for the Band fit on average based on a linear fit of parameters. The high energy photon index β of the Band function fit agrees between the joint fits and the KW fit if we take into account the large uncertainties in the parameter.

4.4. KW, WAM and BAT joint fit

Figure 16 and 17 summarize the joint fit results of all three instruments. The systematic differences in α and E_{peak} which we see in the KW-BAT and the BAT-WAM joint fits are also apparent in this joint fit. α obtained by the joint fit is 0.1 and 0.2 steeper on average than the KW fit for the CPL fit and the Band fit respectively. There are eight spectral regions which the 90% confidence level of α do not overlap between the KW and the KW-WAM-BAT joint fit for the CPL (Table 11, 18, 24, 30, 34, 35, 36 and 38) and the Band fit (Table 24, 33, 34, 35, 36, 38, 41 and 43). The largest un-overlapping confidence level in α between the KW and the KW-WAM-BAT joint fit is seen in GRB 051221A Reg1 of 0.04 for the CPL fit, and GRB 070328 Reg2 and Reg13 of 0.06 for the Band fit. On averaged, the un-overlapping confidence level is 0.03 for the CPL fit and 0.04 for the Band fit. According to a linear fit of parameters, E_{peak} based on the joint fit is 9% and 12% higher on average than the KW fit for the CPL model and the Band function respectively. There are ten and six spectral regions which the 90% confidence level of E_{peak} do not overlap between the KW and the KW-WAM-BAT joint

---

[4] A small incident angle (on-axis) means that the source is coming from an off-axis angle for the WAM because the detector normal is at $\theta = 90°$.

fit for the CPL (Table 26, 28, 30, 33, 34, 35, 36, 38, 41 and 43) and the Band fit (Table 34, 35, 36, 38, 41 and 43) respectively. The largest un-overlapping confidence level in E_{peak} between the KW and the KW-WAM-BAT joint fit is seen in GRB 070328 Reg13 of 51 keV for the CPL fit, and GRB 070328 Reg2 of 151 keV for the Band fit. Also, GRB 070328 Reg2 shows the relatively large gap of 41 keV in the CPL fit, and, similarly, GRB 070328 Reg13 has 142 keV gap in the Band fit. Excluding those four outliers, the averaged un-overlapping confidence level is 15 keV for the CPL fit and 13 keV for the Band fit. The constant factor of the BAT data is systematically smaller by 10% in both a CPL fit and the Band fit. The WAM constant factor is smaller by 5% for a CPL fit and 2% for the Band fit excluding the outliers of GRB 051221A and GRB 060105 (see section 4.2).

5.   Discussion and Conclusion

We report the results of our attempt to use the simultaneously observed GRBs to cross-calibrate the energy response of the KW, the WAM and the BAT instruments. Since every GRBs has a different brightness and spectral shape, it is difficult to use the observed GRB spectrum as "a standard candle" to calibrate the instruments. However, we can reveal the systematic problems among the instruments by comparing the best fit parameters derived for each instrument and from the joint analysis of the data.

First, there is a systematic trend in the joint fits that the low-energy photon index α becomes steeper by 0.2 in the Band function compared to that of the KW fit. The lowering of the low-energy photon index is well represented by the examples of GRB 061007 spectral fit results (e.g. Figure 7). There are systematically positive residuals below 50 keV and also negative residuals above 50 keV in the BAT data from the best fit model of the KW fit to the Band function. Along with the joint fit results, this suggests that the BAT data prefers a steeper power-law slope than that derived from the KW data. Note that the WAM data are less sensitive for deriving α since the lower energy boundary of its spectrum is $\sim$120 keV.

Second, on average, E_{peak} derived from the joint fits are systematically higher than those from the KW fit: 9% higher for the joint KW-BAT fit, 6% higher for the joint KW-WAM fit, 14% higher for the joint BAT-WAM fit, and 12% higher for the joint KW-WAM-BAT fit based on the Band function. We note the relatively large inconsistency in the 90% confidence level of E_{peak} for the spectra of GRB 070328 (Reg2 and Reg13) between the KW fit and the KW-WAM-BAT joint fit. The un-overlapping confidence level of E_{peak} is 40-50 keV for the CPL fit and 140-150 keV for the Band fit for those spectra. The low-energy photon index α and E_{peak} are strongly coupled. E_{peak} will be higher if α goes steeper (left panel of Figure 18). To investigate whether a systematically higher E_{peak} is due to a steeper α, we check the differences in E_{peak} and α derived from the joint BAT-WAM fit (which has the largest inconsistency in α) and the joint KW-BAT fit (which has the smallest inconsistencies in E_{peak} and α combining the BAT data). The result is shown in the right panel of Figure 18. There is a very small

difference in E_{peak} if α derived from the joint BAT-WAM fit is flatter than the joint KW-BAT fit (α (BAT-WAM) - α (KW-BAT) > 0, right side of the figure). However the E_{peak} based on the joint BAT-WAM fit is systematically higher than that of the joint KW-BAT fit if the α based on the joint BAT-WAM fit is steeper than the joint KW-BAT fit (α (BAT-WAM) - α (KW-BAT) < 0, left side of the figure). This demonstrates that a systematically higher E_{peak} in the joint fit is mainly as a result of a steeper α. Therefore, we believe that the fundamental cause of this problem is due to a steeper α which comes when we include the BAT data as we discussed above.

Third, the constant factor of the BAT data shows a systematically smaller value when we fix the constant factor of the KW value to 1. There is no correlation between the BAT smaller constant factor and the spectral parameters such as α, E_{peak}, and β (see Figure 9, 10, 12, 13, 14, 15, 16, and 17). We investigate whether variations in the constant factor are correlated with the incident angle of each instrument or with the observed flux. Figures 19, 20 and 21 show the constant factors of the BAT and the WAM based on the three instrument joint fits plotted with respect to the incident angles of the KW, the WAM and the BAT respectively. Figure 22 shows the constant factors of the joint fits versus the observed flux in the 20-1000 keV band. Although there might be a hint of a correlation between the BAT constant factor and θ, the correlation coefficient is 0.655 in 12 samples. The probability of such a correlation occurring by chance for this sample size is 0.131. We find no systematic trend in the constant factor with either incident angles or the observed fluxes. Therefore, we conclude that the intrinsic effective area of the current energy response file of the BAT is 10-20% smaller than that of the KW. Although there might be a similar trend in the WAM constant factor, the scatter in the WAM constant factor is too large for us to make a solid conclusion.

Despite the systematic problems in the joint fits, we note that the uncertainties in the spectral parameters will improve significantly using the joint fits. The joint KW-BAT fits provides smaller uncertainties in both α and E_{peak}, compared to those of the KW fit. The averaged uncertainties of α and E_{peak} in the joint KW-BAT fits are 0.06 and 63 keV, whereas the uncertainties in the KW fits are 0.1 and 71 keV. This is because the BAT high statistics data will provide a better constraint on α, which also improves the uncertainties in E_{peak}. The KW-WAM joint fits provide better constraints on β than does the KW fit. The averaged uncertainties of β in the joint KW-WAM fits are 0.8, on the other hand, the averaged uncertainty of β on the KW fit is 2.8. The high statistics WAM data above 100 keV helps to constrain β. The three instrument joint fits provide the smallest uncertainties in both α and E_{peak}. The averaged uncertainties in α and E_{peak} in the three instrument fits are 0.04 and 45 keV. The joint fit effort is important not only to enable us to understand the systematic problems among the instruments, but also to reduce the uncertainties in the spectral parameters such as α and E_{peak}, allowing better constraints on the empirical relationships and ultimately better physical models of the prompt emission.

Finally, we want to emphasize that it is very difficult to understand the instrumental effects buried in the scientific results such as GRB empirical relations without these kind of cross-calibration efforts. We believe that the systematic problems in the spectral parameters which we derived in this work by combining different instrument data would be added as a systematic error to the statistical uncertainties of the spectral parameters. This is especially important when we display the spectral parameters derived from different instruments such as the empirical relationships. We hope that this kind of joint analysis effort will expand to the data of the previous missions and also to the current/future missions to understand the instrumental problems and the instrumental effects on the interpretation of GRB prompt emission data.

References

Agostinelli, S. et al. 2003, Nuclear Instruments and Methods in Physics Research, A506, 250

Amati, L., et al. 2002, A&A, 390, 81

Amati, L. 2006, MNRAS, 372, 233

Aptekar, R.L, et al. 1995, Space Sci. Rev., 71, 265

Band, D.L., et al. 1993, ApJ, 413, 281

Barthelmy, S.D., et al. 2005, Space Sci. Rev., 120, 143

Butler, N. R., Kocevski, D., Bloom, J. S., Curtis, J. L. 2007, ApJ, 671, 656

Cabrera, J. I., Firmani, C., Avila-Reese, V., Ghirlanda, G., Ghisellini, G., Nava, L. 2006, MNRAS, 382, 342

Firmani, C, Ghisellini, G., Avila-Reese, V., and Ghirlanda, G. 2006, MNRAS, 370, 185

Gehrels, N., et al. 2004, ApJ, 611, 1005

Ghirlanda, G., Ghisellini, G., Lazzati, D., 2004, ApJ, 616, 331

Ghirlanda, G., Nava, L., Ghisellini, G., Firmani, C. 2007, A&A, 466, 127

Kaneko, Y., et al. 2006, ApJS, 166, 298

Kira, C., et al. 2009, in Proceedings of Astrophysics with All-Sky X-Ray Observations 3rd international MAXI Workshop, 322

Kokubun, M., et al. 2007, PASJ, 59, S53

Liang, E., Zhang, B., ApJ, 633, 611

Mitsuda, K., et al. 2007, PASJ, 59, S1

Ohno, M., et al. 2005, IEEE, Trans, Nucl. Sci., 52, 2758
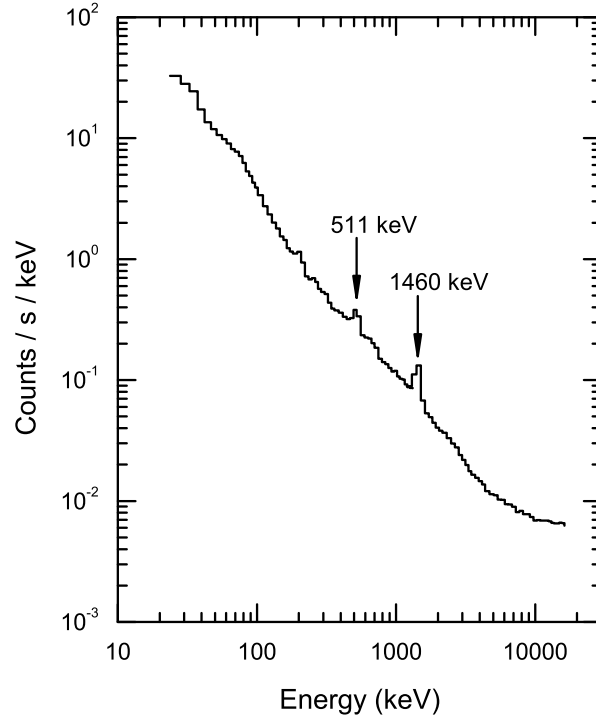
Fig. 1. The background spectrum of the Konus-Wind instrument.

Palmer, D.M., et al. 2005, Nature, 434, 1107

Preece, R.D., Briggs, M.S., Mallozzi, R.S., Pendleton, G.N., Paciesas, W.S., Band, D.L. 1998, Astrophys. Lett., 506, 23

Rossi, F., et al. 2008, MNRAS, 388, 1284

Sakamoto, T. et al. 2008, ApJS, 175, 179

Sakamoto, T. et al. 2009, ApJ, 693, 922

Sakamoto, T. et al. 2010, Submitted to ApJS

Sari, R., Piran, T., Narayan, R. 1998, Astrophys. Lett., 497, 17

Sato, G. et al. 2005, NIM A, 541, 372

Sato, G. et al. 2007, ApJ, 657, 359

Sizun, P. et al. 2004, in Proceedings of the 5th INTEGRAL Workshop on the INTEGRAL Universe, ed. V. Schnfelder, G. Lichti & C. Winkler, ESA SP-552, 815

Suzuki, M. et al. 2005, IEEE Trans. Nucl. Sci., 52, 1033

Takahashi, T., et al. 2007, PASJ, 59, S35

Terekhov, M.M., Aptekar, R.L., Frederiks, D.D., Golenetskii, S.V., Il'inskii, V.N., Mazets, E.P. 1998, in Fourth Huntsville gamma-ray burst symposium, ed. C.A. Meegan, R.D. Preece, & T.M. Koshut (AIP Conference Proceedings), 428, 894

Yamaoka, K., et al. 2009, PASJ, 61, S35

Yonetoku, D., Murakami, T., Nakamura, T., Yamazaki, R., Inoue, A.K., Ioka, K. 2004, ApJ, 609, 935

Zhang, B. 2007, Chinese Journal of Astronomy and Astrophysics, 7, 1
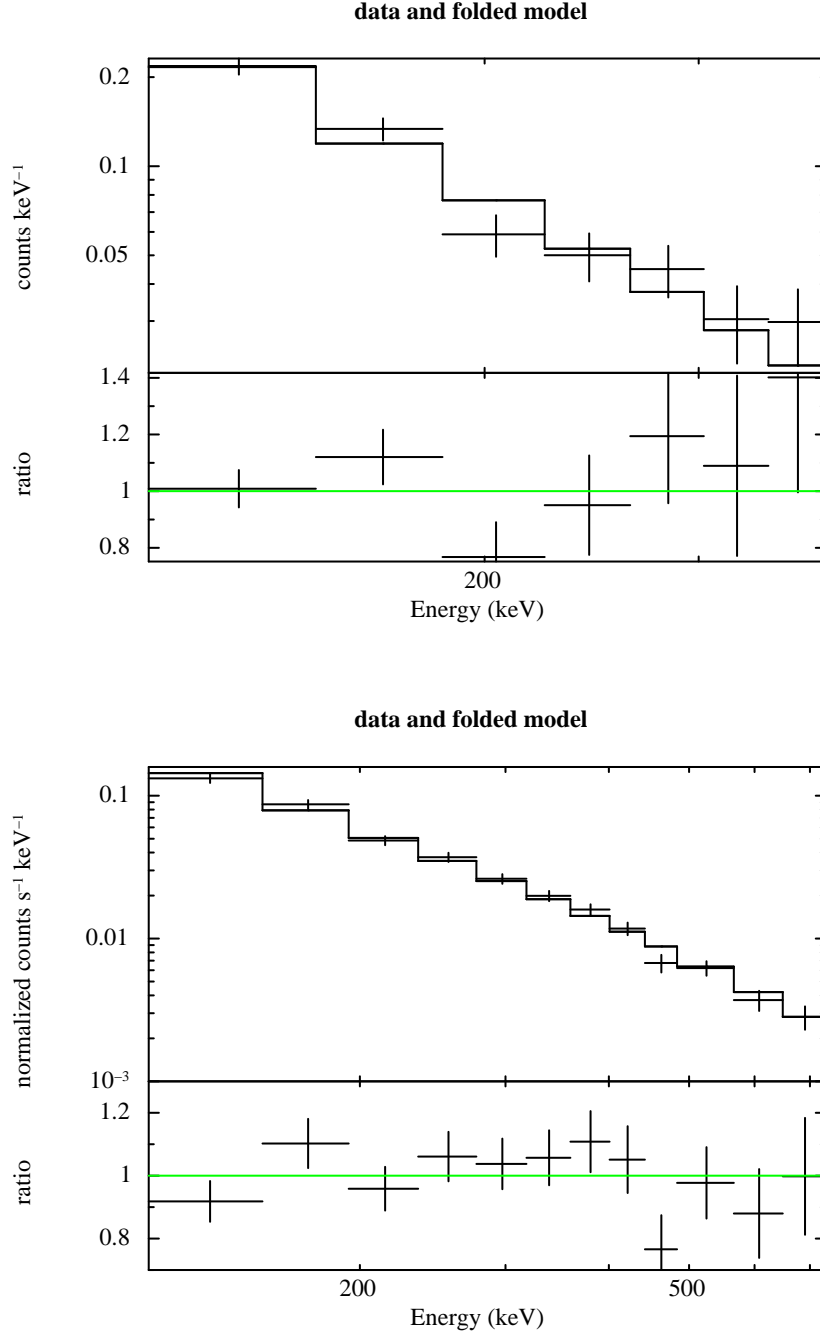
Fig. 2. The WAM Crab spectra obtained by the earth occultation technique. Top panel shows the data integrated about one day. The Crab incident angle is about 20 degrees from the WAM 0 detector. Bottom panel is the three-year integration data. All of the data with incident angles smaller than 30 degrees from the normal direction of each detector are added. The energy response is averaged over each incident angle, weighting by the number of occultation. The spectrum above 100 keV from one-day integration data is well fitted by a single power-law model with a photon index of 2.16 ± 0.27, and its energy flux in the 100-500 keV band is $9.9^{+1.2}_{-1.6} \times 10^{-9}$ erg cm^{-2} s^{-1} (χ^2/d.o.f. $= 6.96/5$). For the three-year integration data, the spectrum is also well fit by a single power-law with a photon index of 2.23 ± 0.09, and its energy flux in the 100-500 keV band is $9.0^{+0.9}_{-1.1} \times 10^{-9}$ cm^{-2} s^{-1} by adding 7% systematic errors for all PHA channels (χ^2/d.o.f. $= 11.79/10$).

Table 1. The GRB trigger time of each instrument. Times are all in UT.

GRB	T_0 (KW)	T_0 (BAT)	T_0 (WAM)
051008	2005/10/08 16:33:20.762	16:33:21.316	16:33:17.470
051221A	2005/12/21 01:51:12.976	01:51:15.868	01:51:15.888
060105	2006/01/05 06:49:04.371	06:49:27.446	06:49:25.696
060117	2006/01/17 06:49:57.852	06:50:01.599	06:50:00.572
060124*	2006/01/24 16:04:13.894	15:54:51.825	16:04:10.646
060502A	2006/05/02 03:03:33.119	03:03:32.144	03:03:31.501
060813	2006/08/13 22:50:21.576	22:50:22.685	22:50:24.295
060814	2006/08/14 23:02:34.447	23:02:19.035	23:02:17.783
060904A	2006/09/04 01:04:13.821	01:03:21.201	01:04:09.040
060912	2006/09/12 13:55:57.788	13:55:54.144	13:55:55.435
061006	2006/10/06 16:45:26.896	16:45:50.510	16:45:27.638
061007	2006/10/07 10:08:09.344	10:08:08.812	10:08:05.628
061222A	2006/12/22 03:30:14.682	03:28:52.110	03:30:13.420
070328	2007/03/28 03:53:49.993	03:53:53.155	03:53:46.348

* The BAT triggered on the weak precursor, whereas the KW and WAM triggered on the main part of the burst which is ∼560 sec later.
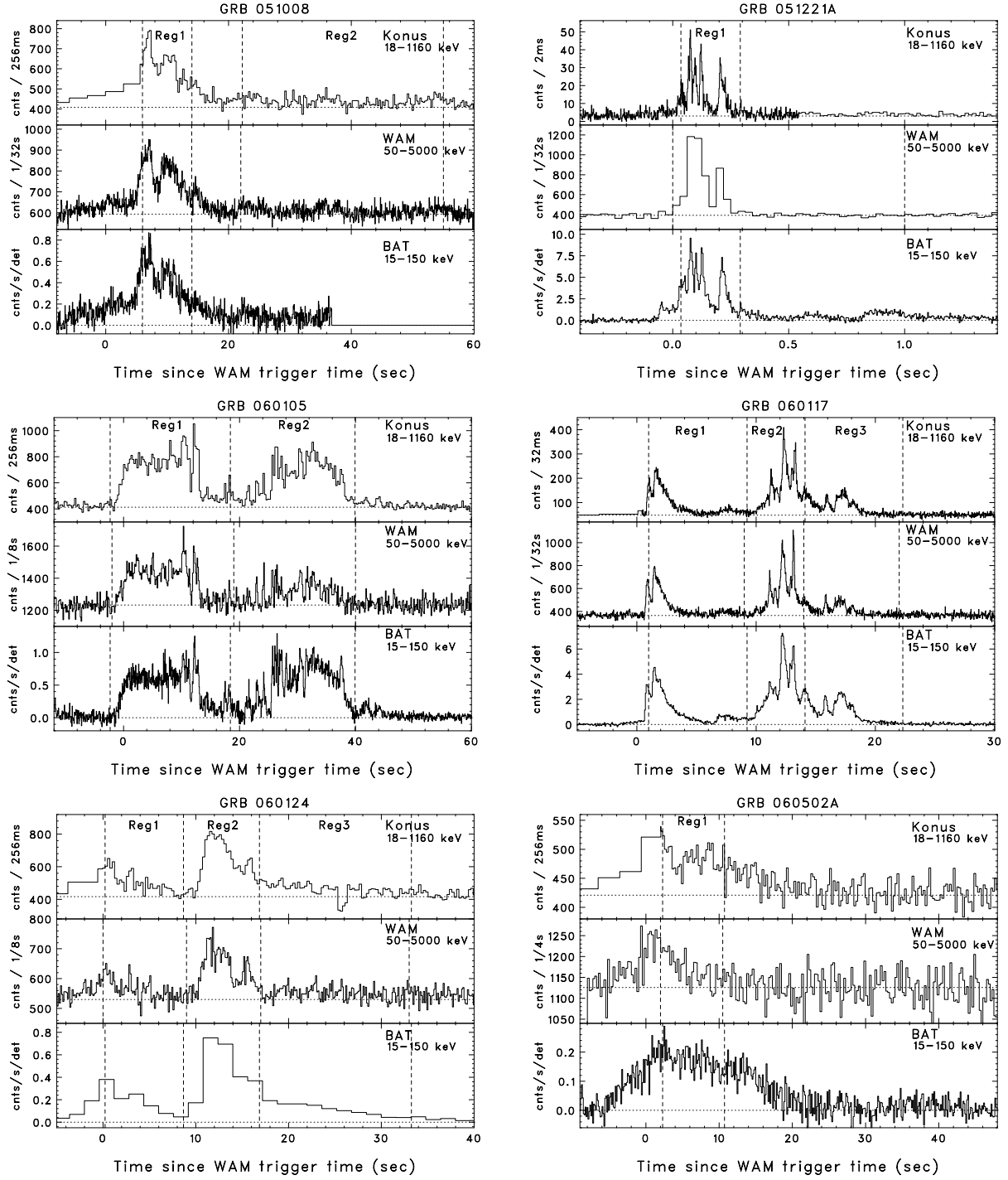
Fig. 3. Light curves of the KW (top), the WAM (middle), and the BAT (bottom) of our samples. Note that the KW light curves before the KW trigger times were recorded in the waiting mode with 2.944 s time resolution.
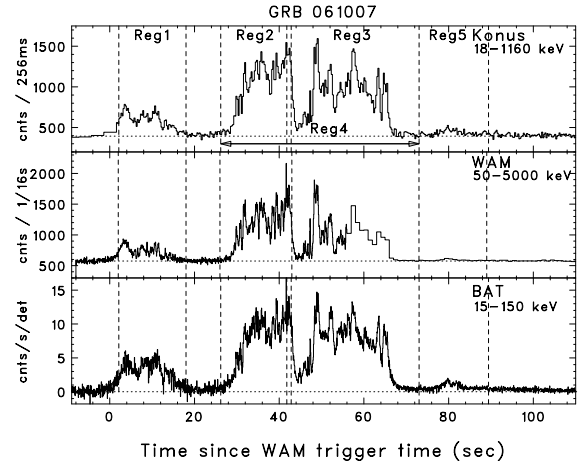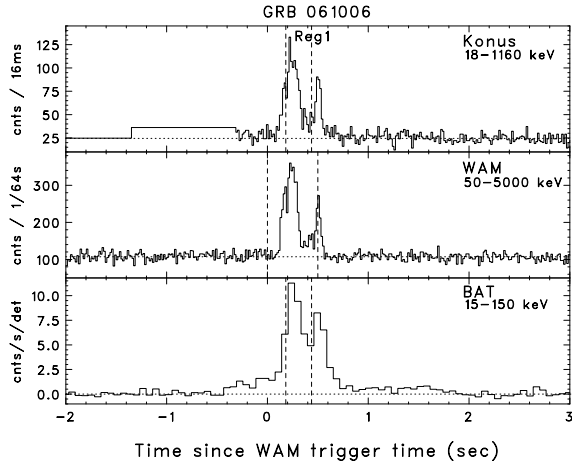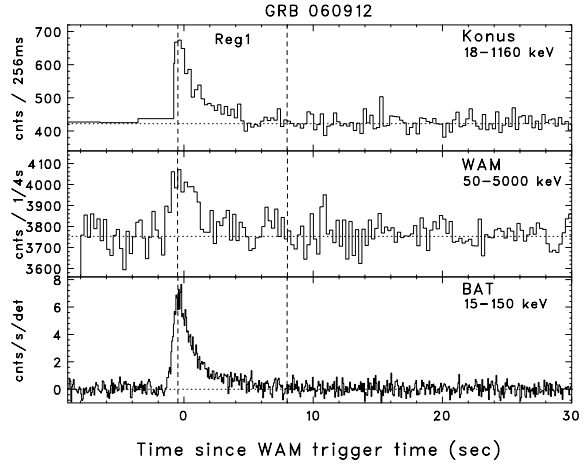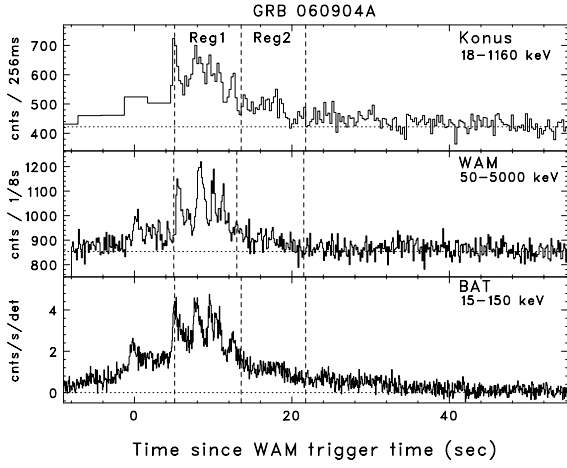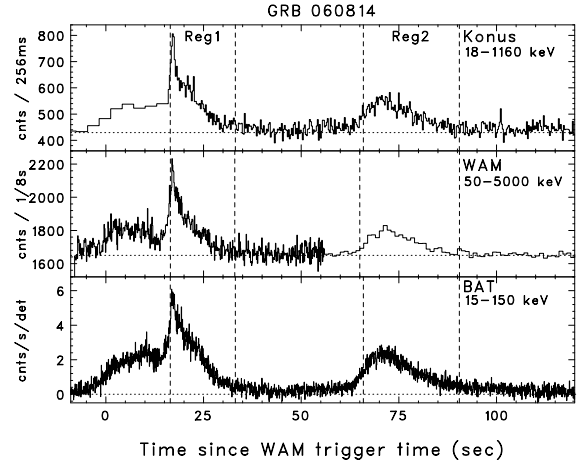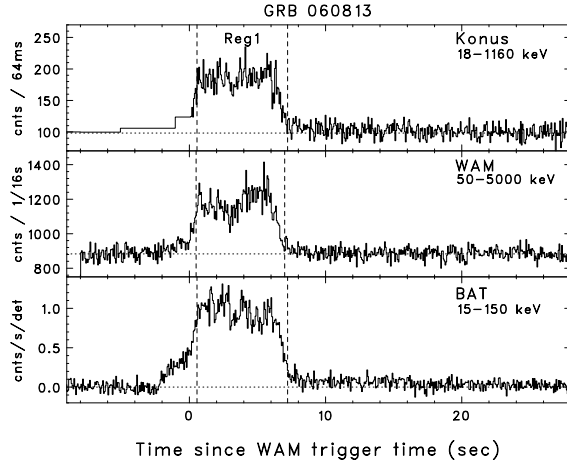
Fig. 4. Light curves (continued)
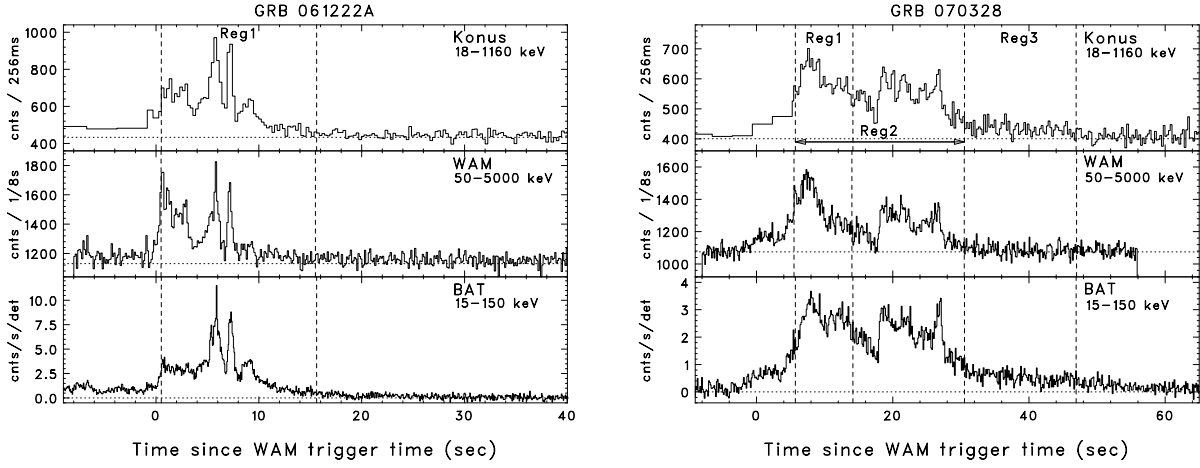
Fig. 5. Light curves (continued)

Table 2. The GRB sky position information from the BAT instrument, the incident angle of GRBs, and the WAM detector ID number used in the analysis for WAM_{SP1} and WAM_{SP2} pair. The KW detector which triggered on the GRB is shown in square brackets in the incidnet angle column of the KW.

GRB	Position (deg)		Incident Angle (deg)		WAM Det ID	
	$(R.A._{J2000}, Dec._{J2000})$	KW (θ)	BAT (θ, ϕ)	WAM (θ, ϕ)	WAM_{SP1}	WAM_{SP2}
051008	$(202.865, +42.103)$	46.9 [S2]	$(44.0, -28.7)$	$(130.3, 133.5)$	0	3
051221A	$(328.715, +16.888)$	27.7 [S2]	$(36.6, -178.6)$	$(148.2, 16.9)$	0	1
060105	$(297.485, +46.356)$	65.2 [S2]	$(42.9, +20.8)$	$(5.7, 145.6)$	0	3
060117	$(327.912, -59.982)$	43.5 [S1]	$(50.1, -159.0)$	$(63.8, 30.8)$	0	1
060124	$(77.097, +69.727)$	46.6 [S2]	$(37.8, -158.3)$	$(134.5, 215.3)$	2	3
060502A	$(240.937, +66.604)$	78.6 [S2]	$(34.9, -131.8)$	$(117.0, 174.4)$	3	-
060813	$(111.890, -29.844)$	39.0 [S1]	$(34.3, -118.4)$	$(72.1, 129.0)$	0	3
060814	$(221.338, +20.591)$	55.4 [S2]	$(28.1, +28.5)$	$(73.4, 22.6)$	0	1
060904A	$(237.731, +44.984)$	27.6 [S2]	$(13.7, +132.6)$	$(93.7, 161.3)$	0	3
060912	$(5.285, +20.971)$	72.9 [S2]	$(33.2, +125.7)$	$(116.4, 274.1)$	2	-
061006	$(110.998, -79.195)$	13.9 [S1]	$(33.6, -20.2)$	$(55.1, 199.8)$	3	-
061007	$(46.299, -50.496)$	27.0 [S1]	$(36.1, +109.8)$	$(91.8, 197.7)$	2	3
061222A	$(358.254, 46.524)$	47.6 [S2]	$(28.0, -136.1)$	$(36.6, 249.3)$	2	3
070328	$(65.113, -34.079)$	35.7 [S1]	$(39.6, -167.9)$	$(92.1, 7.5)$	1	-

20
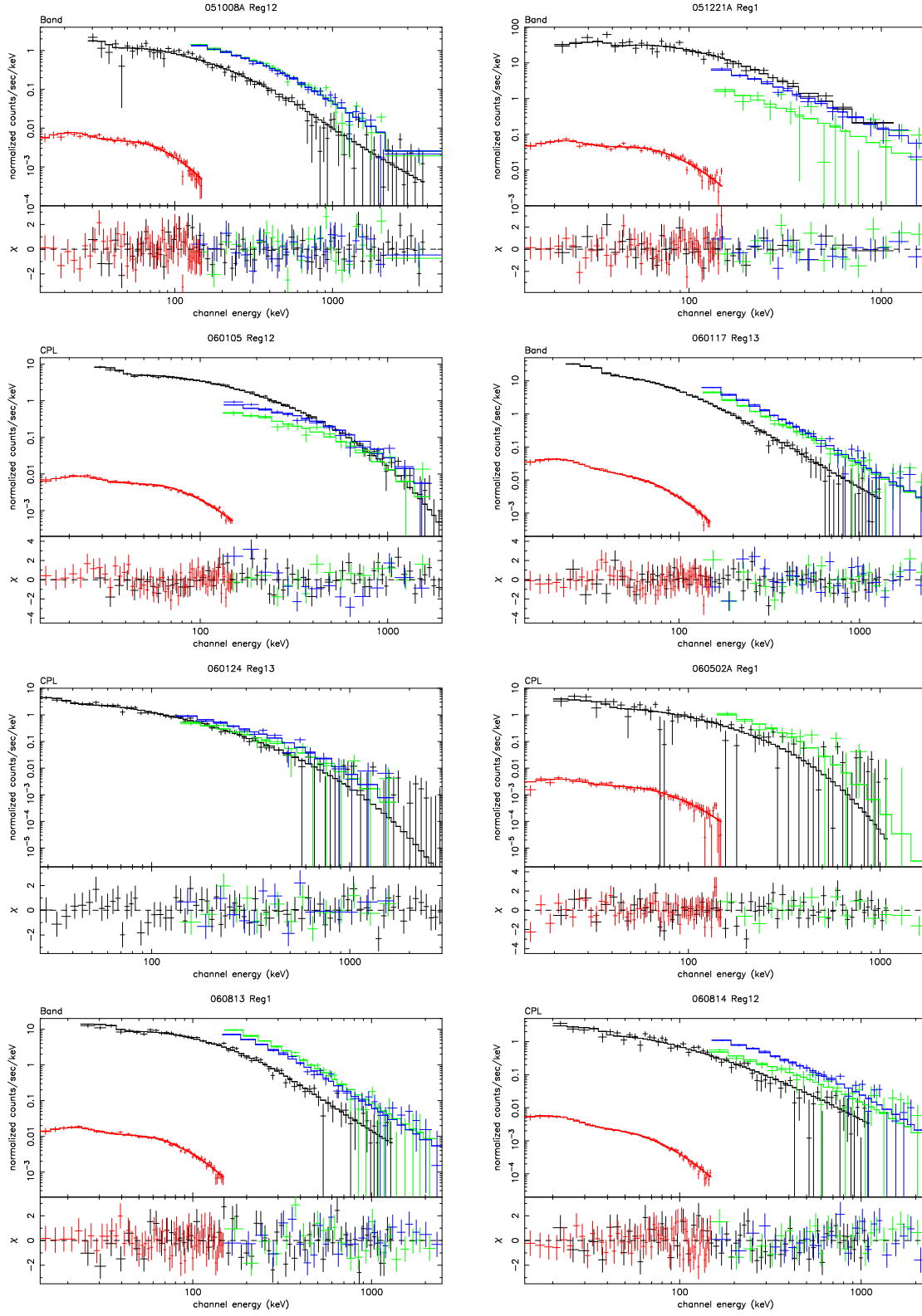
Fig. 6. The joint fit spectra of the KW (black), the WAM (blue and green) and the BAT (red). See text for details (§4).
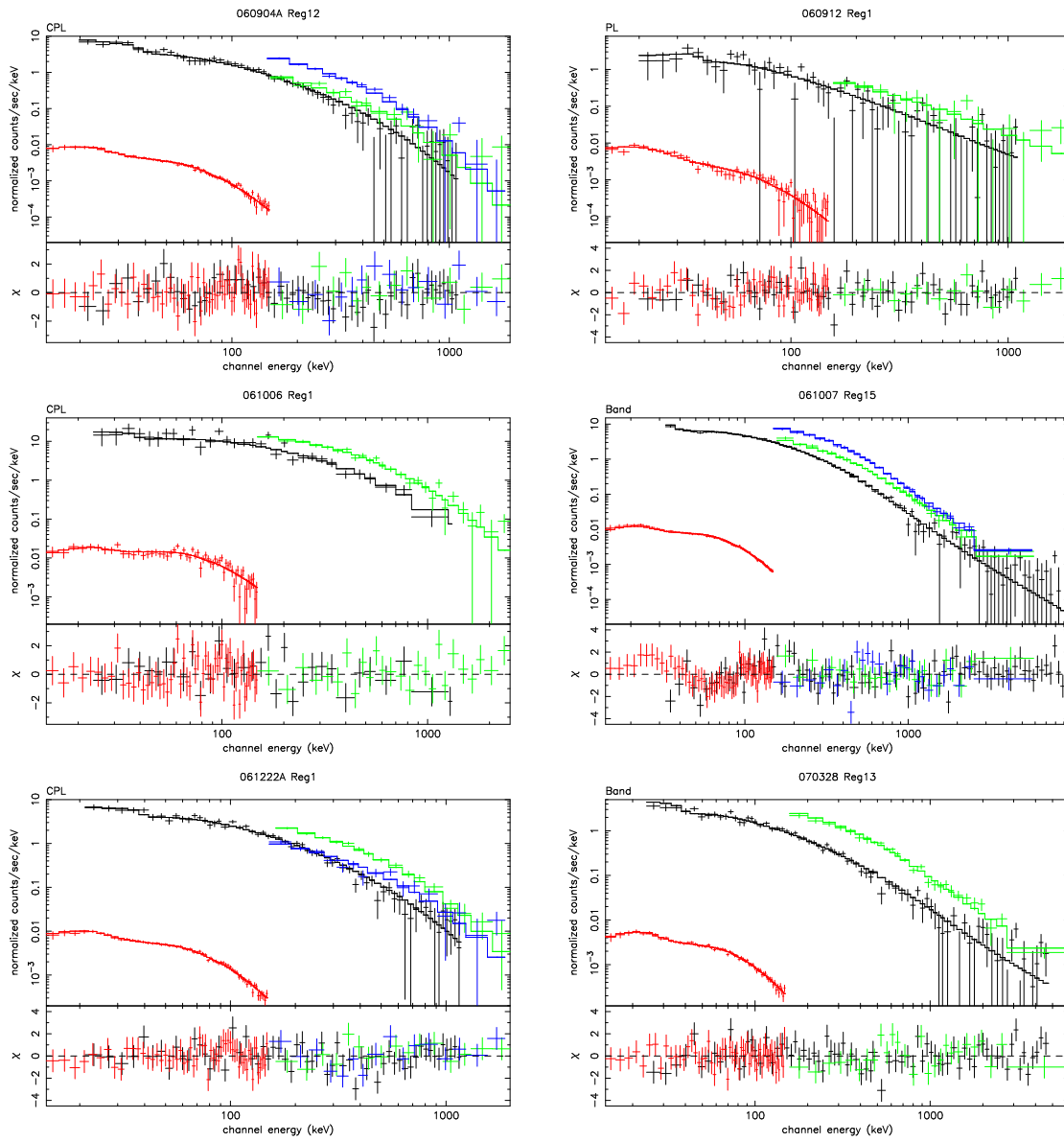
Fig. 7. The joint fit spectra (continued)
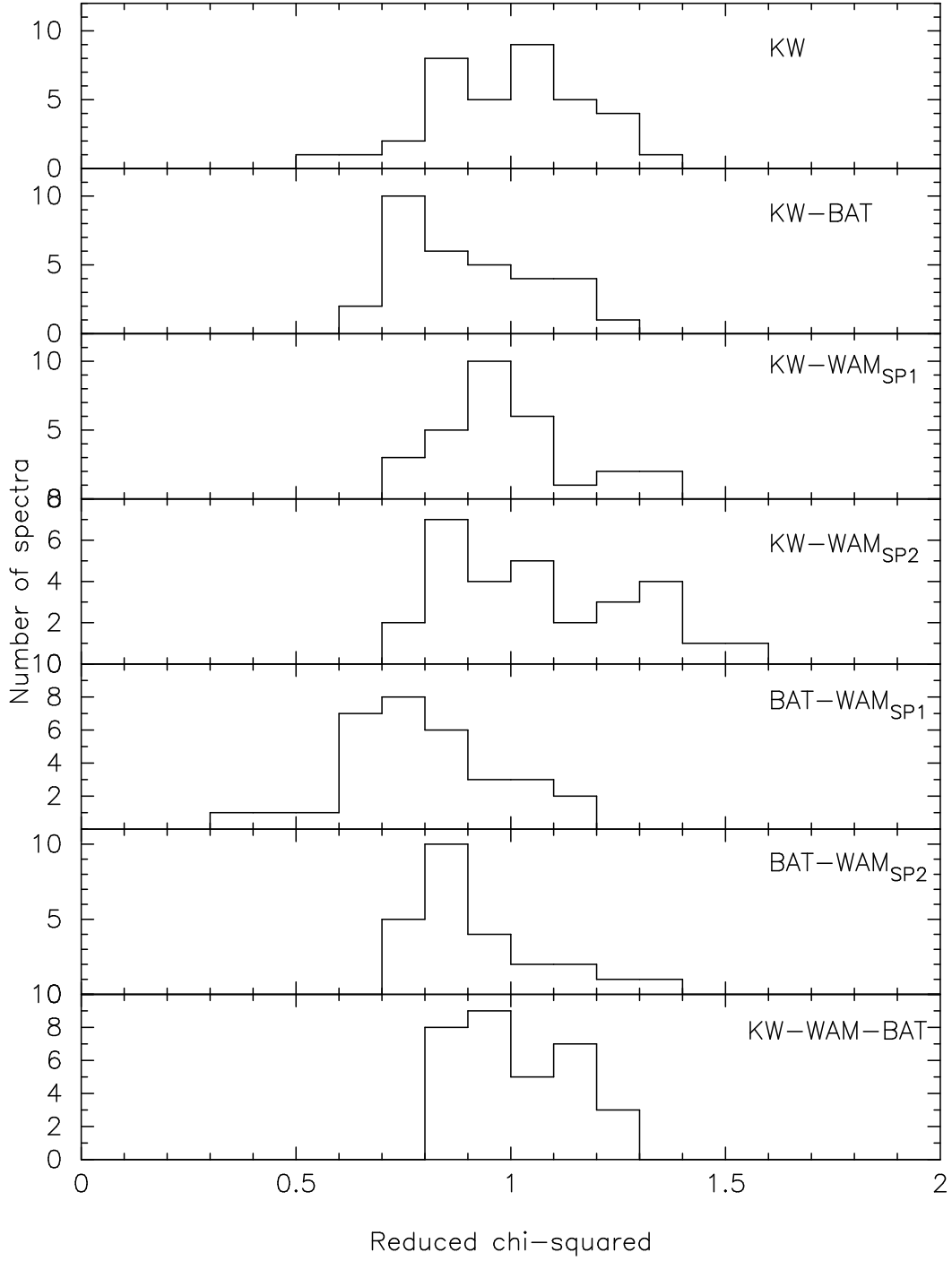
Fig. 8. Histograms of the reduced χ^2 based on the best fit spectral model for the KW and joint fits as indicated on the figures. The best fit spectral model is determined based on the difference in χ^2 between a CPL and the Band function fit. If the value of $\Delta\chi^2$ between a CPL and the Band function fit is greater than 6 ($\Delta\chi^2 \equiv \chi^2_{\mathrm{CPL}} - \chi^2_{\mathrm{Band}} > 6$), we determined that the Band function is a better representative spectral model for the data. Otherwise, the reduced χ^2 for a CPL fit is used.

23
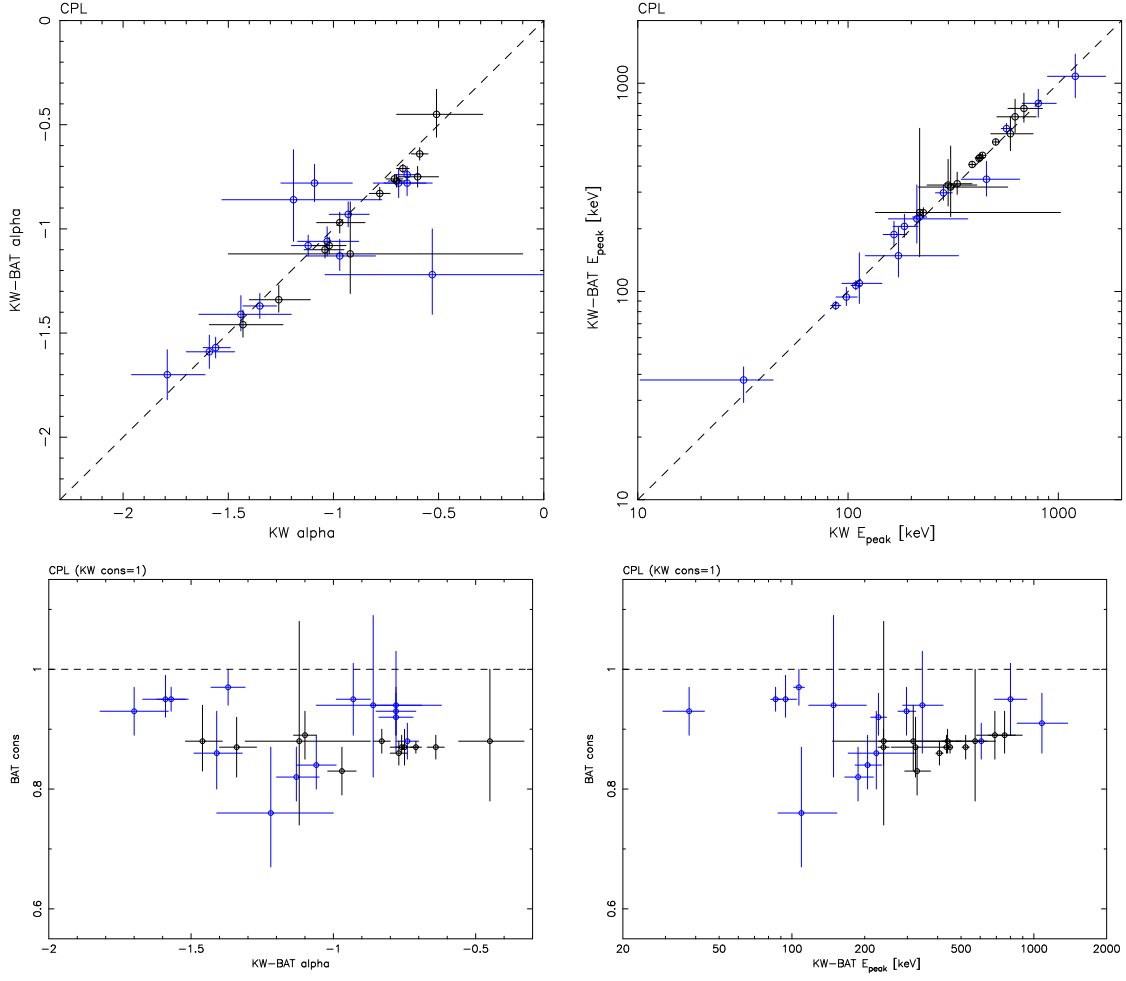
Fig. 9. Correlation between the KW and BAT joint fit spectral parameters, the low-energy photon index α (left-top) and E_{peak} (right-top), and those derived from the KW fit based on a CPL model. The BAT constant factor as a function of α (left-bottom) and E_{peak} (right-bottom) based on a CPL model. The blue data points are not affected by the $Swift$ spacecraft slew. The KW constant factor is fixed to 1.
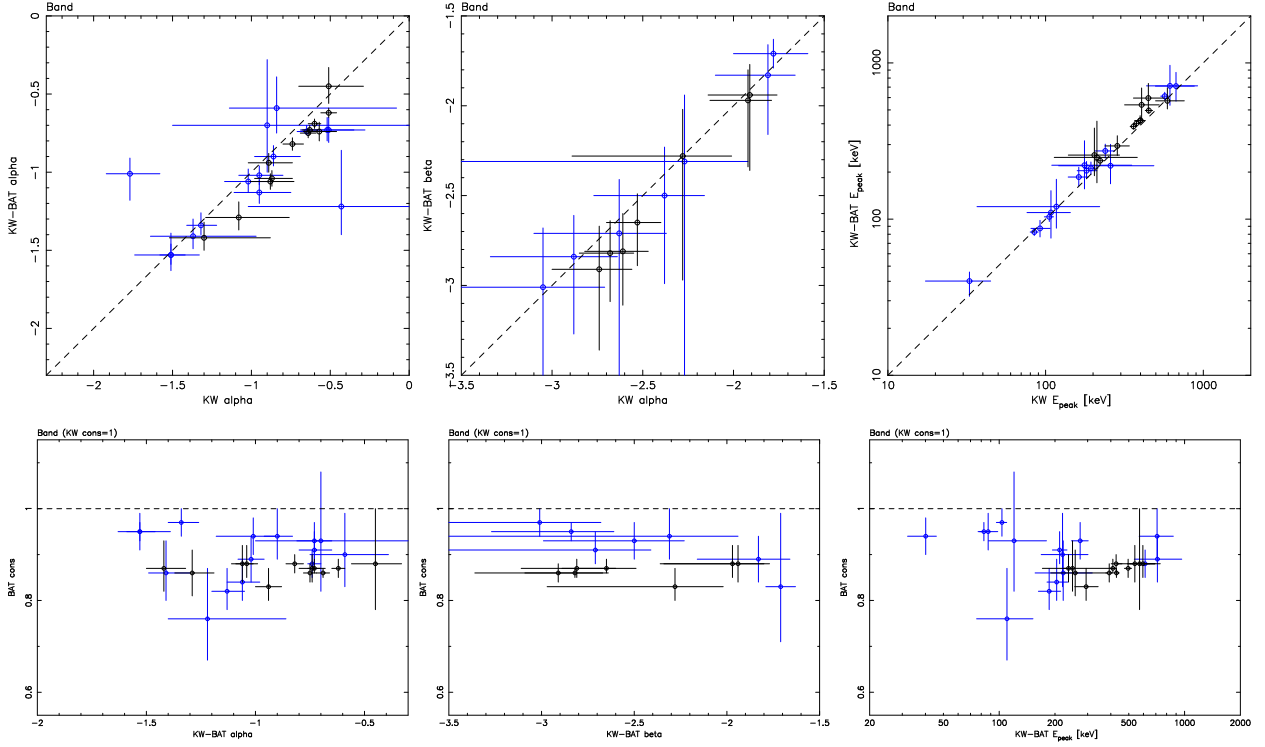
Fig. 10. Correlation between the KW and BAT joint fit spectral parameters, the low-energy photon index α (left-top), the high-energy photon index β (middle-top), and E_{peak} (right-top), and those derived from the KW fit based on the Band function. The BAT constant factor as a function of α (left-bottom), β (middle-bottom) and E_{peak} (right-bottom) based on the Band function. The blue data points are not affected by the $Swift$ spacecraft slew. The KW constant factor is fixed to 1.
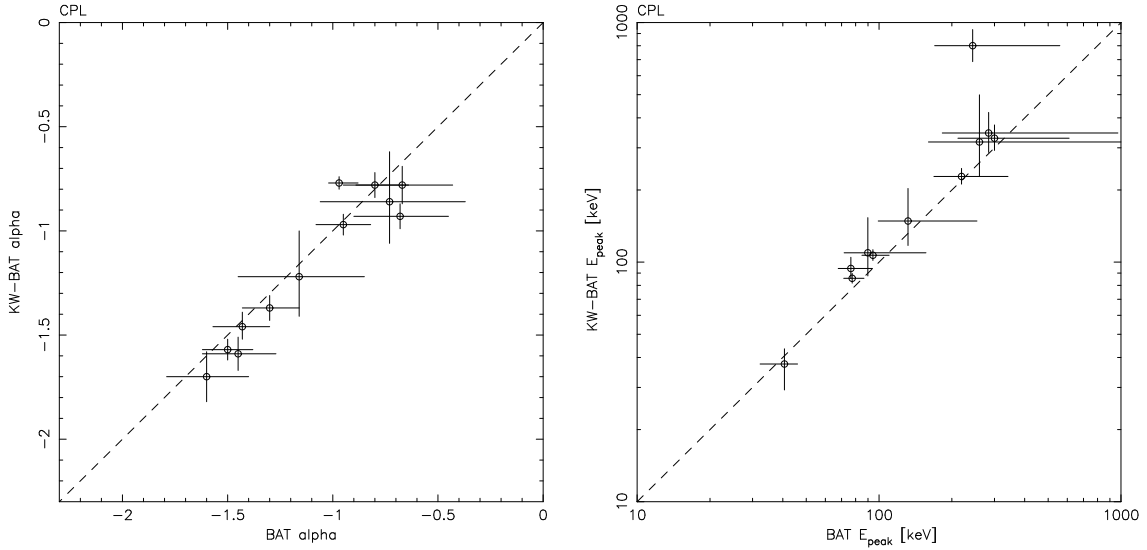
Fig. 11. Correlation between the KW and the BAT joint fit spectral parameters, the low energy photon index α (left) and E_{peak} (right), and those derived from the BAT fit based on a CPL model.
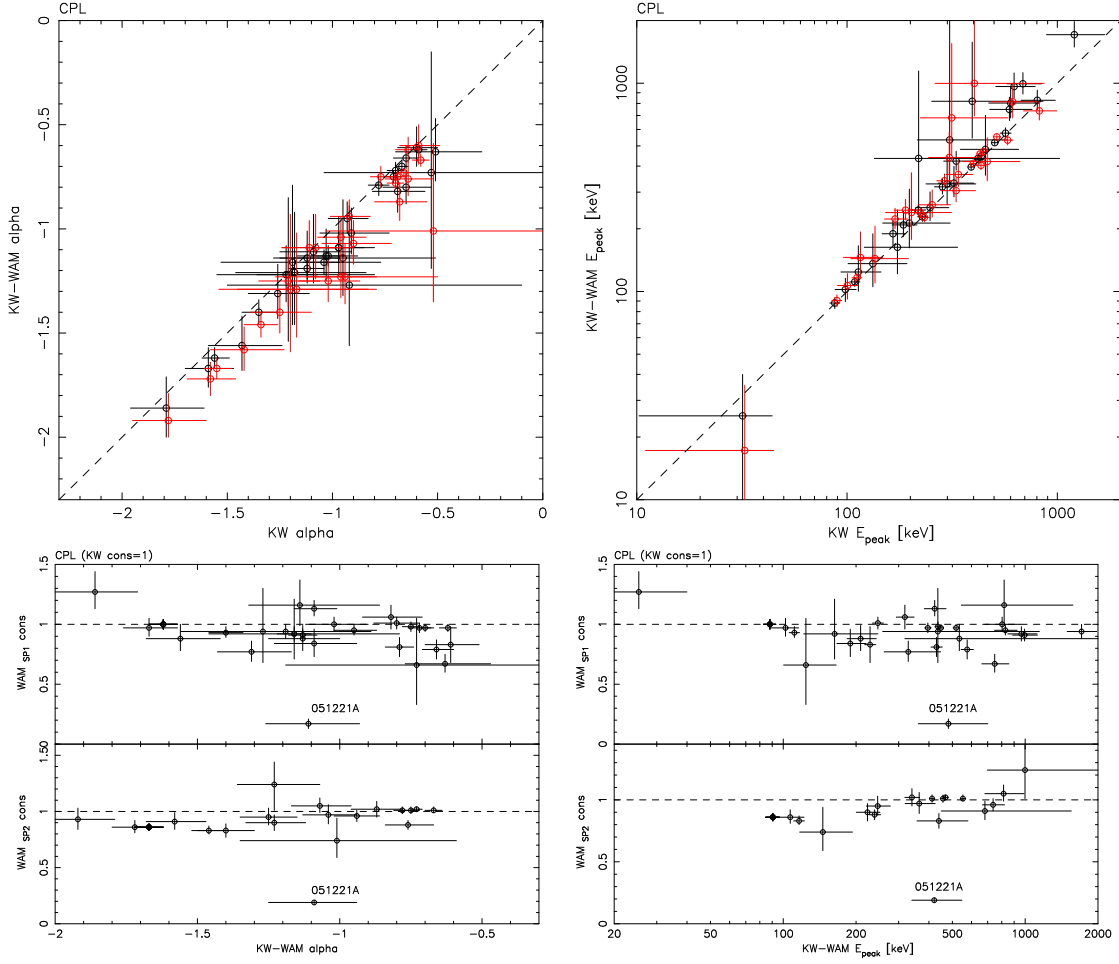
Fig. 12. Correlation between the KW and WAM joint fit spectral parameters, the low-energy photon index α (left-top) and E_{peak} (right-top), and those derived from the KW fit based on a CPL model. The WAM$_{SP1}$ data are shown in black and the WAM$_{SP2}$ data are shown in red. Just for display purposes, the WAM$_{SP2}$ data points are shifted by 0.01 in α and by 2% of their E_{peak} value from the KW fits (x-axis). The WAM$_{SP1}$ and WAM$_{SP2}$ constant factors as a function of α (left-bottom) and E_{peak} (right-bottom) based on a CPL model. The KW constant factor is fixed to 1.
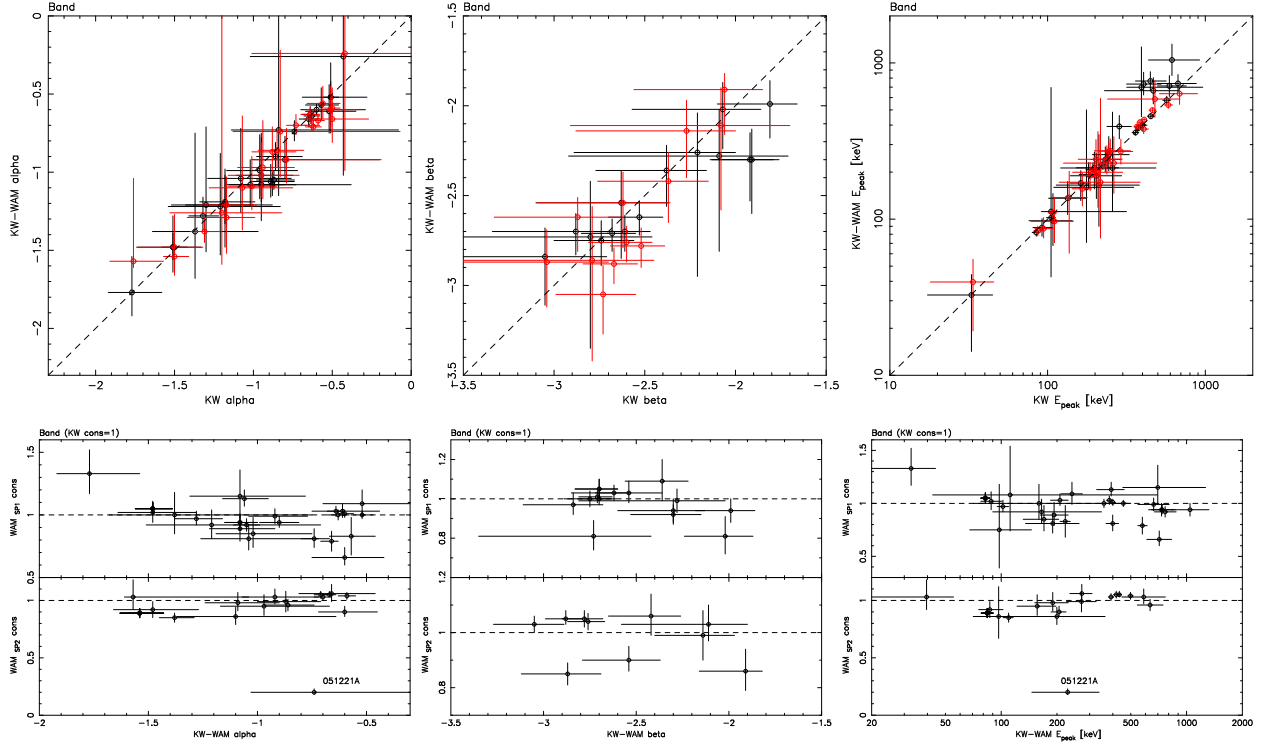
Fig. 13. Correlation between the KW and the WAM joint fit spectral parameters, the low-energy photon index α (left-top), the high-energy photon index β (middle-top), and E_{peak} (right-top), and those derived from the KW fit based on the Band function. The WAM$_{SP1}$ data are shown in black and the WAM$_{SP2}$ data are shown in red. Just for display purposes, the WAM$_{SP2}$ data points are shifted by 0.01 in α and by 2% of their E_{peak} value from the KW fits (x-axis). The WAM$_{SP1}$ and WAM$_{SP2}$ constant factors as a function of α (left-bottom), β (middle-bottom) and E_{peak} (right-bottom) based on the Band function. The KW constant factor is fixed to 1.

27

Fig. 14. Correlation between the BAT and WAM joint fit spectral parameters, the low-energy photon index α (left-top) and E_{peak} (right-top), and those derived from the KW fit based on a CPL model. The WAM$_{SP1}$ data are shown in black and the WAM$_{SP2}$ data are shown in red. Just for display purposes, the WAM$_{SP2}$ data points are shifted by 0.01 in α and by 2% of their E_{peak} value from the KW fits (x-axis). The WAM$_{SP1}$ and WAM$_{SP2}$ constant factors as a function of α (left-bottom) and E_{peak} (right-bottom) based on a CPL model. The BAT constant factor is fixed to 1.
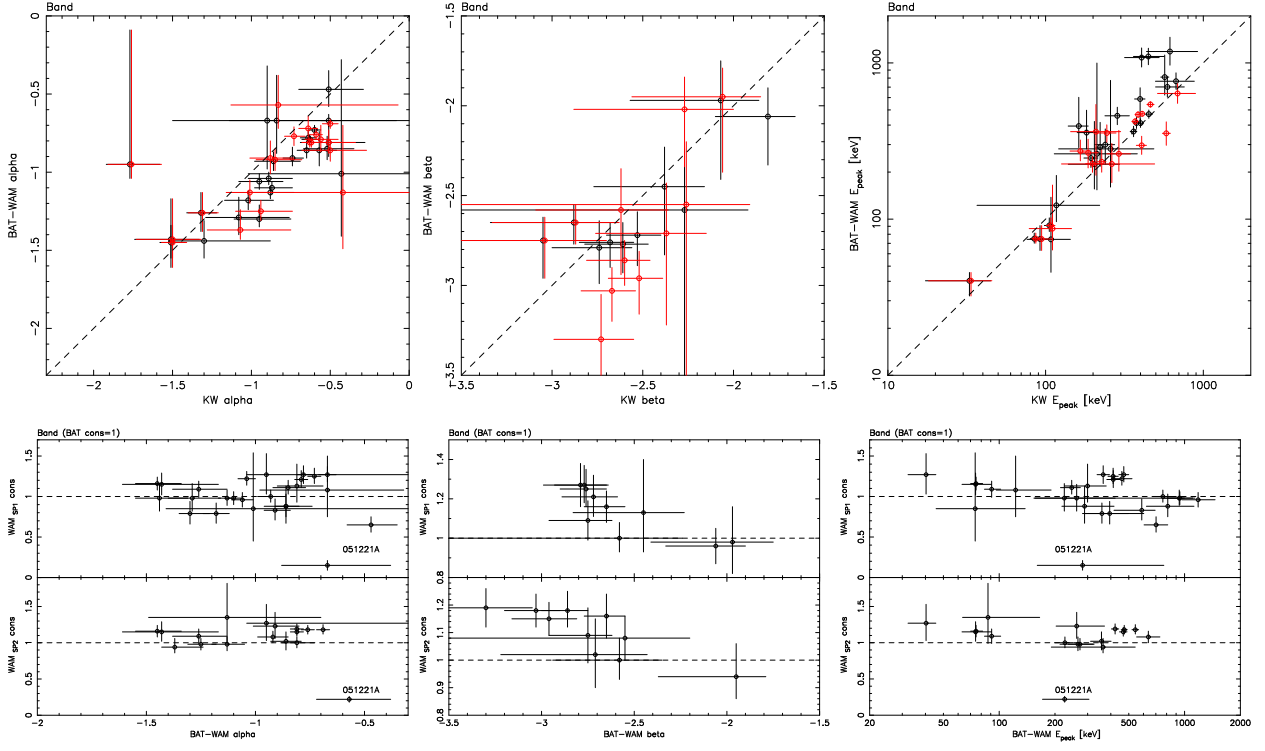
Fig. 15. Correlation between the BAT and the WAM joint fit spectral parameters, the low-energy photon index α (left-top), the high-energy photon index β (middle-top), and E_{peak} (right-top), and those derived from the KW fit based on the Band function. The WAM$_{SP1}$ data are shown in black and the WAM$_{SP2}$ data are shown in red. Just for display purposes, the WAM$_{SP2}$ data points are shifted by 0.01 in α and by 2% of their E_{peak} value from the KW fits (x-axis). The WAM$_{SP1}$ and WAM$_{SP2}$ constant factors as a function of α (left-bottom), β (middle-bottom) and E_{peak} (right-bottom) based on the Band function. The BAT constant factor is fixed to 1.

29

Fig. 16. Correlation between the KW, WAM and BAT joint fit spectral parameters, the low-energy photon index α (left-top) and E_{peak} (right-top), and those derived from the KW fit based on a CPL model. The BAT, WAM1 and WAM2 constant factors as a function of α (left-bottom) and E_{peak} (right-bottom) based on a CPL model. The KW constant factor is fixed to 1.
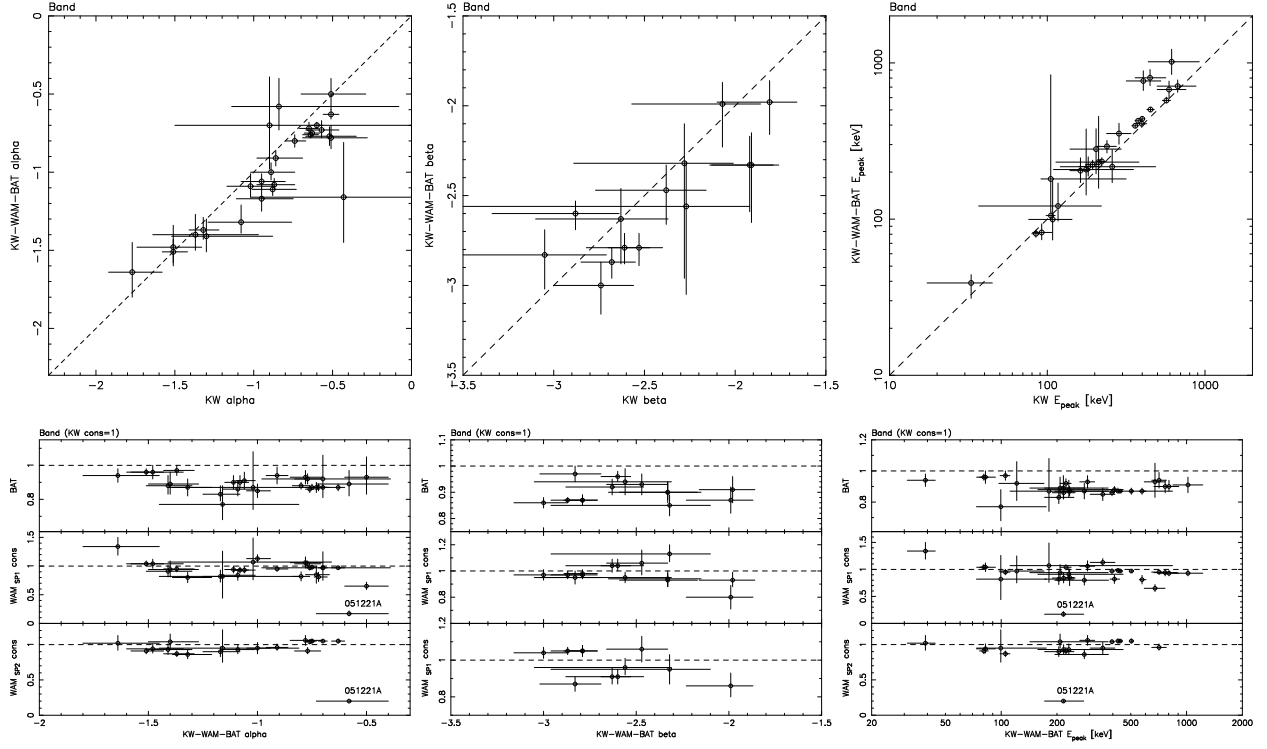
Fig. 17. Correlation between the KW, WAM and BAT joint fit spectral parameters, the low-energy photon index α (left-top), the high-energy photon index β (middle-top), and E_{peak} (right-top), and those derived from the KW fit based on the Band function. The BAT, WAM1 and WAM2 constant factors as a function of α (left-bottom), β (middle-bottom) and E_{peak} (right-bottom) based on the Band function. The KW constant factor is fixed to 1.
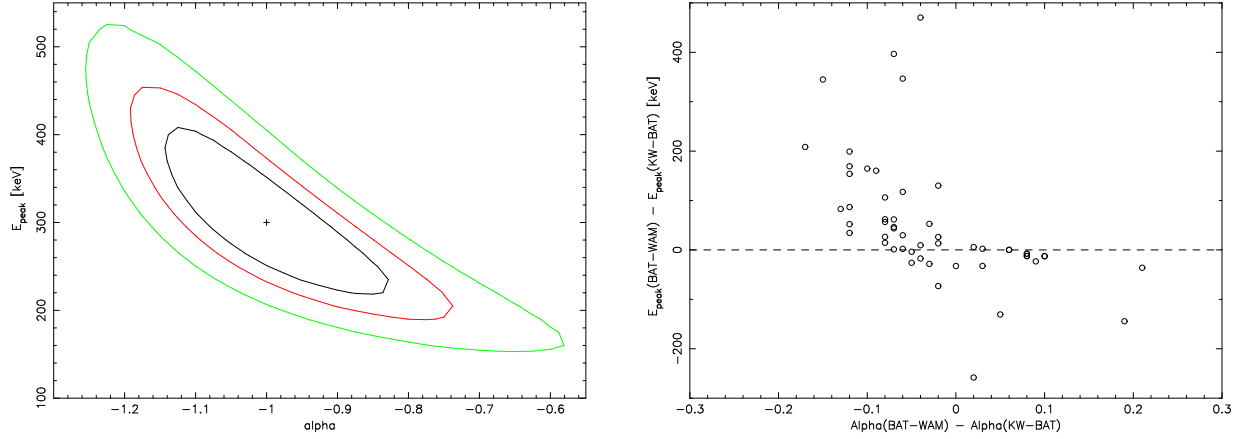
Fig. 18. Left: Confidence contours between E_{peak} and α derived from the KW simulated spectrum with the input Band parameters of $\alpha = -1$, $\beta = -2.5$, and $E_{\text{peak}} = 300\,\text{keV}$. Right: the difference in E_{peak} between the BAT-WAM joint fit and the KW-BAT joint fit vs. the difference in α between the BAT-WAM joint fit and the KW-BAT joint fit.
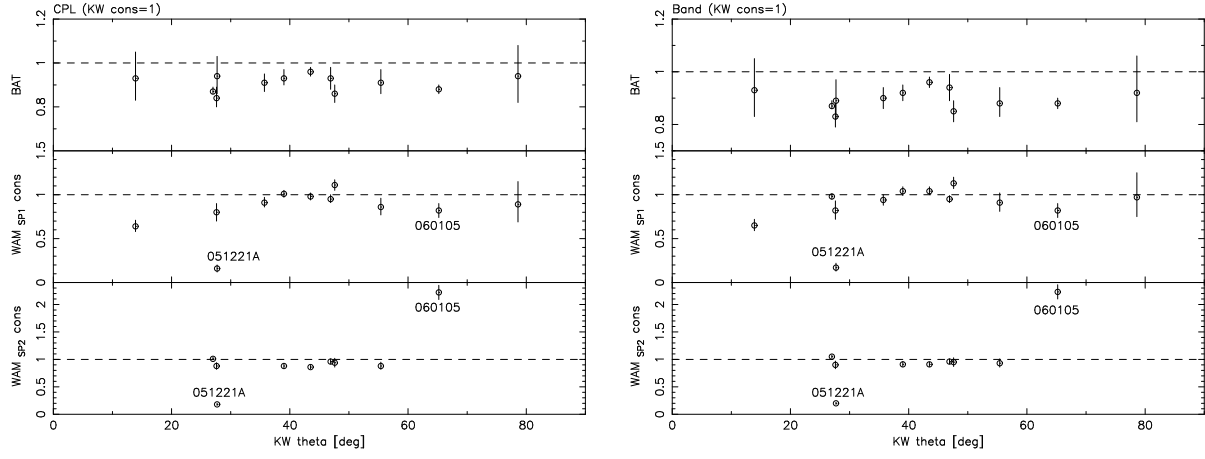
Fig. 19. The BAT, WAM$_{SP1}$ and WAM$_{SP2}$ constant factor based on a CPL fit (left) and the Band fit (right) as a function of the incident angle θ of KW.
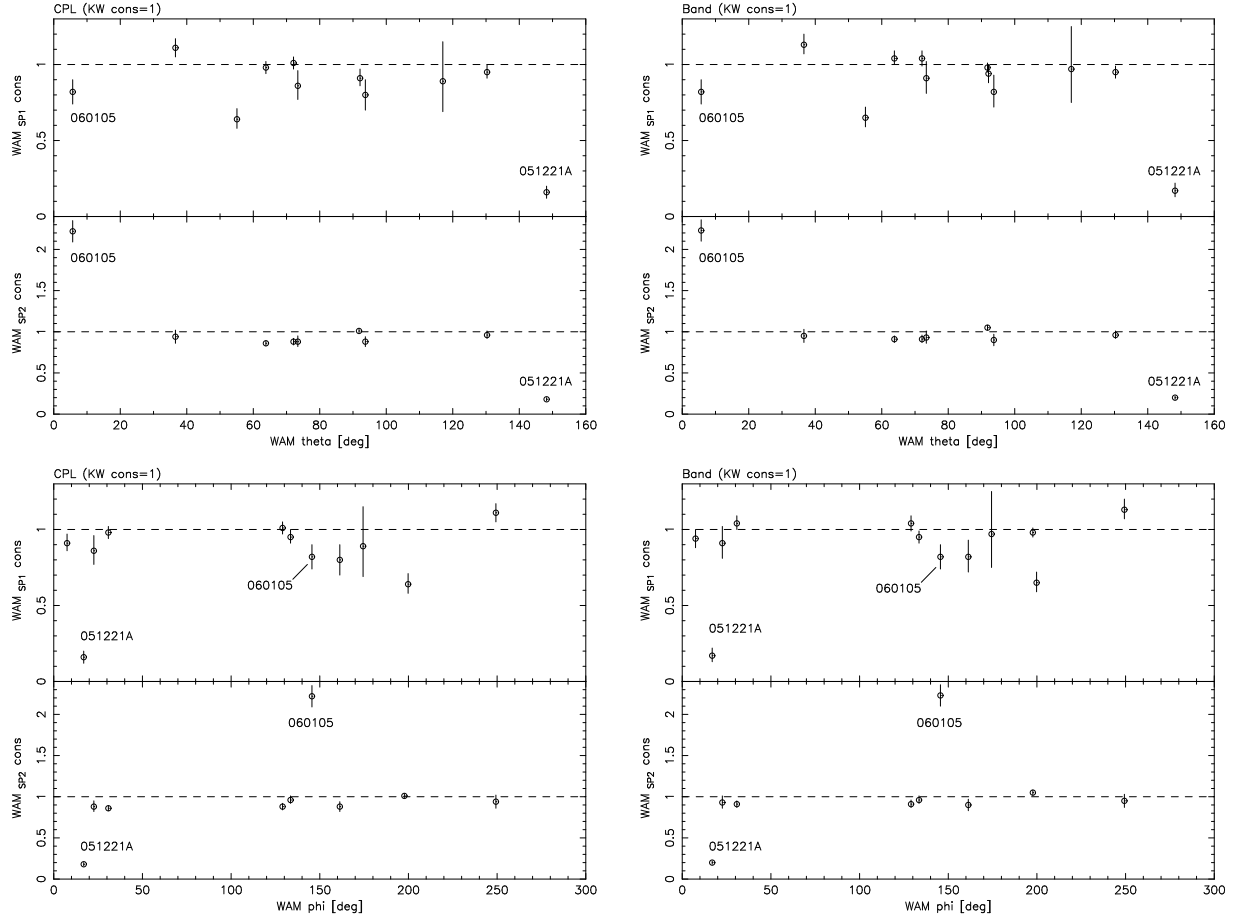
Fig. 20. The WAM$_{SP1}$ and WAM$_{SP2}$ constant factor based on a CPL fit (left) and the Band fit (right) as a function of the incident angle θ (top) and ϕ (bottom) of WAM.

32
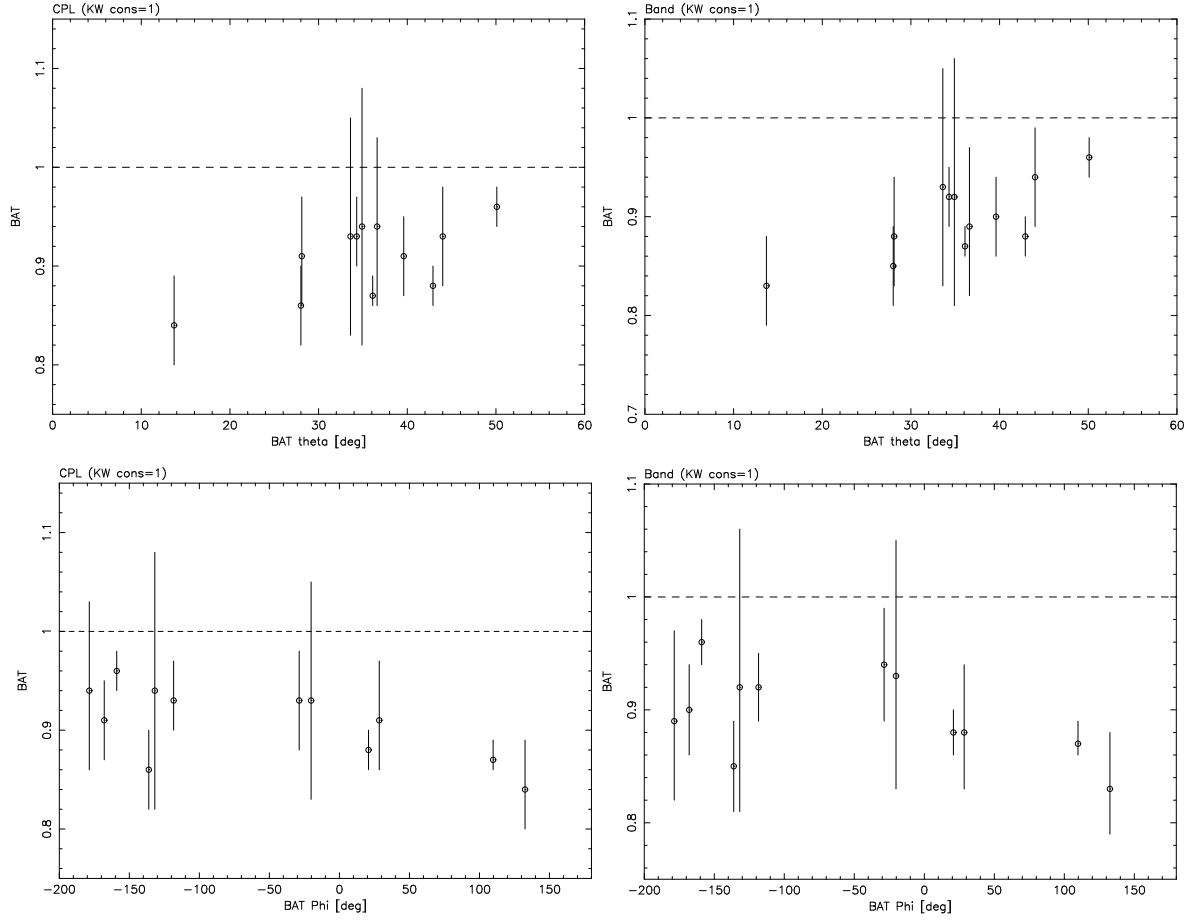
Fig. 21. The BAT constant factor based on a CPL fit (left) and the Band fit (right) as a function of the incident angle θ (top) and ϕ (bottom) of BAT.
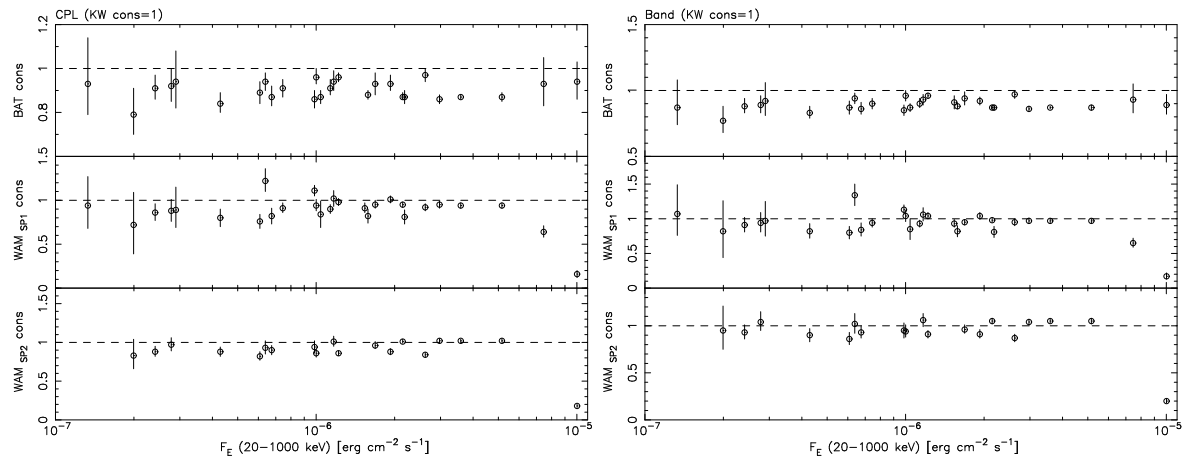
Fig. 22. The BAT, WAM$_{SP1}$ and WAM$_{SP2}$ constant factor based on a CPL fit (left) and the Band fit (right) as a function of the observed energy flux in the 20-1000 keV band.

Table 3. The energy fluence measured with KW, WAM and BAT in their full energy band. The KW, BAT and WAM fluence is measured using the time-averaged spectrum (T_{100} interval). For the KW, in case the burst emission started before the trigger time (e.g. GRB 051008 and GRB 060502A), the fluence for the pre-trigger part is estimated using a product of the count fluence for this part and the conversion factor from a count fluence to an energy fluence using the spectral information of the time-averaged spectrum. Then, the fluence of pre-trigger part is added to the fluence of the main part to obtain the total fluence.

GRB	S^{KW}(20-10000 keV) [erg cm^{-2}]	S^{WAM}(100-1000 keV) [erg cm^{-2}]	S^{BAT}(15-150 keV) [erg cm^{-2}]
051008	$5.2^{+3.0}_{-2.1} \times 10^{-5}$	$(2.85 \pm 0.08) \times 10^{-5}$	-
051221A	$3.4^{+0.8}_{-0.5} \times 10^{-6}$	$(1.5 \pm 0.1) \times 10^{-6}$	$(1.16 \pm 0.04) \times 10^{-6}$
060105	$(7.9 \pm 0.3) \times 10^{-5}$	$(5.0 \pm 0.5) \times 10^{-5}$	$(1.82 \pm 0.03) \times 10^{-5}$
060117	$(3.1 \pm 0.2) \times 10^{-5}$	$(1.54 \pm 0.07) \times 10^{-5}$	$(2.05 \pm 0.03) \times 10^{-5}$
060124	$3.1^{+0.8}_{-0.7} \times 10^{-5}$	$(7.8 \pm 0.9) \times 10^{-6}$	-
060502A	$3.8^{+1.3}_{-0.8} \times 10^{-6}$	$(2.7 \pm 0.5) \times 10^{-6}$	$(2.3 \pm 0.1) \times 10^{-6}$
060813	$1.8^{+0.3}_{-0.2} \times 10^{-5}$	$(1.00 \pm 0.05) \times 10^{-5}$	$(5.5 \pm 0.1) \times 10^{-6}$
060814	$3.7^{+1.1}_{-0.6} \times 10^{-5}$	$(2.5 \pm 0.1) \times 10^{-5}$	$(1.48 \pm 0.02) \times 10^{-5}$
060904A	$1.3^{+0.4}_{-0.2} \times 10^{-5}$	$(6.3 \pm 0.7) \times 10^{-6}$	$(7.8 \pm 0.2) \times 10^{-6}$
060912	$5.7^{+2.2}_{-1.6} \times 10^{-6}$	$(1.3 \pm 0.3) \times 10^{-6}$	$(1.36 \pm 0.06) \times 10^{-6}$
061006	$3.7^{+0.8}_{-0.6} \times 10^{-6}$	$(2.6 \pm 0.1) \times 10^{-6}$	$(1.4 \pm 0.1) \times 10^{-6}$
061007	$(2.6 \pm 0.2) \times 10^{-4}$	$(1.70 \pm 0.07) \times 10^{-4}$	$(4.50 \pm 0.05) \times 10^{-5}$
061222A	$3.4^{+0.9}_{-0.7} \times 10^{-5}$	$(1.75 \pm 0.08) \times 10^{-5}$	$(8.1 \pm 0.2) \times 10^{-6}$
070328	$7.9^{+1.5}_{-1.4} \times 10^{-5}$	$(3.2 \pm 0.2) \times 10^{-5}$	$(9.2 \pm 0.2) \times 10^{-6}$

Table 4. The 1-s peak energy flux measured with KW, WAM and BAT in their full energy band. The KW 1-s peak energy flux is calculated as a product of 1-s peak count-rate and the conversion factor from a count rate to an energy flux using the spectrum accumulated over the time interval which comprises the peak. The BAT and WAM 1-s peak energy flux is measured using the 1-s duration spectrum including the brightest part of the burst emission.

GRB	F_{1s}^{KW}(20-10000 keV) [erg cm^{-2} s^{-1}]	F_{1s}^{WAM}(100-1000 keV) [erg cm^{-2} s^{-1}]	F_{1s}^{BAT}(15-150 keV) [erg cm^{-2} s^{-1}]
051008	$(5.1 \pm 1.1) \times 10^{-6}$	$(2.0 \pm 0.1) \times 10^{-6}$	-
051221A	$3.4^{+0.8}_{-0.5} \times 10^{-6}$	$(1.5 \pm 0.1) \times 10^{-6}$	$(1.02 \pm 0.03) \times 10^{-6}$
060105	$(5.5 \pm 0.6) \times 10^{-6}$	$(3.3 \pm 0.6) \times 10^{-6}$	$(7.1 \pm 0.4) \times 10^{-7}$
060117	$6.5^{+0.6}_{-0.5} \times 10^{-6}$	$(2.9 \pm 0.2) \times 10^{-6}$	$(3.70 \pm 0.08) \times 10^{-6}$
060124	$(3.4 \pm 0.9) \times 10^{-6}$	$(1.0 \pm 0.2) \times 10^{-6}$	-
060502A	$5.5^{+2.2}_{-1.6} \times 10^{-7}$	$(3.8 \pm 1.1) \times 10^{-7}$	$(1.7 \pm 0.2) \times 10^{-7}$
060813	$3.6^{+0.6}_{-0.5} \times 10^{-6}$	$(2.0 \pm 0.2) \times 10^{-6}$	$(8.0 \pm 0.3) \times 10^{-7}$
060814	$(2.1 \pm 0.3) \times 10^{-6}$	$(1.4 \pm 0.1) \times 10^{-6}$	$(6.1 \pm 0.2) \times 10^{-7}$
060904A	$1.3^{+0.4}_{-0.2} \times 10^{-6}$	$(5.4 \pm 1.4) \times 10^{-7}$	$(4.4 \pm 0.2) \times 10^{-7}$
060912	$2.5^{+1.0}_{-0.8} \times 10^{-6}$	$(5.2 \pm 1.5) \times 10^{-7}$	$(5.8 \pm 0.3) \times 10^{-7}$
061006	$3.7^{+0.8}_{-0.6} \times 10^{-6}$	$(2.6 \pm 0.1) \times 10^{-6}$	$(5.3 \pm 0.2) \times 10^{-7}$
061007	$(1.2 \pm 0.1) \times 10^{-5}$	$(9.2 \pm 0.3) \times 10^{-6}$	$(1.56 \pm 0.04) \times 10^{-6}$
061222A	$4.8^{+1.4}_{-1.2} \times 10^{-6}$	$(3.2 \pm 0.2) \times 10^{-6}$	$(5.8 \pm 0.2) \times 10^{-7}$
070328	$(5.9 \pm 1.2) \times 10^{-6}$	$(1.9 \pm 0.1) \times 10^{-6}$	$(3.9 \pm 0.2) \times 10^{-7}$

Table 5. Spectral intervals used in the analysis and time of flight from the spacecraft to the Earth.

GRB	Region	K-W		BAT		WAM		Time of flight		
		t_{start}^{K-W}	t_{stop}^{K-W}	t_{start}^{BAT}	t_{stop}^{BAT}	t_{start}^{WAM}	t_{stop}^{WAM}	K-W→⊕	BAT→⊕	WAM→⊕
051008	Reg1	0.128	8.192	2.152	10.216	6.0	14.0	2.576	−0.001	0.021
	Reg2	16.384	49.152	NA	NA	22.0	55.0			
	Reg12	0.128	49.152	NA	NA	6.0	55.0			
051221A	Reg1	0.0	0.256	0.064	0.320	0.0	1.0	2.962	0.006	0.015
060105	Reg1	16.64	37.376	−4.094	16.642	−2.0	19.0	2.362	0.021	−0.000
	Reg2^S	37.376	58.88	16.642	38.146	19.0	40.0			
	Reg12^S	16.64	58.88	−4.094	16.642	−2.0	40.0			
060117	Reg1	0.192	8.448	−0.055	8.200	1.0	9.0	3.514	0.015	−0.000
	Reg2	8.448	13.312	8.200	13.064	9.0	14.0			
	Reg3	13.312	21.504	13.064	21.256	14.0	22.0			
	Reg13	0.192	21.504	−0.055	21.256	1.0	22.0			
060124	Reg1	0.0	8.448	-	-	0.0	9.0	−3.024	0.011	0.004
	Reg2	8.448	16.640	-	-	9.0	17.0			
	Reg3	16.640	33.024	-	-	17.0	33.0			
	Reg13	0.0	33.024	-	-	0.0	33.0			
060502A	Reg1	0.0	8.448	0.638	9.086	2.0	10.5	−0.326	0.010	0.006
060813	Reg1	0.0	6.656	2.168	8.824	0.5	7.0	3.293	0.016	0.012
060814	Reg1^S	0.0	16.64	15.247	31.887	16.0	33.0	−0.152	0.014	0.015
	Reg2	49.408	73.984	64.655	89.231	65.5	90.5			
	Reg12^S	0.0	73.984	15.247	89.231	16.5	90.5			
060904A	Reg1	0.0	8.448	52.942	61.390	5.0	13.5	0.3267	0.003	0.003
	Reg2	8.448	16.64	61.390	69.582	13.5	21.5			
	Reg12	0.0	16.64	52.942	69.582	5.0	21.5			
060912	Reg1	0.0	8.448	0.319	8.767	-0.5	8.0	−3.306	0.020	0.016
061006	Reg1	0.0	0.256	−22.703	−22.447	0.0	0.5	0.921	0.010	−0.003
061007	Reg1	0.0	15.872	−1.057	14.815	2.0	18.0	−1.577	0.011	0.013
	Reg2^S	24.064	40.704	23.007	39.647	26.0	43.0			
	Reg3^S	39.680	70.912	38.623	69.855	42.0	73.0			
	Reg4^S	24.064	70.912	23.007	69.855	26.0	73.0			
	Reg5	70.912	87.296	69.855	86.239	73.0	89.0			
	Reg15^S	0.0	87.296	−1.057	86.239	2.0	89.0			
061222A	Reg1^S	0.0	15.104	81.808	96.912	0.5	15.5	−0.745	0.018	-0.000
070328	Reg1	0.0	8.448	−1.107	7.341	5.5	14.0	2.071	0.016	0.012

Table 5. (Continued.)

Reg2$^{\mathrm{S}}$	0.0	24.832	-1.107	23.725	5.5	30.5
Reg3$^{\mathrm{S}}$	24.832	41.216	23.725	40.109	30.5	47.0
Reg13$^{\mathrm{S}}$	0.0	41.216	-1.107	40.109	5.5	47.0

$^{\mathrm{S}}$ The spectral interval which contains the $Swift$ spacecraft slew in the BAT data.

Table 6. The best fit parameters by a linear function between parameters in a CPL model derived by the joint fit and the KW fit. For example, the linear function for α in the KW-BAT fits vs. the KW fit is $\alpha_{(\mathrm{KW-BAT})} = \mathrm{a} \times \alpha_{(\mathrm{KW})} + \mathrm{b}$. The "Cons" row is the constant factor of the instrument shown in the parenthesis (B: BAT, W: WAM).

	KW-BAT		KW-WAM		WAM-BAT		KW-WAM-BAT	
	a	b	a	b	a	b	a	b
α	0.92 ± 0.05	$-(0.11 \pm 0.05)$	1.06 ± 0.04	$-(0.01 \pm 0.04)$	0.93 ± 0.04	$-(0.17 \pm 0.04)$	1.00 ± 0.04	$-(0.09 \pm 0.03)$
E_{peak}	1.04 ± 0.03	$-(2 \pm 6)$	1.06 ± 0.02	1 ± 3	1.11 ± 0.03	$-(4 \pm 7)$	1.09 ± 0.03	$-(2 \pm 6)$
Cons	0.886 ± 0.009(B)		0.95 ± 0.01(W)		1.02 ± 0.02(W)		0.900 ± 0.009(B)	0.948 ± 0.011(W)

Table 7. The best fit parameters by a linear function between parameters in the Band function derived by the joint fit and the KW fit. For example, the linear function for α in the KW-BAT fits vs. the KW fit is $\alpha_{(\mathrm{KW-BAT})} = \mathrm{a} \times \alpha_{(\mathrm{KW})} + \mathrm{b}$. The "Cons" row is the constant factor of the instrument shown in the parenthesis (B: BAT, W: WAM).

	KW-BAT		KW-WAM		WAM-BAT		KW-WAM-BAT	
	a	b	a	b	a	b	a	b
α	0.87 ± 0.07	$-(0.20 \pm 0.06)$	0.97 ± 0.07	$-(0.06 \pm 0.05)$	0.87 ± 0.08	$-(0.26 \pm 0.05)$	0.90 ± 0.07	$-(0.20 \pm 0.05)$
E_{peak}	1.09 ± 0.04	$-(7 \pm 7)$	1.06 ± 0.02	$-(6 \pm 6)$	1.14 ± 0.04	$-(12 \pm 6)$	1.12 ± 0.03	$-(9 \pm 6)$
β	0.7 ± 0.2	$-(0.9 \pm 0.4)$	1.15 ± 0.19	0.3 ± 0.5	0.4 ± 0.3	$-(1.7 \pm 0.7)$	0.5 ± 0.2	$-(1.3 \pm 0.4)$
Cons	0.881 ± 0.009(B)		0.97 ± 0.01(W)		1.08 ± 0.02(W)		0.887 ± 0.008(B)	0.981 ± 0.012(W)

Table 8. Spectral parameters: 051008 Reg1

Instrument	Model	α	β	E_{peak} [keV]	C(WAM0)	C(WAM3)	C(BAT)	χ^2/dof
KW	PL	$-1.40^{+0.03}_{-0.03}$	-	-	-	-	-	215/73 (2.95)
KW	CPL	$-0.93^{+0.10}_{-0.09}$	-	803^{+175}_{-130}	-	-	-	77/72 (1.07)
KW	Band	$-0.86^{+0.17}_{-0.12}$	$-2.3^{+0.4}_{-1.3}$	671^{+206}_{-174}	-	-	-	73/71 (1.04)
WAM0	PL	$-1.66^{+0.03}_{-0.03}$	-	-	-	-	-	144/25 (5.79)
WAM0	CPL	$-1.02^{+0.15}_{-0.13}$	-	871^{+155}_{-117}	-	-	-	27/24 (1.13)
WAM0	Band	$-0.91^{+0.21}_{-0.18}$	$-2.6^{+0.3}_{-1.5}$	757^{+170}_{-128}	-	-	-	24/23 (1.05)
WAM3	PL	$-1.72^{+0.04}_{-0.04}$	-	-	-	-	-	111/25 (4.44)
WAM3	CPL	$-1.12^{+0.16}_{-0.14}$	-	783^{+147}_{-110}	-	-	-	23/24 (0.99)
WAM3	Band	$-1.07^{+0.25}_{-0.16}$	> -10	739^{+151}_{-159}	-	-	-	22/23 (0.98)
BAT	PL	$-1.02^{+0.05}_{-0.05}$	-	-	-	-	-	56/57 (1.00)
BAT	CPL	$-0.68^{+0.23}_{-0.22}$	-	244^{+315}_{-74}	-	-	-	49/56 (0.89)
BAT	Band	-	-	-	-	-	-	-
BAT+WAM0	PL	$-1.51^{+0.02}_{-0.03}$	-	-	$1.76^{+0.15}_{-0.11}$	-	-	482/83 (5.82)
BAT+WAM0	CPL	$-0.95^{+0.06}_{-0.06}$	-	821^{+94}_{-81}	$1.00^{+0.08}_{-0.07}$	-	-	81/82 (1.00)
BAT+WAM0	Band	$-0.93^{+0.06}_{-0.06}$	$-2.6^{+0.3}_{-1.1}$	764^{+101}_{-85}	$1.00^{+0.08}_{-0.07}$	-	-	77/81 (0.96)
BAT+WAM3	PL	$-1.54^{+0.02}_{-0.03}$	-	-	-	$1.88^{+0.17}_{-0.12}$	-	494/83 (5.96)
BAT+WAM3	CPL	$-0.94^{+0.06}_{-0.06}$	-	692^{+81}_{-68}	-	$1.08^{+0.09}_{-0.08}$	-	80/82 (0.98)
BAT+WAM3	Band	$-0.92^{+0.07}_{-0.07}$	$-2.6^{+0.4}_{-1.5}$	638^{+99}_{-87}	-	$1.08^{+0.08}_{-0.08}$	-	76/81 (0.95)
KW+BAT	PL	$-1.33^{+0.02}_{-0.02}$	-	-	-	-	$0.86^{+0.05}_{-0.06}$	384/131 (2.93)
KW+BAT	CPL	$-0.93^{+0.06}_{-0.06}$	-	801^{+135}_{-114}	-	-	$0.95^{+0.06}_{-0.06}$	131/130 (1.01)
KW+BAT	Band	$-0.90^{+0.07}_{-0.06}$	$-2.3^{+0.4}_{-1.5}$	711^{+159}_{-142}	-	-	$0.94^{+0.06}_{-0.05}$	127/129 (0.99)
KW+WAM0	PL	$-1.53^{+0.02}_{-0.02}$	-	-	$1.19^{+0.07}_{-0.06}$	-	-	456/99 (4.61)
KW+WAM0	CPL	$-0.95^{+0.08}_{-0.07}$	-	828^{+98}_{-80}	$0.95^{+0.05}_{-0.04}$	-	-	105/98 (1.07)
KW+WAM0	Band	$-0.90^{+0.09}_{-0.09}$	$-2.5^{+0.3}_{-0.6}$	739^{+104}_{-90}	$0.94^{+0.05}_{-0.04}$	-	-	98/97 (1.01)
KW+WAM3	PL	$-1.55^{+0.02}_{-0.02}$	-	-	-	$1.22^{+0.08}_{-0.06}$	-	464/99 (4.70)
KW+WAM3	CPL	$-0.94^{+0.08}_{-0.08}$	-	737^{+85}_{-71}	-	$0.96^{+0.05}_{-0.05}$	-	107/98 (1.10)
KW+WAM3	Band	$-0.86^{+0.12}_{-0.11}$	$-2.4^{+0.3}_{-0.7}$	635^{+111}_{-93}	-	$0.96^{+0.05}_{-0.05}$	-	100/97 (1.04)
KW+2WAM†+BAT	PL	$-1.53^{+0.02}_{-0.02}$	-	-	$1.19^{+0.07}_{-0.05}$	$1.19^{+0.07}_{-0.05}$	$0.65^{+0.03}_{-0.03}$	951/183 (5.20)
KW+2WAM†+BAT	CPL	$-0.95^{+0.05}_{-0.05}$	-	772^{+60}_{-53}	$0.95^{+0.05}_{-0.04}$	$0.96^{+0.05}_{-0.04}$	$0.93^{+0.05}_{-0.05}$	191/182 (1.05)
KW+2WAM†+BAT	Band	$-0.91^{+0.05}_{-0.05}$	$-2.6^{+0.3}_{-0.5}$	710^{+67}_{-62}	$0.95^{+0.04}_{-0.04}$	$0.96^{+0.05}_{-0.04}$	$0.94^{+0.05}_{-0.05}$	181/181 (1.00)

† The joint fit of two WAM spectra.

Table 9. Spectral parameters: 051008 Reg2

Instrument	Model	α	β	E_{peak} [keV]	C(WAM0)	C(WAM3)	χ^2/dof
KW	PL	$-1.45^{+0.11}_{-0.11}$	-	-	-	-	81/60 (1.36)
KW	CPL	$-0.95^{+0.44}_{-0.33}$	-	394^{+462}_{-142}	-	-	73/59 (1.24)
KW	Band	$-0.96^{+0.46}_{-0.20}$	-*	406^{+628}_{-115}	-	-	73/58 (1.26)
WAM0	PL	$-1.54^{+0.00}_{-0.12}$	-	-	-	-	43/23 (1.87)
WAM0	CPL	$-0.61^{+0.66}_{-0.53}$	-	604^{+350}_{-138}	-	-	31/22 (1.45)
WAM0	Band	$-0.62^{+1.78}_{-0.58}$	< -1.78	607^{+286}_{-283}	-	-	31/21 (1.51)
WAM3	PL	$-1.51^{+0.00}_{-0.13}$	-	-	-	-	19/23 (0.86)
WAM3	CPL	$-1.48^{+0.13}_{-0.14}$	-	-*	-	-	19/22 (0.90)
WAM3	Band	$-0.42^{+0.34}_{-14.66}$	$-1.58^{+0.16}_{-0.20}$	335^{+210}_{-184}	-	-	18/21 (0.89)
KW+WAM0	PL	$-1.49^{+0.08}_{-0.08}$	-	-	$1.31^{+0.24}_{-0.19}$	-	125/84 (1.49)
KW+WAM0	CPL	$-1.04^{+0.28}_{-0.23}$	-	672^{+396}_{-174}	$1.14^{+0.20}_{-0.16}$	-	110/83 (1.33)
KW+WAM0	Band	$-1.05^{+0.22}_{-0.23}$	-*	678^{+281}_{-180}	$1.14^{+0.20}_{-0.16}$	-	110/82 (1.34)
KW+WAM3	PL	$-1.47^{+0.08}_{-0.09}$	-	-	-	$1.36^{+0.25}_{-0.20}$	101/84 (1.21)
KW+WAM3	CPL	$-1.23^{+0.19}_{-0.09}$	-	> 650	-	$1.24^{+0.21}_{-0.18}$	98/83 (1.19)
KW+WAM3	Band	$-0.40^{+3.59}_{-0.88}$	$-1.58^{+0.11}_{-0.32}$	167^{+918}_{-105}	-	$1.26^{+0.23}_{-0.18}$	94/82 (1.16)
KW+2WAM†	PL	$-1.51^{+0.07}_{-0.07}$	-	-	$1.30^{+0.23}_{-0.18}$	$1.37^{+0.24}_{-0.19}$	144/106 (1.36)
KW+2WAM†	CPL	$-1.15^{+0.24}_{-0.16}$	-	876^{+742}_{-248}	$1.16^{+0.21}_{-0.16}$	$1.22^{+0.23}_{-0.17}$	133/105 (1.27)
KW+2WAM†	Band	$-1.06^{+0.35}_{-0.25}$	< -1.61	687^{+773}_{-322}	$1.15^{+0.21}_{-0.16}$	$1.21^{+0.22}_{-0.17}$	132/104 (1.28)

* The parameter is not constrained.

† The joint fit of two WAM spectra.

Table 10. Spectral parameters: 051008 Reg12

Instrument	Model	α	β	E_{peak} [keV]	C(WAM0)	C(WAM3)	χ^2/dof
KW	PL	$-1.43^{+0.04}_{-0.04}$	-	-	-	-	129/73 (1.77)
KW	CPL	$-0.91^{+0.17}_{-0.15}$	-	597^{+211}_{-126}	-	-	68/72 (0.96)
KW	Band	$-0.81^{+0.61}_{-0.20}$	$-2.12^{+0.40}_{-1.15}$	477^{+202}_{-248}	-	-	65/71 (0.92)
WAM0	PL	$-1.63^{+0.04}_{-0.04}$	-	-	-	-	101/25 (4.06)
WAM0	CPL	$-1.05^{+0.21}_{-0.24}$	-	885^{+262}_{-175}	-	-	41/24 (1.73)
WAM0	Band	$-0.83^{+0.55}_{-0.25}$	$-2.30^{+0.33}_{-0.71}$	671^{+218}_{-207}	-	-	37/23 (1.62)
WAM3	PL	$-1.66^{+0.05}_{-0.05}$	-	-	-	-	51/25 (2.06)
WAM3	CPL	$-1.24^{+0.15}_{-0.10}$	-	999^{+411}_{-196}	-	-	16/24 (0.69)
WAM3	Band	$-1.22^{+0.35}_{-0.12}$	< -1.99	965^{+418}_{-399}	-	-	16/23 (0.70)
KW+WAM0	PL	$-1.53^{+0.03}_{-0.03}$	-	-	$1.20^{+0.08}_{-0.07}$	-	261/99 (2.64)
KW+WAM0	CPL	$-1.02^{+0.11}_{-0.10}$	-	801^{+159}_{-119}	$1.00^{+0.07}_{-0.06}$	-	113/98 (1.16)
KW+WAM0	Band	$-0.92^{+0.15}_{-0.12}$	$-2.28^{+0.26}_{-0.53}$	664^{+141}_{-118}	$0.99^{+0.06}_{-0.06}$	-	106/97 (1.10)
KW+WAM3	PL	$-1.54^{+0.03}_{-0.03}$	-	-	-	$1.23^{+0.09}_{-0.07}$	218/99 (2.21)
KW+WAM3	CPL	$-1.07^{+0.11}_{-0.10}$	-	812^{+177}_{-131}	-	$1.05^{+0.07}_{-0.06}$	91/98 (0.94)
KW+WAM3	Band	$-0.92^{+0.20}_{-0.15}$	$-2.11^{+0.21}_{-0.47}$	588^{+181}_{-140}	-	$1.03^{+0.07}_{-0.06}$	85/97 (0.88)
KW+2WAM†	PL	$-1.57^{+0.02}_{-0.03}$	-	-	$1.24^{+0.09}_{-0.07}$	$1.27^{+0.09}_{-0.07}$	2.62 (1.24)
KW+2WAM†	CPL	$-1.08^{+0.09}_{-0.08}$	-	857^{+139}_{-110}	$1.02^{+0.07}_{-0.06}$	$1.05^{+0.07}_{-0.06}$	1.08 (1.02)
KW+2WAM†	Band	$-0.95^{+0.15}_{-0.12}$	$-2.25^{+0.22}_{-0.42}$	675^{+140}_{-117}	$1.00^{+0.06}_{-0.06}$	$1.02^{+0.07}_{-0.06}$	1.02 (1.00)

† The joint fit of two WAM spectra.

Table 11. Spectral parameters: 051221A Reg1

Instrument	Model	α	β	E_{peak} [keV]	C(WAM0)	C(WAM1)	C(BAT)	χ^2/dof
KW	PL	$-1.49^{+0.05}_{-0.05}$	-	-	-	-	-	54/37 (1.48)
KW	CPL	$-1.09^{+0.18}_{-0.16}$	-	455^{+200}_{-109}	-	-	-	30/36 (0.83)
KW	Band	$-0.84^{+0.76}_{-0.30}$	$-1.91^{+0.24}_{-2.37}$	258^{+228}_{-137}	-	-	-	27/35 (0.78)
WAM0	PL	$-1.56^{+0.00}_{-0.48}$	-	-	-	-	-	18/14 (1.35)
WAM0	CPL	$-1.54^{+0.42}_{-0.51}$	-	-*	-	-	-	18/13 (1.45)
WAM0	Band	-	-	-	-	-	-	-
WAM1	PL	$-1.98^{+0.00}_{-0.18}$	-	-	-	-	-	7/14 (0.51)
WAM1	CPL	$-2.04^{+0.54}_{-0.27}$	-	-*	-	-	-	7/13 (0.54)
WAM1	Band	-	-	-	-	-	-	-
BAT	PL	$-0.95^{+0.05}_{-0.05}$	-	-	-	-	-	68/57 (1.20)
BAT	CPL	$-0.67^{+0.24}_{-0.22}$	-	284^{+687}_{-101}	-	-	-	63/56 (1.14)
BAT	Band	-	-	-	-	-	-	-
BAT+WAM0	PL	$-0.96^{+0.05}_{-0.05}$	-	-	$0.06^{+0.02}_{-0.02}$	-	-	94/72 (1.31)
BAT+WAM0	CPL	$-0.78^{+0.19}_{-0.15}$	-	431^{+1124}_{-188}	$0.15^{+0.06}_{-0.05}$	-	-	85/71 (1.21)
BAT+WAM0	Band	$-0.67^{+0.29}_{-0.21}$	< -1.12	282^{+491}_{-121}	$0.15^{+0.06}_{-0.06}$	-	-	82/70 (1.18)
BAT+WAM1	PL	$-1.09^{+0.05}_{-0.06}$	-	-	-	$0.10^{+0.02}_{-0.01}$	-	201/72 (2.79)
BAT+WAM1	CPL	$-0.72^{+0.10}_{-0.09}$	-	324^{+91}_{-63}	-	$0.19^{+0.03}_{-0.03}$	-	81/71 (1.15)
BAT+WAM1	Band	$-0.57^{+0.19}_{-0.15}$	$-2.07^{+0.22}_{-0.38}$	225^{+79}_{-54}	-	$0.22^{+0.04}_{-0.04}$	-	72/70 (1.03)
KW+BAT	PL	$-1.22^{+0.04}_{-0.04}$	-	-	-	-	$1.24^{+0.16}_{-0.15}$	258/95 (2.72)
KW+BAT	CPL	$-0.78^{+0.09}_{-0.09}$	-	346^{+75}_{-59}	-	-	$0.94^{+0.09}_{-0.08}$	103/94 (1.10)
KW+BAT	Band	$-0.59^{+0.20}_{-0.16}$	$-1.92^{+0.18}_{-0.37}$	220^{+82}_{-51}	-	-	$0.90^{+0.09}_{-0.07}$	93/93 (1.01)
KW+WAM0	PL	$-1.49^{+0.05}_{-0.05}$	-	-	$0.19^{+0.05}_{-0.04}$	-	-	73/52 (1.42)
KW+WAM0	CPL	$-1.11^{+0.18}_{-0.15}$	-	481^{+219}_{-120}	$0.17^{+0.04}_{-0.04}$	-	-	50/51 (1.00)
KW+WAM0	Band	$-0.73^{+0.76}_{-0.42}$	$-1.81^{+0.16}_{-0.40}$	213^{+272}_{-100}	$0.18^{+0.05}_{-0.05}$	-	-	47/50 (0.94)
KW+WAM1	PL	$-1.55^{+0.05}_{-0.05}$	-	-	-	$0.22^{+0.03}_{-0.03}$	-	87/52 (1.68)
KW+WAM1	CPL	$-1.09^{+0.16}_{-0.15}$	-	421^{+127}_{-81}	-	$0.19^{+0.02}_{-0.02}$	-	45/51 (0.89)
KW+WAM1	Band	$-0.74^{+0.52}_{-0.29}$	$-1.96^{+0.16}_{-0.28}$	228^{+109}_{-82}	-	$0.20^{+0.03}_{-0.02}$	-	36/50 (0.72)
KW+2WAM†+BAT	PL	$-1.29^{+0.04}_{-0.04}$	-	-	$0.16^{+0.04}_{-0.04}$	$0.17^{+0.02}_{-0.02}$	$1.07^{+0.11}_{-0.12}$	355/125 (2.84)
KW+2WAM†+BAT	CPL	$-0.79^{+0.08}_{-0.08}$	-	349^{+59}_{-48}	$0.16^{+0.04}_{-0.04}$	$0.18^{+0.02}_{-0.02}$	$0.94^{+0.09}_{-0.08}$	142/124 (1.15)
KW+2WAM†+BAT	Band	$-0.58^{+0.18}_{-0.15}$	$-1.95^{+0.14}_{-0.22}$	216^{+62}_{-45}	$0.17^{+0.05}_{-0.04}$	$0.20^{+0.02}_{-0.02}$	$0.89^{+0.08}_{-0.07}$	122/123 (0.99)

* The parameter is not constrained.

† The joint fit of two WAM spectra.

Table 12. Spectral parameters: 060105 Reg1

Instrument	Model	α	β	E_{peak} [keV]	C(WAM0)	C(WAM3)	C(BAT)	χ^2/dof
KW	PL	-1.35	-	-	-	-	-	894/62 (14.44)
KW	CPL	$-0.65^{+0.06}_{-0.06}$	-	567^{+37}_{-32}	-	-	-	69/61 (1.13)
KW	Band	$-0.65^{+0.06}_{-0.06}$	-*	569^{+36}_{-32}	-	-	-	69/60 (1.15)
WAM0	PL	$-1.64^{+0.00}_{-0.15}$	-	-	-	-	-	15/14 (1.12)
WAM0	CPL	$-0.69^{+0.82}_{-0.67}$	-	724^{+583}_{-165}	-	-	-	9/13 (0.76)
WAM0	Band	$-0.64^{+1.08}_{-0.69}$	< -1.81	692^{+305}_{-251}	-	-	-	9/12 (0.81)
WAM3	PL	$-2.10^{+0.09}_{-0.09}$	-	-	-	-	-	19/14 (1.39)
WAM3	CPL	$-1.44^{+0.45}_{-0.38}$	-	360^{+80}_{-111}	-	-	-	9/13 (0.71)
WAM3	Band	$-1.23^{+6.23}_{-0.57}$	< -2.18	334^{+104}_{-162}	-	-	-	9/12 (0.75)
BAT	PL	$-0.94^{+0.04}_{-0.04}$	-	-	-	-	-	42/57 (0.74)
BAT	CPL	-	-	-	-	-	-	-
BAT	Band	-	-	-	-	-	-	-
BAT+WAM0	PL	$-0.99^{+0.04}_{-0.04}$	-	-	$0.39^{+0.07}_{-0.06}$	-	-	116/72 (1.62)
BAT+WAM0	CPL	$-0.86^{+0.06}_{-0.05}$	-	814^{+268}_{-181}	$0.88^{+0.15}_{-0.13}$	-	-	55/71 (0.78)
BAT+WAM0	Band	$-0.86^{+0.06}_{-0.05}$	-*	812^{+312}_{-189}	$0.88^{+0.15}_{-0.13}$	-	-	55/70 (0.79)
BAT+WAM3	PL	$-1.08^{+0.04}_{-0.05}$	-	-	-	$0.95^{+0.18}_{-0.14}$	-	417/72 (5.79)
BAT+WAM3	CPL	$-0.75^{+0.06}_{-0.06}$	-	394^{+52}_{-44}	-	$3.43^{+0.40}_{-0.37}$	-	67/71 (0.95)
BAT+WAM3	Band	$-0.72^{+0.08}_{-0.07}$	< -2.38	354^{+65}_{-58}	-	$3.59^{+0.47}_{-0.42}$	-	64/70 (0.93)
KW+BAT	PL	$-1.31^{+0.01}_{-0.01}$	-	-	-	-	$0.78^{+0.03}_{-0.03}$	1168/120 (9.74)
KW+BAT	CPL	$-0.74^{+0.04}_{-0.04}$	-	606^{+36}_{-33}	-	-	$0.88^{+0.03}_{-0.03}$	130/119 (1.10)
KW+BAT	Band	$-0.74^{+0.04}_{-0.02}$	-*	613^{+36}_{-33}	-	-	$0.88^{+0.03}_{-0.03}$	131/118 (1.11)
KW+WAM0	PL	$-1.36^{+0.00}_{+0.00}$	-	-	0.83	-	-	922/77 (11.98)
KW+WAM0	CPL	$-0.66^{+0.06}_{-0.05}$	-	576^{+35}_{-32}	$0.79^{+0.08}_{-0.08}$	-	-	81/76 (1.08)
KW+WAM0	Band	$-0.66^{+0.03}_{-0.05}$	-*	577^{+35}_{-32}	$0.79^{+0.08}_{-0.08}$	-	-	81/75 (1.09)
KW+WAM3	PL	-1.37	-	-	-	1.76	-	1111/77 (14.43)
KW+WAM3	CPL	$-0.62^{+0.06}_{-0.06}$	-	533^{+30}_{-27}	-	$2.06^{+0.13}_{-0.13}$	-	114/76 (1.50)
KW+WAM3	Band	$-0.63^{+0.04}_{-0.05}$	-*	538^{+30}_{-27}	-	$2.07^{+0.13}_{-0.13}$	-	114/75 (1.52)
KW+2WAM†+BAT	PL	$-1.33^{+0.01}_{-0.01}$	-	-	$0.80^{+0.13}_{-0.08}$	$1.63^{+0.13}_{-0.11}$	$0.76^{+0.03}_{-0.03}$	1435/150 (9.57)
KW+2WAM†+BAT	CPL	$-0.72^{+0.04}_{-0.04}$	-	574^{+31}_{-28}	$0.81^{+0.08}_{-0.08}$	$2.07^{+0.13}_{-0.13}$	$0.87^{+0.03}_{-0.03}$	193/149 (1.30)
KW+2WAM†+BAT	Band	$-0.72^{+0.04}_{-0.02}$	-*	575^{+29}_{-19}	$0.81^{+0.08}_{-0.08}$	$2.07^{+0.07}_{-0.13}$	$0.87^{+0.02}_{-0.02}$	193/148 (1.31)

* The parameter is not constrained.

† The joint fit of two WAM spectra.

Table 13. Spectral parameters: 060105 Reg2

Instrument	Model	α	β	E_{peak} [keV]	C(WAM0)	C(WAM3)	C(BAT)	χ^2/dof
KW	PL	-1.61	-	-	-	-	-	626/62 (10.11)
KW	CPL	$-0.60^{+0.10}_{-0.09}$	-	228^{+13}_{-12}	-	-	-	50/61 (0.83)
KW	Band	$-0.57^{+0.11}_{-0.10}$	< -2.79	222^{+15}_{-14}	-	-	-	47/60 (0.80)
WAM0	PL	$-2.27^{+0.34}_{-0.43}$	-	-	-	-	-	18/14 (1.32)
WAM0	CPL	$-1.70^{+4.23}_{-0.54}$	-	$-^{*}$	-	-	-	18/13 (1.40)
WAM0	Band	$-^{*}$	$-2.55^{+0.54}_{-1.15}$	185^{+52}_{-164}	-	-	-	17/12 (1.44)
WAM3	PL	$-2.52^{+0.19}_{-0.21}$	-	-	-	-	-	20/14 (1.49)
WAM3	CPL	$-0.96^{+2.01}_{-1.13}$	-	197^{+60}_{-197}	-	-	-	15/13 (1.16)
WAM3	Band	$-0.63^{+5.63}_{-1.13}$	< -2.58	202^{+52}_{-111}	-	-	-	14/12 (1.21)
BAT	PL	$-1.11^{+0.04}_{-0.04}$	-	-	-	-	-	53/57 (0.93)
BAT	CPL	$-0.92^{+0.15}_{-0.14}$	-	362^{+799}_{-130}	-	-	-	48/56 (0.86)
BAT	Band	-	-	-	-	-	-	-
BAT+WAM0	PL	$-1.12^{+0.04}_{-0.04}$	-	-	$0.24^{+0.06}_{-0.06}$	-	-	108/72 (1.50)
BAT+WAM0	CPL	$-0.87^{+0.11}_{-0.10}$	-	297^{+132}_{-73}	$0.87^{+0.25}_{-0.21}$	-	-	67/71 (0.95)
BAT+WAM0	Band	$-0.86^{+0.12}_{-0.10}$	< -2.03	289^{+128}_{-71}	$0.88^{+0.25}_{-0.21}$	-	-	66/70 (0.96)
BAT+WAM3	PL	$-1.14^{+0.04}_{-0.04}$	-	-	-	$0.49^{+0.10}_{-0.09}$	-	229/72 (3.19)
BAT+WAM3	CPL	$-0.79^{+0.09}_{-0.08}$	-	233^{+44}_{-33}	-	$2.99^{+0.53}_{-0.48}$	-	66/71 (0.94)
BAT+WAM3	Band	$-0.79^{+0.09}_{-0.08}$	$\pm\infty$	233^{+44}_{-33}	-	$2.99^{+0.53}_{-0.25}$	-	66/70 (0.95)
KW+BAT	PL	$-1.49^{+0.02}_{-0.02}$	-	-	-	-	$0.92^{+0.03}_{-0.04}$	1103/120 (9.20)
KW+BAT	CPL	$-0.75^{+0.05}_{-0.05}$	-	239^{+14}_{-12}	-	-	$0.87^{+0.03}_{-0.03}$	110/119 (0.93)
KW+BAT	Band	$-0.74^{+0.06}_{-0.06}$	< -2.87	237^{+14}_{-14}	-	-	$0.87^{+0.03}_{-0.03}$	109/118 (0.92)
KW+WAM0	PL	$-1.61^{+0.02}_{-0.02}$	-	-	$0.78^{+0.16}_{-0.15}$	-	-	656/77 (8.53)
KW+WAM0	CPL	$-0.61^{+0.10}_{-0.09}$	-	229^{+13}_{-11}	$0.83^{+0.15}_{-0.15}$	-	-	69/76 (0.91)
KW+WAM0	Band	$-0.57^{+0.11}_{-0.10}$	$-3.22^{+0.45}_{-1.90}$	221^{+14}_{-14}	$0.83^{+0.15}_{-0.15}$	-	-	65/75 (0.88)
KW+WAM3	PL	$-1.62^{+0.02}_{-0.02}$	-	-	-	$1.85^{+0.25}_{-0.22}$	-	721/77 (9.37)
KW+WAM3	CPL	$-0.60^{+0.10}_{-0.09}$	-	227^{+12}_{-11}	-	$2.47^{+0.26}_{-0.26}$	-	66/76 (0.87)
KW+WAM3	Band	$-0.56^{+0.11}_{-0.10}$	$-3.37^{+0.48}_{-2.84}$	221^{+14}_{-13}	-	$2.46^{+0.26}_{-0.26}$	-	63/75 (0.84)
KW+2WAM†+BAT	PL	$-1.50^{+0.02}_{-0.02}$	-	-	$0.67^{+0.14}_{-0.13}$	$1.49^{+0.20}_{-0.18}$	$0.91^{+0.03}_{-0.04}$	1253/150 (8.36)
KW+2WAM†+BAT	CPL	$-0.74^{+0.05}_{-0.05}$	-	237^{+13}_{-12}	$0.84^{+0.15}_{-0.15}$	$2.48^{+0.26}_{-0.26}$	$0.87^{+0.03}_{-0.03}$	145/149 (0.97)
KW+2WAM†+BAT	Band	$-0.73^{+0.06}_{-0.05}$	< -2.96	234^{+13}_{-13}	$0.85^{+0.15}_{-0.15}$	$2.48^{+0.26}_{-0.26}$	$0.87^{+0.03}_{-0.03}$	143/148 (0.97)

* The parameter is not constrained.

† The joint fit of two WAM spectra.

Table 14. Spectral parameters: 060105 Reg12

Instrument	Model	α	β	E_{peak} [keV]	C(WAM0)	C(WAM3)	C(BAT)	χ^2/dof
KW	PL	-1.45	-	-	-	-	-	1043/62 (16.84)
KW	CPL	$-0.78^{+0.05}_{-0.05}$	-	424^{+24}_{-22}	-	-	-	61/61 (1.00)
KW	Band	$-0.74^{+0.07}_{-0.06}$	$-2.80^{+0.34}_{-0.80}$	398^{+29}_{-31}	-	-	-	57/60 (0.95)
WAM0	PL	$-1.81^{+0.00}_{-0.15}$	-	-	-	-	-	12/14 (0.88)
WAM0	CPL	$-1.30^{+0.70}_{-0.58}$	-	> 495	-	-	-	10/13 (0.78)
WAM0	Band	$-1.27^{+6.27}_{-8.73}$	< -1.75	-*	-	-	-	10/12 (0.84)
WAM3	PL	$-2.24^{+0.09}_{-0.09}$	-	-	-	-	-	27/14 (1.98)
WAM3	CPL	$-1.52^{+0.49}_{-0.39}$	-	256^{+66}_{-154}	-	-	-	15/13 (1.23)
WAM3	Band	$-1.04^{+1.94}_{-3.49}$	< -2.60	255^{+114}_{-34}	-	-	-	15/12 (1.25)
BAT	PL	$-1.03^{+0.03}_{-0.03}$	-	-	-	-	-	40/57 (0.70)
BAT	CPL	-	-	-	-	-	-	-
BAT	Band	-	-	-	-	-	-	-
BAT+WAM0	PL	$-1.06^{+0.03}_{-0.03}$	-	-	$0.34^{+0.05}_{-0.04}$	-	-	132/72 (1.84)
BAT+WAM0	CPL	$-0.92^{+0.05}_{-0.05}$	-	611^{+189}_{-131}	$0.82^{+0.13}_{-0.12}$	-	-	52/71 (0.74)
BAT+WAM0	Band	$-0.91^{+0.07}_{-0.05}$	< -1.91	588^{+106}_{-172}	$0.83^{+0.14}_{-0.12}$	-	-	52/70 (0.75)
BAT+WAM3	PL	$-1.12^{+0.03}_{-0.03}$	-	-	-	$0.76^{+0.11}_{-0.09}$	-	516/72 (7.17)
BAT+WAM3	CPL	$-0.79^{+0.05}_{-0.05}$	-	321^{+38}_{-33}	-	$3.19^{+0.33}_{-0.30}$	-	71/71 (1.01)
BAT+WAM3	Band	$-0.77^{+0.06}_{-0.06}$	< -2.58	297^{+42}_{-37}	-	$3.30^{+0.35}_{-0.33}$	-	68/70 (0.98)
KW+BAT	PL	-1.39	-	-	-	-	0.84	1527/120 (12.73)
KW+BAT	CPL	$-0.83^{+0.03}_{-0.03}$	-	440^{+23}_{-21}	-	-	$0.88^{+0.02}_{-0.02}$	109/119 (0.92)
KW+BAT	Band	$-0.82^{+0.04}_{-0.04}$	< -2.61	427^{+32}_{-26}	-	-	$0.88^{+0.02}_{-0.02}$	109/118 (0.93)
KW+WAM0	PL	-1.45	-	-	0.80	-	-	1075/77 (13.96)
KW+WAM0	CPL	$-0.79^{+0.05}_{-0.05}$	-	430^{+24}_{-22}	$0.81^{+0.08}_{-1.08}$	-	-	76/76 (1.00)
KW+WAM0	Band	$-0.74^{+0.07}_{-0.06}$	$-2.73^{+0.31}_{-0.62}$	399^{+30}_{-32}	$0.81^{+0.08}_{-0.07}$	-	-	70/75 (0.95)
KW+WAM3	PL	-1.47	-	-	-	1.77	-	1306/77 (16.96)
KW+WAM3	CPL	$-0.75^{+0.05}_{-0.05}$	-	403^{+20}_{-19}	-	$2.23^{+0.13}_{-0.13}$	-	102/76 (1.35)
KW+WAM3	Band	$-0.70^{+0.07}_{-0.06}$	$-2.86^{+0.30}_{-0.56}$	377^{+25}_{-25}	-	$2.23^{+0.13}_{-0.13}$	-	97/75 (1.30)
KW+2WAM†+BAT	PL	-1.41	-	-	0.75	1.60	0.82	1859/150 (12.40)
KW+2WAM†+BAT	CPL	$-0.82^{+0.03}_{-0.03}$	-	424^{+20}_{-18}	$0.82^{+0.08}_{-0.08}$	$2.22^{+0.13}_{-0.13}$	$0.88^{+0.02}_{-0.02}$	170/149 (1.14)
KW+2WAM†+BAT	Band	$-0.80^{+0.04}_{-0.04}$	< -2.66	408^{+28}_{-22}	$0.82^{+0.08}_{-0.08}$	$2.23^{+0.13}_{-0.13}$	$0.88^{+0.02}_{-0.02}$	168/148 (1.14)

* The parameter is not constrained.

† The joint fit of two WAM spectra.

Table 15. Spectral parameters: 060117 Reg1

Instrument	Model	α	β	$E_{\rm peak}$ [keV]	C(WAM0)	C(WAM1)	C(BAT)	χ^2/dof
KW	PL	$-2.02^{+0.03}_{-0.03}$	-	-	-	-	-	135/61 (2.22)
KW	CPL	$-1.59^{+0.12}_{-0.11}$	-	98^{+12}_{-10}	-	-	-	73/60 (1.22)
KW	Band	$-1.51^{+0.18}_{-0.17}$	< -2.41	92^{+15}_{-11}	-	-	-	72/59 (1.23)
WAM0	PL	$-2.41^{+0.14}_{-0.16}$	-	-	-	-	-	29/22 (1.33)
WAM0	CPL	-	-	-	-	-	-	-
WAM0	Band	-	-	-	-	-	-	-
WAM1	PL	$-2.32^{+0.11}_{-0.12}$	-	-	-	-	-	26/22 (1.19)
WAM1	CPL	-	-	-	-	-	-	-
WAM1	Band	-	-	-	-	-	-	-
BAT	PL	$-1.85^{+0.04}_{-0.04}$	-	-	-	-	-	61/57 (1.07)
BAT	CPL	$-1.45^{+0.18}_{-0.17}$	-	76^{+18}_{-9}	-	-	-	44/56 (0.80)
BAT	Band	$-1.10^{+0.75}_{-0.40}$	$-2.04^{+0.11}_{-0.55}$	56^{+23}_{-14}	-	-	-	42/55 (0.76)
BAT+WAM0	PL	$-1.90^{+0.04}_{-0.04}$	-	-	$0.79^{+0.07}_{-0.06}$	-	-	132/80 (1.66)
BAT+WAM0	CPL	$-1.69^{+0.08}_{-0.08}$	-	108^{+28}_{-18}	$0.98^{+0.11}_{-0.10}$	-	-	89/79 (1.13)
BAT+WAM0	Band	$-1.43^{+0.26}_{-0.18}$	$-2.40^{+0.16}_{-0.18}$	75^{+16}_{-12}	$1.15^{+0.14}_{-0.13}$	-	-	73/78 (0.95)
BAT+WAM1	PL	$-1.92^{+0.04}_{-0.04}$	-	-	-	$0.76^{+0.06}_{-0.05}$	-	138/80 (1.73)
BAT+WAM1	CPL	$-1.72^{+0.07}_{-0.06}$	-	122^{+27}_{-20}	-	$0.85^{+0.07}_{-0.07}$	-	79/79 (1.01)
BAT+WAM1	Band	$-1.39^{+0.32}_{-0.21}$	$-2.31^{+0.12}_{-0.13}$	72^{+19}_{-12}	-	$1.01^{+0.10}_{-0.10}$	-	70/78 (0.91)
KW+BAT	PL	$-1.95^{+0.03}_{-0.03}$	-	-	-	-	$1.00^{+0.04}_{-0.04}$	224/119 (1.88)
KW+BAT	CPL	$-1.59^{+0.08}_{-0.08}$	-	94^{+11}_{-8}	-	-	$0.95^{+0.04}_{-0.04}$	121/118 (1.03)
KW+BAT	Band	$-1.53^{+0.13}_{-0.10}$	< -2.42	87^{+7}_{-10}	-	-	$0.95^{+0.04}_{-0.04}$	119/117 (1.02)
KW+WAM0	PL	$-2.04^{+0.03}_{-0.03}$	-	-	$0.97^{+0.08}_{-0.07}$	-	-	184/84 (2.20)
KW+WAM0	CPL	$-1.67^{+0.10}_{-0.09}$	-	102^{+13}_{-13}	$0.97^{+0.08}_{-0.07}$	-	-	115/83 (1.39)
KW+WAM0	Band	$-1.48^{+0.20}_{-0.16}$	$-2.50^{+0.14}_{-0.22}$	88^{+12}_{-11}	$1.02^{+0.09}_{-0.08}$	-	-	103/82 (1.26)
KW+WAM1	PL	$-2.05^{+0.03}_{-0.03}$	-	-	-	$0.90^{+0.06}_{-0.06}$	-	182/84 (2.17)
KW+WAM1	CPL	$-1.72^{+0.08}_{-0.08}$	-	107^{+15}_{-15}	-	$0.86^{+0.06}_{-0.05}$	-	107/83 (1.30)
KW+WAM1	Band	$-1.48^{+0.21}_{-0.18}$	$-2.41^{+0.10}_{-0.19}$	87^{+16}_{-11}	-	$0.92^{+0.07}_{-0.07}$	-	102/82 (1.25)
KW+2WAM†+BAT	PL	$-1.99^{+0.02}_{-0.03}$	-	-	$0.90^{+0.06}_{-0.06}$	$0.83^{+0.05}_{-0.05}$	$0.98^{+0.04}_{-0.04}$	345/169 (2.04)
KW+2WAM†+BAT	CPL	$-1.70^{+0.05}_{-0.05}$	-	108^{+12}_{-11}	$0.94^{+0.07}_{-0.06}$	$0.86^{+0.05}_{-0.05}$	$0.96^{+0.04}_{-0.03}$	205/168 (1.22)
KW+2WAM†+BAT	Band	$-1.48^{+0.14}_{-0.12}$	$-2.39^{+0.08}_{-0.11}$	82^{+11}_{-9}	$1.04^{+0.08}_{-0.08}$	$0.94^{+0.07}_{-0.06}$	$0.96^{+0.04}_{-0.04}$	184/167 (1.11)

† The joint fit of two WAM spectra.

Table 16. Spectral parameters: 060117 Reg2

Instrument	Model	α	β	E_{peak} [keV]	C(WAM0)	C(WAM1)	C(BAT)	χ^2/dof
KW	PL	$-1.98^{+0.02}_{-0.02}$	-	-	-	-	-	335/60 (5.60)
KW	CPL	$-1.35^{+0.08}_{-0.08}$	-	109^{+6}_{-6}	-	-	-	58/59 (0.99)
KW	Band	$-1.32^{+0.10}_{-0.09}$	$-3.05^{+0.34}_{-0.71}$	106^{+7}_{-7}	-	-	-	53/58 (0.92)
WAM0	PL	$-2.70^{+0.10}_{-0.10}$	-	-	-	-	-	20/22 (0.95)
WAM0	CPL	-	-	-	-	-	-	-
WAM0	Band	-	-	-	-	-	-	-
WAM1	PL	$-2.53^{+0.07}_{-0.07}$	-	-	-	-	-	31/22 (1.43)
WAM1	CPL	$-1.91^{+0.36}_{-0.10}$	-	< 118	-	-	-	18/21 (0.90)
WAM1	Band	$-1.09^{+3.09}_{-1.20}$	$-2.88^{+0.20}_{-0.31}$	139^{+29}_{-76}	-	-	-	16/20 (0.83)
BAT	PL	$-1.74^{+0.03}_{-0.03}$	-	-	-	-	-	75/57 (1.33)
BAT	CPL	$-1.30^{+0.14}_{-0.13}$	-	94^{+16}_{-9}	-	-	-	41/56 (0.74)
BAT	Band	$-1.30^{+0.14}_{-0.13}$	< -2.08	94^{+16}_{-9}	-	-	-	41/55 (0.76)
BAT+WAM0	PL	$-1.89^{+0.03}_{-0.03}$	-	-	$0.71^{+0.05}_{-0.04}$	-	-	434/80 (5.43)
BAT+WAM0	CPL	$-1.44^{+0.06}_{-0.06}$	-	110^{+9}_{-8}	$0.97^{+0.07}_{-0.06}$	-	-	81/79 (1.03)
BAT+WAM0	Band	$-1.26^{+0.13}_{-0.12}$	$-2.75^{+0.13}_{-0.21}$	91^{+11}_{-8}	$1.09^{+0.10}_{-0.10}$	-	-	64/78 (0.83)
BAT+WAM1	PL	$-1.93^{+0.02}_{-0.03}$	-	-	-	$0.73^{+0.05}_{-0.04}$	-	471/80 (5.90)
BAT+WAM1	CPL	$-1.49^{+0.05}_{-0.05}$	-	122^{+9}_{-9}	-	$0.83^{+0.05}_{-0.04}$	-	70/79 (0.89)
BAT+WAM1	Band	$-1.43^{+0.09}_{-0.07}$	$-2.83^{+0.21}_{-0.36}$	112^{+11}_{-12}	-	$0.86^{+0.06}_{-0.05}$	-	62/78 (0.80)
KW+BAT	PL	$-1.91^{+0.02}_{-0.02}$	-	-	-	-	$1.04^{+0.03}_{-0.03}$	523/118 (4.43)
KW+BAT	CPL	$-1.37^{+0.06}_{-0.06}$	-	107^{+6}_{-5}	-	-	$0.97^{+0.03}_{-0.03}$	102/117 (0.88)
KW+BAT	Band	$-1.34^{+0.08}_{-0.06}$	$-3.01^{+0.33}_{-0.66}$	103^{+6}_{-7}	-	-	$0.97^{+0.03}_{-0.03}$	97/116 (0.84)
KW+WAM0	PL	$-2.03^{+0.02}_{-0.02}$	-	-	$0.93^{+0.05}_{-0.04}$	-	-	548/83 (6.61)
KW+WAM0	CPL	$-1.40^{+0.06}_{-0.06}$	-	111^{+6}_{-5}	$0.93^{+0.05}_{-0.04}$	-	-	97/82 (1.19)
KW+WAM0	Band	$-1.28^{+0.12}_{-0.10}$	$-2.84^{+0.16}_{-0.27}$	102^{+8}_{-7}	$0.97^{+0.06}_{-0.05}$	-	-	79/81 (0.98)
KW+WAM1	PL	$-2.05^{+0.02}_{-0.02}$	-	-	-	$0.89^{+0.04}_{-0.04}$	-	557/83 (6.72)
KW+WAM1	CPL	$-1.46^{+0.06}_{-0.06}$	-	116^{+6}_{-6}	-	$0.83^{+0.04}_{-0.03}$	-	92/82 (1.12)
KW+WAM1	Band	$-1.38^{+0.09}_{-0.07}$	$-2.87^{+0.18}_{-0.25}$	110^{+6}_{-7}	-	$0.85^{+0.04}_{-0.04}$	-	76/81 (0.95)
KW+2WAM†+BAT	PL	$-2.00^{+0.01}_{-0.02}$	-	-	$0.88^{+0.04}_{-0.04}$	$0.83^{+0.04}_{-0.03}$	$1.01^{+0.03}_{-0.03}$	1055/168 (6.28)
KW+2WAM†+BAT	CPL	$-1.45^{+0.04}_{-0.04}$	-	115^{+5}_{-5}	$0.92^{+0.04}_{-0.04}$	$0.84^{+0.03}_{-0.03}$	$0.97^{+0.03}_{-0.03}$	175/167 (1.05)
KW+2WAM†+BAT	Band	$-1.37^{+0.08}_{-0.06}$	$-2.83^{+0.14}_{-0.19}$	105^{+6}_{-7}	$0.95^{+0.05}_{-0.05}$	$0.87^{+0.04}_{-0.04}$	$0.97^{+0.03}_{-0.03}$	148/166 (0.89)

† The joint fit of two WAM spectra.

Table 17. Spectral parameters: 060117 Reg3

Instrument	Model	α	β	E_{peak} [keV]	C(WAM0)	C(WAM1)	C(BAT)	χ^2/dof
KW	PL	$-2.31^{+0.05}_{-0.05}$	-	-	-	-	-	107/60 (1.79)
KW	CPL	$-1.79^{+0.18}_{-0.17}$	-	32^{+12}_{-22}	-	-	-	67/59 (1.14)
KW	Band	$-1.77^{+0.19}_{-0.15}$	$-3.62^{+6.28}_{-0.83}$	33^{+12}_{-16}	-	-	-	67/58 (1.16)
WAM0	PL	$-2.95^{+0.28}_{-0.32}$	-	-	-	-	-	29/22 (1.33)
WAM0	CPL	-	-	-	-	-	-	-
WAM0	Band	-	-	-	-	-	-	-
WAM1	PL	$-2.73^{+0.22}_{-0.25}$	-	-	-	-	-	35/22 (1.62)
WAM1	CPL	-	-	-	-	-	-	-
WAM1	Band	-	-	-	-	-	-	-
BAT	PL	$-2.11^{+0.04}_{-0.04}$	-	-	-	-	-	82/57 (1.45)
BAT	CPL	$-1.60^{+0.20}_{-0.19}$	-	41^{+5}_{-8}	-	-	-	60/56 (1.08)
BAT	Band	$-0.98^{+1.17}_{-0.42}$	$-2.33^{+0.10}_{-0.14}$	38^{+4}_{-5}	-	-	-	53/55 (0.97)
BAT+WAM0	PL	$-2.14^{+0.04}_{-0.04}$	-	-	$0.86^{+0.10}_{-0.09}$	-	-	141/80 (1.77)
BAT+WAM0	CPL	$-1.77^{+0.14}_{-0.13}$	-	36^{+8}_{-13}	$1.35^{+0.24}_{-0.20}$	-	-	98/79 (1.24)
BAT+WAM0	Band	$-0.95^{+0.86}_{-0.09}$	$-2.50^{+0.33}_{-0.39}$	40^{+5}_{-8}	$1.27^{+0.26}_{-0.24}$	-	-	93/78 (1.20)
BAT+WAM1	PL	$-2.14^{+0.04}_{-0.04}$	-	-	-	$0.68^{+0.07}_{-0.06}$	-	142/80 (1.78)
BAT+WAM1	CPL	$-1.85^{+0.11}_{-0.10}$	-	31^{+11}_{-17}	-	$0.93^{+0.13}_{-0.11}$	-	104/79 (1.32)
BAT+WAM1	Band	$-0.93^{+0.73}_{-0.82}$	$-2.46^{+0.12}_{-0.48}$	40^{+6}_{-4}	-	$0.95^{+0.22}_{-0.15}$	-	95/78 (1.22)
KW+BAT	PL	$-2.21^{+0.03}_{-0.03}$	-	-	-	-	$0.97^{+0.04}_{-0.04}$	216/118 (1.83)
KW+BAT	CPL	$-1.70^{+0.12}_{-0.12}$	-	38^{+6}_{-8}	-	-	$0.93^{+0.04}_{-0.04}$	129/117 (1.10)
KW+BAT	Band	$-1.01^{+0.10}_{-0.17}$	$-2.51^{+0.78}_{-6.39}$	40^{+6}_{-8}	-	-	$0.94^{+0.04}_{-0.04}$	139/116 (1.20)
KW+WAM0	PL	$-2.33^{+0.05}_{-0.05}$	-	-	$1.13^{+0.13}_{-0.12}$	-	-	152/83 (1.84)
KW+WAM0	CPL	$-1.86^{+0.15}_{-0.14}$	-	25^{+15}_{-22}	$1.27^{+0.17}_{-0.14}$	-	-	101/82 (1.24)
KW+WAM0	Band	$-1.77^{+0.23}_{-0.15}$	$-3.13^{+0.33}_{-0.69}$	33^{+12}_{-19}	$1.33^{+0.19}_{-0.16}$	-	-	97/81 (1.21)
KW+WAM1	PL	$-2.33^{+0.05}_{-0.05}$	-	-	-	$0.88^{+0.09}_{-0.08}$	-	153/83 (1.85)
KW+WAM1	CPL	$-1.92^{+0.13}_{-0.08}$	-	17^{+18}_{-15}	-	$0.93^{+0.10}_{-0.09}$	-	107/82 (1.31)
KW+WAM1	Band	$-1.57^{+0.53}_{-0.04}$	< -2.56	40^{+16}_{-20}	-	$1.03^{+0.15}_{-0.11}$	-	107/81 (1.33)
KW+2WAM†+BAT	PL	$-2.23^{+0.03}_{-0.03}$	-	-	$0.97^{+0.09}_{-0.09}$	$0.77^{+0.07}_{-0.06}$	$0.96^{+0.04}_{-0.04}$	325/168 (1.94)
KW+2WAM†+BAT	CPL	$-1.84^{+0.09}_{-0.08}$	-	30^{+9}_{-12}	$1.22^{+0.14}_{-0.12}$	$0.93^{+0.09}_{-0.08}$	$0.94^{+0.04}_{-0.04}$	216/167 (1.30)
KW+2WAM†+BAT	Band	$-1.64^{+0.19}_{-0.16}$	$-2.86^{+0.17}_{-0.25}$	39^{+5}_{-8}	$1.34^{+0.16}_{-0.15}$	$1.02^{+0.11}_{-0.10}$	$0.94^{+0.04}_{-0.04}$	205/166 (1.24)

† The joint fit of two WAM spectra.

Table 18. Spectral parameters: 060117 Reg13

Instrument	Model	α	β	E_{peak} [keV]	C(WAM0)	C(WAM1)	C(BAT)	χ^2/dof
KW	PL	$-2.05^{+0.02}_{-0.02}$	-	-	-	-	-	302/60 (5.04)
KW	CPL	$-1.56^{+0.07}_{-0.06}$	-	87^{+5}_{-5}	-	-	-	50/59 (0.86)
KW	Band	$-1.51^{+0.09}_{-0.07}$	$-2.88^{+0.24}_{-0.46}$	85^{+5}_{-5}	-	-	-	45/58 (0.78)
WAM0	PL	$-2.63^{+0.09}_{-0.09}$	-	-	-	-	-	20/22 (0.92)
WAM0	CPL	-	-	-	-	-	-	-
WAM0	Band	-	-	-	-	-	-	-
WAM1	PL	$-2.48^{+0.06}_{-0.07}$	-	-	-	-	-	33/22 (1.53)
WAM1	CPL	-	-	-	-	-	-	-
WAM1	Band	-	-	-	-	-	-	-
BAT	PL	$-1.88^{+0.03}_{-0.03}$	-	-	-	-	-	74/57 (1.31)
BAT	CPL	$-1.50^{+0.12}_{-0.12}$	-	77^{+9}_{-6}	-	-	-	40/56 (0.73)
BAT	Band	$-1.50^{+0.12}_{-0.12}$	$-8.80^{+0.06}_{-0.07}$	77^{+12}_{-9}	-	-	-	40/55 (0.74)
BAT+WAM0	PL	$-1.98^{+0.02}_{-0.03}$	-	-	$0.82^{+0.05}_{-0.04}$	-	-	329/80 (4.12)
BAT+WAM0	CPL	$-1.65^{+0.05}_{-0.05}$	-	88^{+8}_{-7}	$1.03^{+0.06}_{-0.06}$	-	-	95/79 (1.20)
BAT+WAM0	Band	$-1.46^{+0.11}_{-0.10}$	$-2.65^{+0.10}_{-0.12}$	75^{+6}_{-5}	$1.16^{+0.08}_{-0.08}$	-	-	63/78 (0.81)
BAT+WAM1	PL	$-2.00^{+0.02}_{-0.03}$	-	-	-	$0.77^{+0.04}_{-0.03}$	-	342/80 (4.28)
BAT+WAM1	CPL	$-1.69^{+0.05}_{-0.04}$	-	96^{+9}_{-9}	-	$0.86^{+0.04}_{-0.04}$	-	84/79 (1.06)
BAT+WAM1	Band	$-1.53^{+0.14}_{-0.16}$	$-2.51^{+0.08}_{-0.32}$	79^{+16}_{-8}	-	$0.95^{+0.07}_{-0.09}$	-	73/78 (0.95)
KW+BAT	PL	$-2.00^{+0.01}_{-0.01}$	-	-	-	-	$1.01^{+0.02}_{-0.02}$	444/118 (3.77)
KW+BAT	CPL	$-1.57^{+0.05}_{-0.05}$	-	86^{+4}_{-4}	-	-	$0.95^{+0.02}_{-0.02}$	94/117 (0.80)
KW+BAT	Band	$-1.53^{+0.07}_{-0.06}$	$-2.84^{+0.22}_{-0.43}$	83^{+4}_{-4}	-	-	$0.95^{+0.02}_{-0.02}$	88/116 (0.76)
KW+WAM0	PL	$-2.08^{+0.02}_{-0.02}$	-	-	$0.97^{+0.04}_{-0.04}$	-	-	467/83 (5.64)
KW+WAM0	CPL	$-1.62^{+0.05}_{-0.05}$	-	88^{+5}_{-5}	$1.00^{+0.04}_{-0.04}$	-	-	104/82 (1.27)
KW+WAM0	Band	$-1.48^{+0.09}_{-0.08}$	$-2.70^{+0.10}_{-0.13}$	82^{+5}_{-4}	$1.05^{+0.05}_{-0.05}$	-	-	71/81 (0.88)
KW+WAM1	PL	$-2.09^{+0.02}_{-0.02}$	-	-	-	$0.88^{+0.03}_{-0.03}$	-	467/83 (5.63)
KW+WAM1	CPL	$-1.67^{+0.05}_{-0.05}$	-	91^{+6}_{-6}	-	$0.86^{+0.03}_{-0.03}$	-	101/82 (1.23)
KW+WAM1	Band	$-1.54^{+0.11}_{-0.09}$	$-2.62^{+0.11}_{-0.19}$	84^{+6}_{-6}	-	$0.89^{+0.04}_{-0.04}$	-	84/81 (1.04)
KW+2WAM†+BAT	PL	$-2.06^{+0.01}_{-0.01}$	-	-	$0.93^{+0.04}_{-0.03}$	$0.84^{+0.03}_{-0.03}$	$1.00^{+0.02}_{-0.02}$	832/168 (4.96)
KW+2WAM†+BAT	CPL	$-1.66^{+0.03}_{-0.03}$	-	90^{+5}_{-5}	$0.98^{+0.04}_{-0.04}$	$0.86^{+0.03}_{-0.03}$	$0.96^{+0.02}_{-0.02}$	207/167 (1.24)
KW+2WAM†+BAT	Band	$-1.51^{+0.08}_{-0.07}$	$-2.60^{+0.07}_{-0.09}$	81^{+5}_{-4}	$1.04^{+0.05}_{-0.04}$	$0.91^{+0.04}_{-0.04}$	$0.96^{+0.02}_{-0.02}$	158/166 (0.95)

$\dagger$ The joint fit of two WAM spectra.

Table 19. Spectral parameters: 060124 Reg1

Instrument	Model	α	β	E_{peak} [keV]	C(WAM2)	C(WAM3)	χ^2/dof
KW	PL	$-1.71^{+0.09}_{-0.09}$	-	-	-	-	83/60 (1.39)
KW	CPL	$-1.18^{+0.33}_{-0.28}$	-	198^{+112}_{-50}	-	-	70/59 (1.19)
KW	Band	$-1.17^{+0.33}_{-0.27}$	-*	199^{+110}_{-64}	-	-	70/58 (1.21)
WAM2	PL	$-2.17^{+0.45}_{-0.62}$	-	-	-	-	10/14 (0.72)
WAM2	CPL	-	-	-	-	-	-
WAM2	Band	-	-	-	-	-	-
WAM3	PL	$-2.00^{+0.31}_{-0.39}$	-	-	-	-	14/14 (1.02)
WAM3	CPL	-	-	-	-	-	-
WAM3	Band	-	-	-	-	-	-
KW+WAM2	PL	$-1.73^{+0.09}_{-0.09}$	-	-	$0.77^{+0.27}_{-0.22}$	-	96/75 (1.29)
KW+WAM2	CPL	$-1.21^{+0.29}_{-0.25}$	-	213^{+97}_{-51}	$0.81^{+0.26}_{-0.22}$	-	78/74 (1.06)
KW+WAM2	Band	$-1.30^{+0.28}_{-0.16}$	-*	228^{+97}_{-51}	$0.82^{+0.26}_{-0.22}$	-	79/73 (1.08)
KW+WAM3	PL	$-1.73^{+0.09}_{-0.09}$	-	-	-	$0.78^{+0.20}_{-0.16}$	100/75 (1.33)
KW+WAM3	CPL	$-1.29^{+0.27}_{-0.23}$	-	239^{+133}_{-61}	-	$0.74^{+0.17}_{-0.15}$	85/74 (1.15)
KW+WAM3	Band	$-1.29^{+0.21}_{-0.13}$	-*	240^{+132}_{-54}	-	$0.74^{+0.15}_{-0.13}$	85/73 (1.17)
KW+2WAM†	PL	$-1.82^{+0.10}_{-0.11}$	-	-	$0.83^{+0.29}_{-0.24}$	$0.82^{+0.21}_{-0.17}$	105/88 (1.20)
KW+2WAM†	CPL	$-1.33^{+0.30}_{-0.26}$	-	244^{+119}_{-60}	$0.80^{+0.25}_{-0.22}$	$0.74^{+0.18}_{-0.15}$	91/87 (1.05)
KW+2WAM†	Band	$-1.44^{+0.43}_{-0.16}$	-*	268^{+119}_{-60}	$0.82^{+0.25}_{-0.22}$	$0.76^{+0.18}_{-0.15}$	91/86 (1.07)

* The parameter is not constrained.

† The joint fit of two WAM spectra.

Table 20. Spectral parameters: 060124 Reg2

Instrument	Model	α	β	E_{peak} [keV]	C(WAM2)	C(WAM3)	χ^2/dof
KW	PL	$-1.63^{+0.04}_{-0.04}$	-	-	-	-	133/69 (1.94)
KW	CPL	$-1.12^{+0.15}_{-0.13}$	-	323^{+78}_{-52}	-	-	60/68 (0.90)
KW	Band	$-0.96^{+0.24}_{-0.21}$	$-2.21^{+0.21}_{-0.68}$	244^{+85}_{-52}	-	-	55/67 (0.83)
WAM2	PL	$-2.02^{+0.18}_{-0.20}$	-	-	-	-	17/14 (1.23)
WAM2	CPL	$-1.21^{+1.20}_{-0.78}$	-	< 785	-	-	14/13 (1.11)
WAM2	Band	-	-	-	-	-	-
WAM3	PL	$-2.11^{+0.13}_{-0.14}$	-	-	-	-	18/14 (1.30)
WAM3	CPL	$-1.23^{+0.83}_{-0.65}$	-	281^{+74}_{-132}	-	-	12/13 (0.94)
WAM3	Band	$-1.19^{+1.20}_{-0.67}$	< -2.27	279^{+72}_{-65}	-	-	11/12 (1.00)
KW+WAM2	PL	$-1.65^{+0.03}_{-0.04}$	-	-	$0.70^{+0.08}_{-0.08}$	-	164/84 (1.95)
KW+WAM2	CPL	$-1.14^{+0.13}_{-0.12}$	-	331^{+67}_{-47}	$0.66^{+0.07}_{-0.07}$	-	75/83 (0.91)
KW+WAM2	Band	$-0.99^{+0.23}_{-0.18}$	$-2.26^{+0.22}_{-0.69}$	259^{+79}_{-56}	$0.66^{+0.08}_{-0.07}$	-	70/82 (0.86)
KW+WAM3	PL	$-1.67^{+0.03}_{-0.04}$	-	-	-	$0.70^{+0.07}_{-0.06}$	189/84 (2.26)
KW+WAM3	CPL	$-1.09^{+0.13}_{-0.12}$	-	305^{+47}_{-35}	-	$0.64^{+0.05}_{-0.05}$	73/83 (0.89)
KW+WAM3	Band	$-1.02^{+0.21}_{-0.14}$	$-2.51^{+0.36}_{-1.06}$	274^{+51}_{-57}	-	$0.64^{+0.06}_{-0.05}$	69/82 (0.85)
KW+2WAM†	PL	$-1.69^{+0.03}_{-0.04}$	-	-	$0.73^{+0.09}_{-0.08}$	$0.72^{+0.07}_{-0.08}$	217/99 (2.20)
KW+2WAM†	CPL	$-1.11^{+0.12}_{-0.11}$	-	313^{+45}_{-34}	$0.66^{+0.07}_{-0.07}$	$0.64^{+0.05}_{-0.05}$	88/98 (0.91)
KW+2WAM†	Band	$-1.03^{+0.19}_{-0.14}$	$-2.50^{+0.32}_{-0.93}$	279^{+51}_{-54}	$0.66^{+0.08}_{-0.07}$	$0.64^{+0.05}_{-0.05}$	84/97 (0.87)

† The joint fit of two WAM spectra.

Table 21. Spectral parameters: 060124 Reg3

Instrument	Model	α	β	$E_{\rm peak}$ [keV]	C(WAM2)	C(WAM3)	χ^2/dof
KW	PL	$-1.85^{+0.11}_{-0.11}$	-	-	-	-	80/60 (1.34)
KW	CPL	$-1.21^{+0.41}_{-0.34}$	-	133^{+60}_{-32}	-	-	66/59 (1.13)
KW	Band	$-1.20^{+0.21}_{-0.35}$	< -2.32	132^{+40}_{-31}	-	-	66/58 (1.15)
WAM2	PL	$-2.42^{+0.67}_{-1.02}$	-	-	-	-	11/14 (0.85)
WAM2	CPL	< 2.5	-	231^{+41}_{-62}	-	-	9/13 (0.71)
WAM2	Band	-	-	-	-	-	-
WAM3	PL	$-2.29^{+0.46}_{-0.62}$	-	-	-	-	20/14 (1.49)
WAM3	CPL	-	-	-	-	-	-
WAM3	Band	-	-	-	-	-	-
KW+WAM2	PL	$-1.86^{+0.11}_{-0.11}$	-	-	$0.88^{+0.39}_{-0.32}$	-	94/75 (1.26)
KW+WAM2	CPL	$-1.22^{+0.37}_{-0.32}$	-	136^{+53}_{-31}	$0.97^{+0.41}_{-0.33}$	-	77/74 (1.05)
KW+WAM2	Band	$-1.22^{+0.34}_{-0.30}$	< -2.44	137^{+39}_{-30}	$0.97^{+0.40}_{-0.16}$	-	77/73 (1.07)
KW+WAM3	PL	$-1.87^{+0.10}_{-0.11}$	-	-	-	$0.98^{+0.30}_{-0.24}$	103/75 (1.39)
KW+WAM3	CPL	$-1.29^{+0.36}_{-0.30}$	-	144^{+62}_{-34}	-	$0.94^{+0.28}_{-0.22}$	89/74 (1.21)
KW+WAM3	Band	$-1.24^{+1.57}_{-0.35}$	< -2.11	136^{+66}_{-85}	-	$0.96^{+0.32}_{-0.24}$	89/73 (1.22)
KW+2WAM†	PL	$-2.00^{+0.12}_{-0.14}$	-	-	$0.98^{+0.44}_{-0.35}$	$1.05^{+0.33}_{-0.26}$	108/88 (1.24)
KW+2WAM†	CPL	$-1.44^{+0.40}_{-0.35}$	-	139^{+61}_{-43}	$0.97^{+0.41}_{-0.33}$	$0.96^{+0.30}_{-0.23}$	99/87 (1.14)
KW+2WAM†	Band	$-1.42^{+0.46}_{-0.36}$	< -2.24	137^{+60}_{-42}	$0.97^{+0.41}_{-0.33}$	$0.97^{+0.30}_{-0.23}$	99/86 (1.15)

† The joint fit of two WAM spectra.

Table 22. Spectral parameters: 060124 Reg13

Instrument	Model	α	β	$E_{\rm peak}$ [keV]	C(WAM2)	C(WAM3)	χ^2/dof
KW	PL	$-1.72^{+0.04}_{-0.04}$	-	-	-	-	111/69 (1.61)
KW	CPL	$-1.22^{+0.15}_{-0.14}$	-	248^{+57}_{-36}	-	-	55/68 (0.81)
KW	Band	$-1.18^{+0.19}_{-0.16}$	< -2.17	232^{+60}_{-44}	-	-	54/67 (0.81)
WAM2	PL	$-2.14^{+0.22}_{-0.25}$	-	-	-	-	17/14 (1.24)
WAM2	CPL	$0.15^{+2.85}_{-1.77}$	-	284^{+76}_{-73}	-	-	11/13 (0.88)
WAM2	Band	$3.32^{+1.77}_{-4.45}$	< -2.26	242^{+85}_{-51}	-	-	9/12 (0.82)
WAM3	PL	$-2.10^{+0.15}_{-0.17}$	-	-	-	-	19/14 (1.39)
WAM3	CPL	$-1.60^{+0.80}_{-0.59}$	-	< 414	-	-	17/13 (1.33)
WAM3	Band	-	-	-	-	-	-
KW+WAM2	PL	$-1.74^{+0.04}_{-0.04}$	-	-	$0.74^{+0.10}_{-0.09}$	-	138/84 (1.65)
KW+WAM2	CPL	$-1.22^{+0.14}_{-0.13}$	-	253^{+48}_{-34}	$0.73^{+0.09}_{-0.09}$	-	68/83 (0.82)
KW+WAM2	Band	$-1.19^{+0.17}_{-0.14}$	$-2.76^{+0.50}_{-7.24}$	241^{+50}_{-41}	$0.73^{+0.09}_{-0.09}$	-	67/82 (0.82)
KW+WAM3	PL	$-1.75^{+0.04}_{-0.04}$	-	-	$0.77^{+0.07}_{-0.07}$	-	148/84 (1.77)
KW+WAM3	CPL	$-1.25^{+0.13}_{-0.12}$	-	261^{+46}_{-33}	$0.71^{+0.06}_{-0.06}$	-	73/83 (0.89)
KW+WAM3	Band	$-1.21^{+0.18}_{-0.14}$	$-2.62^{+0.42}_{-7.38}$	242^{+53}_{-48}	$0.71^{+0.07}_{-0.06}$	-	72/82 (0.88)
KW+2WAM†	PL	$-1.77^{+0.04}_{-0.04}$	-	-	$0.77^{+0.10}_{-0.10}$	$0.78^{+0.08}_{-0.07}$	174/99 (1.76)
KW+2WAM†	CPL	$-1.25^{+0.13}_{-0.12}$	-	261^{+41}_{-31}	$0.73^{+0.09}_{-0.09}$	$0.71^{+0.06}_{-0.06}$	86/98 (0.88)
KW+2WAM†	Band	$-1.22^{+0.16}_{-0.13}$	$-2.74^{+0.46}_{-7.26}$	248^{+45}_{-42}	$0.73^{+0.09}_{-0.09}$	$0.71^{+0.07}_{-0.06}$	84/97 (0.88)

† The joint fit of two WAM spectra.

Table 23. Spectral parameters: 060502A Reg1

Instrument	Model	α	β	E_{peak} [keV]	C(WAM3)	C(BAT)	χ^2/dof
KW	PL	$-1.71^{+0.10}_{-0.11}$	-	-	-	-	73/60 (1.22)
KW	CPL	$-1.19^{+0.42}_{-0.34}$	-	174^{+162}_{-53}	-	-	64/59 (1.10)
KW	Band	$-0.90^{+4.75}_{-0.60}$	< -1.79	117^{+103}_{-80}	-	-	64/58 (1.11)
WAM3	PL	$-2.75^{+0.58}_{-0.81}$	-	-	-	-	11/14 (0.81)
WAM3	CPL	-	-	-	-	-	-
WAM3	Band	-	-	-	-	-	-
BAT	PL	$-1.26^{+0.08}_{-0.08}$	-	-	-	-	54/57 (0.96)
BAT	CPL	$-0.73^{+0.36}_{-0.33}$	-	132^{+122}_{-33}	-	-	47/56 (0.84)
BAT	Band	-	-	-	-	-	-
BAT+WAM3	PL	$-1.32^{+0.08}_{-0.08}$	-	-	$0.41^{+0.12}_{-0.10}$	-	94/72 (1.31)
BAT+WAM3	CPL	$-0.79^{+0.29}_{-0.24}$	-	141^{+75}_{-33}	$0.98^{+0.40}_{-0.29}$	-	60/71 (0.85)
BAT+WAM3	Band	$-0.67^{+0.35}_{-0.31}$	< -2.12	123^{+68}_{-26}	$1.08^{+0.42}_{-0.33}$	-	59/70 (0.84)
KW+BAT	PL	$-1.43^{+0.07}_{-0.07}$	-	-	-	$1.27^{+0.24}_{-0.19}$	158/118 (1.35)
KW+BAT	CPL	$-0.86^{+0.24}_{-0.20}$	-	149^{+55}_{-31}	-	$0.94^{+0.15}_{-0.12}$	114/117 (0.97)
KW+BAT	Band	$-0.70^{+0.42}_{-0.30}$	< -1.88	120^{+60}_{-33}	-	$0.93^{+0.15}_{-0.11}$	112/116 (0.97)
KW+WAM3	PL	$-1.76^{+0.10}_{-0.11}$	-	-	$0.94^{+0.30}_{-0.22}$	-	95/75 (1.27)
KW+WAM3	CPL	$-1.16^{+0.37}_{-0.30}$	-	163^{+83}_{-42}	$0.92^{+0.29}_{-0.21}$	-	77/74 (1.05)
KW+WAM3	Band	$-0.87^{+0.83}_{-0.57}$	< -2.07	119^{+113}_{-44}	$1.02^{+0.35}_{-0.29}$	-	76/73 (1.05)
KW+WAM3+BAT	PL	$-1.46^{+0.06}_{-0.07}$	-	-	$0.67^{+0.17}_{-0.14}$	$1.21^{+0.21}_{-0.18}$	191/133 (1.44)
KW+WAM3+BAT	CPL	$-0.87^{+0.21}_{-0.18}$	-	150^{+46}_{-29}	$0.89^{+0.26}_{-0.20}$	$0.94^{+0.14}_{-0.12}$	126/132 (0.96)
KW+WAM3+BAT	Band	$-0.70^{+0.31}_{-0.28}$	< -2.10	121^{+49}_{-24}	$0.97^{+0.28}_{-0.22}$	$0.92^{+0.14}_{-0.11}$	124/131 (0.95)

Table 24. Spectral parameters: 060813 Reg1

Instrument	Model	α	β	E_{peak} [keV]	C(WAM0)	C(WAM3)	C(BAT)	χ^2/dof
KW	PL	$-1.57^{+0.02}_{-0.02}$	-	-	-	-	-	431/60 (7.18)
KW	CPL	$-0.65^{+0.12}_{-0.11}$	-	218^{+18}_{-16}	-	-	-	82/59 (1.40)
KW	Band	$-0.52^{+0.17}_{-0.15}$	$-2.63^{+0.26}_{-0.47}$	194^{+21}_{-19}	-	-	-	74/58 (1.28)
WAM0	PL	$-2.23^{+0.07}_{-0.07}$	-	-	-	-	-	42/22 (1.94)
WAM0	CPL	$-1.48^{+0.34}_{-0.30}$	-	223^{+38}_{-71}	-	-	-	20/21 (0.98)
WAM0	Band	-	-	-	-	-	-	-
WAM3	PL	$-2.19^{+0.07}_{-0.08}$	-	-	-	-	-	38/22 (1.76)
WAM3	CPL	$-1.59^{+0.48}_{-0.38}$	-	< 260	-	-	-	30/21 (1.44)
WAM3	Band	$-0.71^{+5.71}_{-0.80}$	$-2.58^{+0.24}_{-0.39}$	227^{+26}_{-40}	-	-	-	22/20 (1.14)
BAT	PL	$-1.13^{+0.04}_{-0.04}$	-	-	-	-	-	53/57 (0.94)
BAT	CPL	$-0.80^{+0.16}_{-0.15}$	-	219^{+122}_{-51}	-	-	-	38/56 (0.69)
BAT	Band	-	-	-	-	-	-	-
BAT+WAM0	PL	-1.51	-	-	1.07	-	-	832/80 (10.40)
BAT+WAM0	CPL	$-0.87^{+0.05}_{-0.05}$	-	259^{+19}_{-17}	$1.08^{+0.07}_{-0.07}$	-	-	67/79 (0.86)
BAT+WAM0	Band	$-0.85^{+0.08}_{-0.07}$	< -2.47	246^{+28}_{-32}	$1.11^{+0.09}_{-0.08}$	-	-	66/78 (0.86)
BAT+WAM3	PL	$-1.45^{+0.03}_{-0.03}$	-	-	-	$0.81^{+0.08}_{-0.05}$	-	703/80 (8.80)
BAT+WAM3	CPL	$-0.86^{+0.06}_{-0.06}$	-	251^{+21}_{-19}	-	$0.96^{+0.07}_{-0.06}$	-	75/79 (0.95)
BAT+WAM3	Band	$-0.81^{+0.08}_{-0.07}$	$-2.58^{+0.23}_{-0.36}$	226^{+25}_{-27}	-	$1.00^{+0.08}_{-0.07}$	-	61/78 (0.79)
KW+BAT	PL	$-1.44^{+0.02}_{-0.02}$	-	-	-	-	$1.03^{+0.04}_{-0.05}$	753/118 (6.38)
KW+BAT	CPL	$-0.78^{+0.06}_{-0.06}$	-	228^{+18}_{-16}	-	-	$0.92^{+0.04}_{-0.03}$	126/117 (1.08)
KW+BAT	Band	$-0.73^{+0.08}_{-0.07}$	$-2.71^{+0.30}_{-0.84}$	212^{+20}_{-18}	-	-	$0.91^{+0.04}_{-0.03}$	122/116 (1.05)
KW+WAM0	PL	$-1.69^{+0.02}_{-0.03}$	-	-	$1.30^{+0.08}_{-0.06}$	-	-	766/83 (9.24)
KW+WAM0	CPL	$-0.80^{+0.08}_{-0.08}$	-	246^{+13}_{-12}	$1.01^{+0.05}_{-0.05}$	-	-	120/82 (1.47)
KW+WAM0	Band	$-0.61^{+0.17}_{-0.14}$	$-2.54^{+0.18}_{-0.31}$	207^{+22}_{-23}	$1.03^{+0.06}_{-0.05}$	-	-	109/81 (1.36)
KW+WAM3	PL	$-1.67^{+0.02}_{-0.03}$	-	-	-	$1.08^{+0.07}_{-0.05}$	-	695/83 (8.38)
KW+WAM3	CPL	$-0.76^{+0.09}_{-0.08}$	-	239^{+14}_{-13}	-	$0.88^{+0.04}_{-0.04}$	-	124/82 (1.52)
KW+WAM3	Band	$-0.60^{+0.15}_{-0.12}$	$-2.54^{+0.17}_{-0.25}$	205^{+19}_{-19}	-	$0.90^{+0.05}_{-0.04}$	-	101/81 (1.25)
KW+2WAM†+BAT	PL	$-1.62^{+0.02}_{-0.02}$	-	-	$1.16^{+0.06}_{-0.05}$	$0.99^{+0.06}_{-0.04}$	$0.85^{+0.03}_{-0.03}$	1607/167 (9.63)
KW+2WAM†+BAT	CPL	$-0.84^{+0.05}_{-0.05}$	-	249^{+11}_{-10}	$1.01^{+0.04}_{-0.04}$	$0.88^{+0.04}_{-0.04}$	$0.93^{+0.04}_{-0.03}$	197/166 (1.19)
KW+2WAM†+BAT	Band	$-0.77^{+0.06}_{-0.06}$	$-2.63^{+0.17}_{-0.25}$	223^{+15}_{-16}	$1.04^{+0.05}_{-0.05}$	$0.91^{+0.05}_{-0.04}$	$0.92^{+0.03}_{-0.03}$	177/165 (1.08)

† The joint fit of two WAM spectra.

Table 25. Spectral parameters: 060814 Reg1

Instrument	Model	α	β	E_{peak} [keV]	C(WAM0)	C(WAM1)	C(BAT)	χ^2/dof
KW	PL	$-1.64^{+0.04}_{-0.04}$	-	-	-	-	-	76/60 (1.28)
KW	CPL	$-1.26^{+0.15}_{-0.14}$	-	299^{+111}_{-62}	-	-	-	45/59 (0.78)
KW	Band	$-1.08^{+0.32}_{-0.21}$	$-2.07^{+0.21}_{-0.50}$	204^{+91}_{-65}	-	-	-	41/58 (0.72)
WAM0	PL	$-2.01^{+0.23}_{-0.27}$	-	-	-	-	-	16/22 (0.73)
WAM0	CPL	-	-	-	-	-	-	-
WAM0	Band	-	-	-	-	-	-	-
WAM1	PL	$-1.84^{+0.09}_{-0.09}$	-	-	-	-	-	27/22 (1.24)
WAM1	CPL	-	-	-	-	-	-	-
WAM1	Band	-	-	-	-	-	-	-
BAT	PL	$-1.47^{+0.04}_{-0.04}$	-	-	-	-	-	40/57 (0.70)
BAT	CPL	$-1.33^{+0.15}_{-0.15}$	-	> 165	-	-	-	37/56 (0.67)
BAT	Band	-	-	-	-	-	-	-
BAT+WAM0	PL	$-1.49^{+0.04}_{-0.04}$	-	-	$0.68^{+0.09}_{-0.08}$	-	-	74/80 (0.93)
BAT+WAM0	CPL	$-1.38^{+0.09}_{-0.07}$	-	$386.5^{+405.7}_{-143.4}$	$0.88^{+0.16}_{-0.13}$	-	-	58/79 (0.74)
BAT+WAM0	Band	$-1.29^{+0.13}_{-0.11}$	$-1.97^{+0.22}_{-0.44}$	225^{+198}_{-69}	$0.98^{+0.18}_{-0.16}$	-	-	54/78 (0.70)
BAT+WAM1	PL	$-1.54^{+0.03}_{-0.03}$	-	-	-	$0.83^{+0.07}_{-0.06}$	-	112/80 (1.41)
BAT+WAM1	CPL	$-1.41^{+0.05}_{-0.05}$	-	521^{+201}_{-121}	-	$0.90^{+0.07}_{-0.07}$	-	66/79 (0.85)
BAT+WAM1	Band	$-1.37^{+0.13}_{-0.06}$	$-1.95^{+0.16}_{-0.42}$	363^{+179}_{-172}	-	$0.94^{+0.12}_{-0.08}$	-	62/78 (0.81)
KW+BAT	PL	$-1.54^{+0.03}_{-0.03}$	-	-	-	-	$0.95^{+0.06}_{-0.05}$	139/118 (1.18)
KW+BAT	CPL	$-1.34^{+0.07}_{-0.06}$	-	324^{+106}_{-67}	-	-	$0.87^{+0.05}_{-0.05}$	84/117 (0.72)
KW+BAT	Band	$-1.29^{+0.10}_{-0.08}$	< -1.85	257^{+126}_{-67}	-	-	$0.86^{+0.05}_{-0.05}$	82/116 (0.71)
KW+WAM0	PL	$-1.65^{+0.04}_{-0.04}$	-	-	$0.80^{+0.09}_{-0.09}$	-	-	100/83 (1.21)
KW+WAM0	CPL	$-1.31^{+0.14}_{-0.12}$	-	329^{+119}_{-67}	$0.77^{+0.09}_{-0.08}$	-	-	68/82 (0.83)
KW+WAM0	Band	$-1.04^{+0.32}_{-0.22}$	$-2.02^{+0.15}_{-0.22}$	190^{+74}_{-54}	$0.81^{+0.10}_{-0.09}$	-	-	58/81 (0.72)
KW+WAM1	PL	$-1.68^{+0.04}_{-0.04}$	-	-	-	$0.91^{+0.07}_{-0.06}$	-	116/83 (1.40)
KW+WAM1	CPL	$-1.40^{+0.10}_{-0.10}$	-	440^{+140}_{-83}	-	$0.83^{+0.06}_{-0.06}$	-	79/82 (0.97)
KW+WAM1	Band	$-1.10^{+0.46}_{-0.27}$	$-1.91^{+0.09}_{-0.25}$	200^{+164}_{-81}	-	$0.86^{+0.08}_{-0.07}$	-	71/81 (0.88)
KW+2WAM†+BAT	PL	$-1.59^{+0.04}_{-0.03}$	-	-	$0.75^{+0.08}_{-0.08}$	$0.82^{+0.06}_{-0.05}$	$0.91^{+0.05}_{-0.05}$	242/166 (1.46)
KW+2WAM†+BAT	CPL	$-1.39^{+0.05}_{-0.05}$	-	425^{+96}_{-69}	$0.76^{+0.08}_{-0.08}$	$0.82^{+0.06}_{-0.05}$	$0.89^{+0.05}_{-0.05}$	142/165 (0.87)
KW+2WAM†+BAT	Band	$-1.32^{+0.11}_{-0.07}$	$-1.99^{+0.12}_{-0.24}$	281^{+98}_{-86}	$0.80^{+0.09}_{-0.09}$	$0.86^{+0.07}_{-0.06}$	$0.87^{+0.05}_{-0.05}$	136/164 (0.83)

† The joint fit of two WAM spectra.

Table 26. Spectral parameters: 060814 Reg2

Instrument	Model	α	β	$E_{\rm peak}$ [keV]	C(WAM0)	C(WAM1)	C(BAT)	χ^2/dof
KW	PL	$-1.78^{+0.07}_{-0.07}$	-	-	-	-	-	63/60 (1.07)
KW	CPL	$-1.44^{+0.24}_{-0.20}$	-	212^{+159}_{-57}	-	-	-	53/59 (0.91)
KW	Band	$-1.37^{+0.40}_{-0.27}$	<-1.92	177^{+176}_{-67}	-	-	-	53/58 (0.92)
WAM0	PL	$-1.61^{-0.22}_{-0.27}$	-	-	-	-	-	16/22 (0.77)
WAM0	CPL	-	-	-	-	-	-	-
WAM0	Band	-	-	-	-	-	-	-
WAM1	PL	$-1.77^{+0.11}_{-0.12}$	-	-	-	-	-	22/22 (1.04)
WAM1	CPL	-	-	-	-	-	-	-
WAM1	Band	-	-	-	-	-	-	-
BAT	PL	$-1.55^{+0.04}_{-0.04}$	-	-	-	-	-	38/57 (0.67)
BAT	CPL	-	-	-	-	-	-	-
BAT	Band	-	-	-	-	-	-	-
BAT+WAM0	PL	$-1.56^{+0.04}_{-0.04}$	-	-	$0.80^{+0.12}_{-0.11}$	-	-	55/80 (0.69)
BAT+WAM0	CPL	-	-	-	-	-	-	-
BAT+WAM0	Band	-	-	-	-	-	-	-
BAT+WAM1	PL	$-1.58^{+0.04}_{-0.04}$	-	-	-	$0.93^{+0.08}_{-0.07}$	-	70/80 (0.88)
BAT+WAM1	CPL	$-1.52^{+0.05}_{-0.05}$	-	825^{+1099}_{-324}	-	$0.99^{+0.09}_{-0.08}$	-	61/79 (0.77)
BAT+WAM1	Band	$-1.47^{+0.15}_{-0.10}$	<-1.66	339^{+1425}_{-183}	-	$1.06^{+0.14}_{-0.15}$	-	60/78 (0.78)
KW+BAT	PL	$-1.61^{+0.03}_{-0.03}$	-	-	-	-	$0.97^{+0.08}_{-0.07}$	124/118 (1.05)
KW+BAT	CPL	$-1.41^{+0.09}_{-0.08}$	-	223^{+102}_{-53}	-	-	$0.86^{+0.07}_{-0.06}$	92/117 (0.79)
KW+BAT	Band	$-1.41^{+0.11}_{-0.08}$	<-1.97	221^{+96}_{-65}	-	-	$0.86^{+0.07}_{-0.06}$	92/116 (0.80)
KW+WAM0	PL	$-1.77^{+0.07}_{-0.07}$	-	-	$0.99^{+0.17}_{-0.15}$	-	-	81/83 (0.99)
KW+WAM0	CPL	$-1.65^{+0.19}_{-0.15}$	-	>242	$0.97^{+0.17}_{-0.15}$	-	-	79/82 (0.97)
KW+WAM0	Band	$-1.38^{+0.63}_{-0.30}$	$-1.95^{+0.15}_{-0.36}$	160^{+341}_{-89}	$1.00^{+0.18}_{-0.15}$	-	-	76/81 (0.94)
KW+WAM1	PL	$-1.78^{+0.06}_{-0.06}$	-	-	-	$1.11^{+0.13}_{-0.11}$	-	86/83 (1.05)
KW+WAM1	CPL	$-1.68^{+0.12}_{-0.11}$	-	>405	-	$1.06^{+0.13}_{-0.11}$	-	84/82 (1.03)
KW+WAM1	Band	$-1.43^{+0.92}_{-0.31}$	$-1.87^{+0.10}_{-0.11}$	165^{+1277}_{-111}	-	$1.09^{+0.13}_{-0.11}$	-	82/81 (1.01)
KW+2WAM†+BAT	PL	$-1.63^{+0.03}_{-0.03}$	-	-	$0.87^{+0.13}_{-0.12}$	$0.97^{+0.09}_{-0.08}$	$0.96^{+0.08}_{-0.07}$	175/166 (1.06)
KW+2WAM†+BAT	CPL	$-1.53^{+0.05}_{-0.05}$	-	540^{+304}_{-151}	$0.88^{+0.13}_{-0.12}$	$0.97^{+0.09}_{-0.08}$	$0.92^{+0.08}_{-0.07}$	150/165 (0.91)
KW+2WAM†+BAT	Band	$-1.40^{+0.13}_{-0.10}$	$-1.86^{+0.09}_{-0.12}$	208^{+170}_{-65}	$0.94^{+0.15}_{-0.13}$	$1.04^{+0.11}_{-0.09}$	$0.89^{+0.07}_{-0.06}$	145/164 (0.89)

† The joint fit of two WAM spectra.

Table 27. Spectral parameters: 060814 Reg12

Instrument	Model	α	β	E_{peak} [keV]	C(WAM0)	C(WAM1)	C(BAT)	χ^2/dof
KW	PL	$-1.70^{+0.06}_{-0.06}$	-	-	-	-	-	72/60 (1.20)
KW	CPL	$-1.43^{+0.19}_{-0.16}$	-	308^{+268}_{-92}	-	-	-	61/59 (1.04)
KW	Band	$-1.30^{+0.42}_{-0.22}$	< -1.81	212^{+170}_{-98}	-	-	-	59/58 (1.02)
WAM0	PL	$-1.76^{+0.21}_{-0.25}$	-	-	-	-	-	15/22 (0.71)
WAM0	CPL	-	-	-	-	-	-	-
WAM0	Band	-	-	-	-	-	-	-
WAM1	PL	$-1.77^{+0.09}_{-0.10}$	-	-	-	-	-	19/22 (0.88)
WAM1	CPL	-	-	-	-	-	-	-
WAM1	Band	-	-	-	-	-	-	-
BAT	PL	$-1.56^{+0.03}_{-0.03}$	-	-	-	-	-	45/57 (0.79)
BAT	CPL	-	-	-	-	-	-	-
BAT	Band	-	-	-	-	-	-	-
BAT+WAM0	PL	$-1.57^{+0.03}_{-0.03}$	-	-	$0.82^{+0.09}_{-0.09}$	-	-	63/80 (0.79)
BAT+WAM0	CPL	$-1.54^{+0.06}_{-0.05}$	-	$\pm\infty$	$0.89^{+0.13}_{-0.12}$	-	-	62/79 (0.78)
BAT+WAM0	Band	$-1.44^{+0.13}_{-0.11}$	$-1.76^{+0.16}_{-0.24}$	262^{+736}_{-108}	$0.98^{+0.17}_{-0.16}$	-	-	58/78 (0.75)
BAT+WAM1	PL	$-1.59^{+0.03}_{-0.03}$	-	-	-	$0.89^{+0.06}_{-0.06}$	-	77/80 (0.97)
BAT+WAM1	CPL	$-1.53^{+0.04}_{-0.02}$	-	772^{+696}_{-270}	-	$0.94^{+0.07}_{-0.03}$	-	63/79 (0.81)
BAT+WAM1	Band	$-1.44^{+0.14}_{-0.11}$	< -1.70	> 156	-	$1.02^{+0.10}_{-0.12}$	-	62/78 (0.80)
KW+BAT	PL	$-1.60^{+0.03}_{-0.03}$	-	-	-	-	$0.96^{+0.06}_{-0.06}$	128/118 (1.09)
KW+BAT	CPL	$-1.46^{+0.07}_{-0.06}$	-	317^{+182}_{-89}	-	-	$0.88^{+0.06}_{-0.05}$	104/117 (0.89)
KW+BAT	Band	$-1.42^{+0.10}_{-0.08}$	< -1.80	249^{+175}_{-78}	-	-	$0.87^{+0.06}_{-0.05}$	103/116 (0.89)
KW+WAM0	PL	$-1.70^{+0.05}_{-0.06}$	-	-	$0.91^{+0.12}_{-0.11}$	-	-	87/83 (1.06)
KW+WAM0	CPL	$-1.56^{+0.14}_{-0.12}$	-	534^{+1641}_{-216}	$0.88^{+0.12}_{-0.10}$	-	-	83/82 (1.02)
KW+WAM0	Band	$-1.21^{+0.50}_{-0.30}$	$-1.90^{+0.13}_{-0.19}$	165^{+182}_{-75}	$0.92^{+0.12}_{-0.11}$	-	-	76/81 (0.95)
KW+WAM1	PL	$-1.72^{+0.05}_{-0.05}$	-	-	-	$0.96^{+0.09}_{-0.08}$	-	92/83 (1.12)
KW+WAM1	CPL	$-1.58^{+0.11}_{-0.10}$	-	682^{+870}_{-231}	-	$0.91^{+0.08}_{-0.07}$	-	85/82 (1.04)
KW+WAM1	Band	$-1.27^{+0.76}_{-0.32}$	$-1.83^{+0.08}_{-0.15}$	172^{+420}_{-97}	-	$0.93^{+0.09}_{-0.08}$	-	81/81 (1.01)
KW+2WAM†+BAT	PL	$-1.62^{+0.03}_{-0.03}$	-	-	$0.84^{+0.10}_{-0.09}$	$0.88^{+0.07}_{-0.06}$	$0.94^{+0.06}_{-0.06}$	183/166 (1.10)
KW+2WAM†+BAT	CPL	$-1.53^{+0.04}_{-0.04}$	-	612^{+295}_{-160}	$0.86^{+0.10}_{-0.09}$	$0.88^{+0.07}_{-0.06}$	$0.91^{+0.06}_{-0.05}$	151/165 (0.92)
KW+2WAM†+BAT	Band	$-1.41^{+0.11}_{-0.10}$	$-1.83^{+0.08}_{-0.13}$	232^{+223}_{-74}	$0.91^{+0.11}_{-0.10}$	$0.93^{+0.08}_{-0.07}$	$0.88^{+0.06}_{-0.05}$	146/164 (0.89)

† The joint fit of two WAM spectra.

Table 28. Spectral parameters: 060904A Reg1

Instrument	Model	α	β	E_{peak} [keV]	C(WAM0)	C(WAM1)	C(BAT)	χ^2/dof
KW	PL	$-1.67^{+0.04}_{-0.04}$	-	-	-	-	-	128/60 (2.15)
KW	CPL	$-1.03^{+0.15}_{-0.14}$	-	186^{+30}_{-22}	-	-	-	45/59 (0.77)
KW	Band	$-1.02^{+0.16}_{-0.15}$	< -2.44	182^{+30}_{-23}	-	-	-	44/58 (0.77)
WAM0	PL	$-2.16^{+0.21}_{-0.25}$	-	-	-	-	-	14/14 (1.03)
WAM0	CPL	$-1.07^{+1.36}_{-0.66}$	-	< 430	-	-	-	10/13 (0.84)
WAM0	Band	$-1.14^{+6.02}_{-0.99}$	< -2.25	309^{+122}_{-145}	-	-	-	10/12 (0.91)
WAM3	PL	$-2.10^{+0.09}_{-0.10}$	-	-	-	-	-	10/14 (0.73)
WAM3	CPL	$-1.83^{+0.37}_{-0.29}$	-	< 334	-	-	-	7/13 (0.59)
WAM3	Band	$-1.83^{+0.33}_{-0.17}$	< -2.07	210^{+124}_{-140}	-	-	-	7/12 (0.64)
BAT	PL	$-1.31^{+0.04}_{-0.04}$	-	-	-	-	-	38/57 (0.67)
BAT	CPL	-	-	-	-	-	-	-
BAT	Band	-	-	-	-	-	-	-
BAT+WAM0	PL	$-1.35^{+0.04}_{-0.04}$	-	-	$0.46^{+0.07}_{-0.06}$	-	-	109/72 (1.51)
BAT+WAM0	CPL	$-1.18^{+0.07}_{-0.06}$	-	357^{+142}_{-83}	$0.79^{+0.13}_{-0.12}$	-	-	54/71 (0.76)
BAT+WAM0	Band	$-1.18^{+0.06}_{-0.06}$	< -2.28	358^{+140}_{-77}	$0.79^{+0.13}_{-0.12}$	-	-	54/70 (0.77)
BAT+WAM3	PL	$-1.47^{+0.03}_{-0.03}$	-	-	-	$0.77^{+0.07}_{-0.06}$	-	268/72 (3.73)
BAT+WAM3	CPL	$-1.16^{+0.06}_{-0.05}$	-	300^{+47}_{-37}	-	$0.94^{+0.08}_{-0.07}$	-	60/71 (0.85)
BAT+WAM3	Band	$-1.13^{+0.08}_{-0.07}$	< -2.13	266^{+59}_{-53}	-	$0.98^{+0.10}_{-0.09}$	-	57/70 (0.82)
KW+BAT	PL	$-1.49^{+0.03}_{-0.03}$	-	-	-	-	$1.03^{+0.06}_{-0.06}$	287/118 (2.43)
KW+BAT	CPL	$-1.06^{+0.07}_{-0.07}$	-	205^{+30}_{-23}	-	-	$0.84^{+0.05}_{-0.04}$	98/117 (0.84)
KW+BAT	Band	$-1.06^{+0.08}_{-0.07}$	< -2.63	204^{+30}_{-23}	-	-	$0.84^{+0.05}_{-0.04}$	98/116 (0.85)
KW+WAM0	PL	$-1.70^{+0.04}_{-0.04}$	-	-	$0.87^{+0.12}_{-0.11}$	-	-	158/75 (2.12)
KW+WAM0	CPL	$-1.13^{+0.13}_{-0.12}$	-	209^{+34}_{-25}	$0.88^{+0.11}_{-0.10}$	-	-	62/74 (0.84)
KW+WAM0	Band	$-1.08^{+0.16}_{-0.14}$	< -2.31	193^{+37}_{-30}	$0.89^{+0.12}_{-0.10}$	-	-	60/73 (0.83)
KW+WAM3	PL	$-1.76^{+0.04}_{-0.04}$	-	-	-	$1.13^{+0.10}_{-0.09}$	-	194/75 (2.59)
KW+WAM3	CPL	$-1.25^{+0.10}_{-0.10}$	-	246^{+31}_{-25}	-	$0.95^{+0.08}_{-0.07}$	-	69/74 (0.94)
KW+WAM3	Band	$-1.09^{+0.19}_{-0.15}$	$-2.30^{+0.16}_{-0.30}$	190^{+40}_{-38}	-	$0.98^{+0.09}_{-0.07}$	-	61/73 (0.84)
KW+2WAM†+BAT	PL	$-1.57^{+0.02}_{-0.03}$	-	-	$0.73^{+0.09}_{-0.08}$	$0.88^{+0.06}_{-0.05}$	$0.94^{+0.05}_{-0.05}$	478/148 (3.23)
KW+2WAM†+BAT	CPL	$-1.15^{+0.05}_{-0.05}$	-	253^{+26}_{-22}	$0.82^{+0.09}_{-0.09}$	$0.90^{+0.06}_{-0.06}$	$0.87^{+0.05}_{-0.04}$	134/147 (0.91)
KW+2WAM†+BAT	Band	$-1.09^{+0.08}_{-0.07}$	$-2.41^{+0.19}_{-0.46}$	217^{+33}_{-29}	$0.84^{+0.10}_{-0.09}$	$0.93^{+0.07}_{-0.06}$	$0.86^{+0.05}_{-0.04}$	127/146 (0.88)

† The joint fit of two WAM spectra.

Table 29. Spectral parameters: 060904A Reg2

Instrument	Model	α	β	E_{peak} [keV]	C(WAM0)	C(WAM1)	C(BAT)	χ^2/dof
KW	PL	$-1.76^{+0.11}_{-0.11}$	-	-	-	-	-	60/60 (1.01)
KW	CPL	$-0.53^{+0.65}_{-0.51}$	-	113^{+32}_{-20}	-	-	-	36/59 (0.62)
KW	Band	$-0.43^{+1.17}_{-0.59}$	< -2.26	108^{+35}_{-32}	-	-	-	36/58 (0.62)
WAM0	PL	$-1.76^{+0.65}_{-1.03}$	-	-	-	-	-	14/14 (1.06)
WAM0	CPL	-	-	-	-	-	-	-
WAM0	Band	-	-	-	-	-	-	-
WAM3	PL	$-2.38^{+0.38}_{-0.48}$	-	-	-	-	-	32/14 (2.31)
WAM3	CPL	-	-	-	-	-	-	-
WAM3	Band	-	-	-	-	-	-	-
BAT	PL	$-1.62^{+0.07}_{-0.07}$	-	-	-	-	-	67/57 (1.19)
BAT	CPL	$-1.16^{+0.31}_{-0.29}$	-	90^{+66}_{-18}	-	-	-	60/56 (1.08)
BAT	Band	$-1.02^{+0.70}_{-0.50}$	< -1.70	75^{+64}_{-15}	-	-	-	59/55 (1.08)
BAT+WAM0	PL	$-1.62^{+0.07}_{-0.07}$	-	-	$0.57^{+0.27}_{-0.25}$	-	-	82/72 (1.15)
BAT+WAM0	CPL	$-1.31^{+0.30}_{-0.28}$	-	111^{+374}_{-32}	$1.08^{+0.78}_{-0.53}$	-	-	78/71 (1.11)
BAT+WAM0	Band	$-1.01^{+0.73}_{-0.40}$	$-1.91^{+0.21}_{-0.75}$	74^{+64}_{-29}	$0.85^{+0.69}_{-0.40}$	-	-	74/70 (1.07)
BAT+WAM3	PL	$-1.65^{+0.07}_{-0.07}$	-	-	-	$0.70^{+0.16}_{-0.13}$	-	112/72 (1.57)
BAT+WAM3	CPL	$-1.42^{+0.18}_{-0.14}$	-	146^{+106}_{-45}	-	$1.07^{+0.35}_{-0.25}$	-	94/71 (1.33)
BAT+WAM3	Band	$-1.13^{+0.43}_{-0.36}$	< -1.97	87^{+78}_{-24}	-	$1.35^{+0.47}_{-0.36}$	-	92/70 (1.32)
KW+BAT	PL	$-1.66^{+0.06}_{-0.06}$	-	-	-	-	$0.92^{+0.15}_{-0.12}$	131/118 (1.12)
KW+BAT	CPL	$-1.22^{+0.22}_{-0.19}$	-	109^{+44}_{-22}	-	-	$0.76^{+0.11}_{-0.09}$	105/117 (0.90)
KW+BAT	Band	$-1.22^{+0.36}_{-0.18}$	< -2.03	110^{+42}_{-35}	-	-	$0.76^{+0.11}_{-0.09}$	105/116 (0.91)
KW+WAM0	PL	$-1.76^{+0.11}_{-0.11}$	-	-	$0.65^{+0.34}_{-0.29}$	-	-	75/75 (1.01)
KW+WAM0	CPL	$-0.73^{+0.58}_{-0.46}$	-	124^{+42}_{-24}	$0.66^{+0.39}_{-0.33}$	-	-	55/74 (0.75)
KW+WAM0	Band	$-0.26^{+1.36}_{-0.76}$	< -2.13	98^{+48}_{-30}	$0.75^{+0.43}_{-0.36}$	-	-	53/73 (0.73)
KW+WAM3	PL	$-1.82^{+0.10}_{-0.11}$	-	-	-	$0.81^{+0.25}_{-0.18}$	-	100/75 (1.34)
KW+WAM3	CPL	$-1.01^{+0.42}_{-0.34}$	-	146^{+48}_{-29}	-	$0.74^{+0.20}_{-0.15}$	-	73/74 (0.99)
KW+WAM3	Band	$-0.24^{+1.27}_{-0.75}$	$-2.53^{+0.32}_{-0.42}$	97^{+41}_{-26}	-	$0.86^{+0.26}_{-0.19}$	-	69/73 (0.95)
KW+2WAM†+BAT	PL	$-1.69^{+0.06}_{-0.06}$	-	-	$0.59^{+0.28}_{-0.26}$	$0.67^{+0.15}_{-0.13}$	$0.91^{+0.14}_{-0.11}$	190/148 (1.29)
KW+2WAM†+BAT	CPL	$-1.36^{+0.15}_{-0.13}$	-	143^{+58}_{-32}	$0.72^{+0.37}_{-0.33}$	$0.83^{+0.21}_{-0.17}$	$0.79^{+0.12}_{-0.09}$	156/147 (1.06)
KW+2WAM†+BAT	Band	$-1.16^{+0.35}_{-0.29}$	< -2.06	100^{+76}_{-26}	$0.82^{+0.44}_{-0.38}$	$0.95^{+0.26}_{-0.20}$	$0.77^{+0.11}_{-0.09}$	154/146 (1.06)

† The joint fit of two WAM spectra.

Table 30. Spectral parameters: 060904A Reg12

Instrument	Model	α	β	E_{peak} [keV]	C(WAM0)	C(WAM1)	C(BAT)	χ^2/dof
KW	PL	$-1.69^{+0.04}_{-0.04}$	-	-	-	-	-	120/60 (2.02)
KW	CPL	$-0.97^{+0.17}_{-0.16}$	-	165^{+25}_{-19}	-	-	-	32/59 (0.56)
KW	Band	$-0.95^{+0.20}_{-0.16}$	< -2.42	162^{+24}_{-23}	-	-	-	31/58 (0.55)
WAM0	PL	$-2.06^{+0.22}_{-0.26}$	-	-	-	-	-	14/14 (1.06)
WAM0	CPL	$-0.57^{+2.12}_{-1.33}$	-	333^{+163}_{-169}	-	-	-	10/13 (0.84)
WAM0	Band	$0.80^{+4.20}_{-2.63}$	< -2.08	285^{+187}_{-96}	-	-	-	10/12 (0.89)
WAM3	PL	$-2.14^{+0.10}_{-0.11}$	-	-	-	-	-	15/14 (1.13)
WAM3	CPL	$-1.73^{+0.44}_{-0.21}$	-	< 300	-	-	-	11/13 (0.89)
WAM3	Band	$-1.72^{+0.43}_{-0.26}$	< -2.24	211^{+89}_{-102}	-	-	-	11/12 (0.96)
BAT	PL	$-1.40^{+0.04}_{-0.04}$	-	-	-	-	-	40/57 (0.71)
BAT	CPL	-	-	-	-	-	-	-
BAT	Band	-	-	-	-	-	-	-
BAT+WAM0	PL	$-1.43^{+0.04}_{-0.04}$	-	-	$0.52^{+0.08}_{-0.07}$	-	-	83/72 (1.17)
BAT+WAM0	CPL	$-1.29^{+0.07}_{-0.06}$	-	362^{+208}_{-105}	$0.80^{+0.15}_{-0.13}$	-	-	53/71 (0.75)
BAT+WAM0	Band	$-1.30^{+0.09}_{-0.05}$	< -2.03	395^{+208}_{-107}	$0.79^{+0.15}_{-0.13}$	-	-	53/70 (0.76)
BAT+WAM3	PL	$-1.53^{+0.03}_{-0.03}$	-	-	-	$0.79^{+0.07}_{-0.06}$	-	220/72 (3.07)
BAT+WAM3	CPL	$-1.25^{+0.06}_{-0.05}$	-	274^{+48}_{-37}	-	$0.98^{+0.08}_{-0.08}$	-	57/71 (0.81)
BAT+WAM3	Band	$-1.25^{+0.07}_{-0.06}$	< -4.3	273^{+48}_{-37}	-	$0.98^{+0.08}_{-0.08}$	-	57/70 (0.82)
KW+BAT	PL	$-1.53^{+0.03}_{-0.03}$	-	-	-	-	$0.99^{+0.06}_{-0.06}$	235/118 (1.99)
KW+BAT	CPL	$-1.13^{+0.08}_{-0.07}$	-	188^{+30}_{-23}	-	-	$0.82^{+0.05}_{-0.04}$	83/117 (0.72)
KW+BAT	Band	$-1.13^{+0.08}_{-0.07}$	< -2.45	186^{+29}_{-23}	-	-	$0.82^{+0.05}_{-0.04}$	83/116 (0.72)
KW+WAM0	PL	$-1.70^{+0.04}_{-0.04}$	-	-	$0.82^{+0.12}_{-0.11}$	-	-	143/75 (1.92)
KW+WAM0	CPL	$-1.09^{+0.15}_{-0.14}$	-	189^{+31}_{-23}	$0.84^{+0.12}_{-0.11}$	-	-	54/74 (0.74)
KW+WAM0	Band	$-1.02^{+0.27}_{-0.17}$	$-2.60^{+0.39}_{-1.50}$	170^{+34}_{-39}	$0.85^{+0.13}_{-0.11}$	-	-	51/73 (0.71)
KW+WAM3	PL	$-1.77^{+0.04}_{-0.04}$	-	-	-	$1.05^{+0.10}_{-0.08}$	-	190/75 (2.54)
KW+WAM3	CPL	$-1.23^{+0.11}_{-0.10}$	-	223^{+28}_{-23}	-	$0.90^{+0.07}_{-0.07}$	-	61/74 (0.83)
KW+WAM3	Band	$-0.97^{+0.30}_{-0.20}$	$-2.28^{+0.14}_{-0.26}$	156^{+41}_{-35}	-	$0.95^{+0.10}_{-0.08}$	-	54/73 (0.74)
KW+2WAM†+BAT	PL	$-1.60^{+0.02}_{-0.03}$	-	-	$0.71^{+0.09}_{-0.09}$	$0.84^{+0.06}_{-0.05}$	$0.93^{+0.05}_{-0.05}$	395/148 (2.67)
KW+2WAM†+BAT	CPL	$-1.22^{+0.05}_{-0.05}$	-	235^{+27}_{-23}	$0.80^{+0.10}_{-0.10}$	$0.88^{+0.06}_{-0.06}$	$0.84^{+0.05}_{-0.04}$	120/147 (0.82)
KW+2WAM†+BAT	Band	$-1.17^{+0.09}_{-0.08}$	< -2.22	204^{+42}_{-33}	$0.82^{+0.11}_{-0.10}$	$0.90^{+0.07}_{-0.07}$	$0.83^{+0.05}_{-0.04}$	117/146 (0.81)

† The joint fit of two WAM spectra.

Table 31. Spectral parameters: 060912 Reg1

Instrument	Model	α	β	E_{peak} [keV]	C(WAM2)	C(BAT)	χ^2/dof
KW	PL	$-1.92^{+0.15}_{-0.16}$	-	-	-	-	63/60 (1.06)
KW	CPL	-	-	-	-	-	-
KW	Band	-	-	-	-	-	-
WAM2	PL	$-1.71^{+0.51}_{-0.78}$	-	-	-	-	8/14 (0.58)
WAM2	CPL	-	-	-	-	-	-
WAM2	Band	-	-	-	-	-	-
BAT	PL	$-1.82^{+0.10}_{-0.10}$	-	-	-	-	57/57 (1.01)
BAT	CPL	-	-	-	-	-	-
BAT	Band	-	-	-	-	-	-
BAT+WAM2	PL	$-1.81^{+0.10}_{-0.10}$	-	-	$0.91^{+0.34}_{-0.28}$	-	65/72 (0.91)
BAT+WAM2	CPL	-	-	-	-	-	-
BAT+WAM2	Band	-	-	-	-	-	-
KW+BAT	PL	$-1.85^{+0.08}_{-0.08}$	-	-	-	$0.79^{+0.15}_{-0.11}$	121/118 (1.03)
KW+BAT	CPL	-	-	-	-	-	-
KW+BAT	Band	-	-	-	-	-	-
KW+WAM2	PL	$-1.91^{+0.15}_{-0.16}$	-	-	$0.82^{+0.33}_{-0.25}$	-	72/75 (0.96)
KW+WAM2	CPL	-	-	-	-	-	-
KW+WAM2	Band	-	-	-	-	-	-
KW+WAM2+BAT	PL	$-1.85^{+0.08}_{-0.08}$	-	-	$0.77^{+0.26}_{-0.22}$	$0.79^{+0.15}_{-0.11}$	130/133 (0.98)
KW+WAM2+BAT	CPL	-	-	-	-	-	-
KW+WAM2+BAT	Band	-	-	-	-	-	-

Table 32. Spectral parameters: 061006 Reg1

Instrument	Model	α	β	E_{peak} [keV]	C(WAM3)	C(BAT)	$\chi^2/$dof
KW	PL	$-1.20^{+0.06}_{-0.06}$	-	-	-	-	87/31 (2.81)
KW	CPL	$-0.51^{+0.22}_{-0.19}$	-	592^{+166}_{-115}	-	-	37/30 (1.25)
KW	Band	$-0.51^{+0.22}_{-0.19}$	-*	592^{+166}_{-94}	-	-	37/29 (1.29)
WAM3	PL	$-1.59^{+0.06}_{-0.07}$	-	-	-	-	65/24 (2.72)
WAM3	CPL	$-0.64^{+0.33}_{-0.29}$	-	795^{+170}_{-116}	-	-	22/23 (0.96)
WAM3	Band	$-0.44^{+0.57}_{-0.41}$	<-2.07	693^{+209}_{-150}	-	-	20/22 (0.93)
BAT	PL	$-0.61^{+0.09}_{-0.09}$	-	-	-	-	60/57 (1.07)
BAT	CPL	-	-	-	-	-	-
BAT	Band	-	-	-	-	-	-
BAT+WAM3	PL	$-1.34^{+0.05}_{-0.06}$	-	-	$1.58^{+0.33}_{-0.22}$	-	334/82 (4.08)
BAT+WAM3	CPL	$-0.50^{+0.11}_{-0.10}$	-	753^{+95}_{-81}	$0.65^{+0.10}_{-0.09}$	-	83/81 (1.03)
BAT+WAM3	Band	$-0.47^{+0.12}_{-0.11}$	<-2.09	702^{+110}_{-98}	$0.65^{+0.10}_{-0.09}$	-	81/80 (1.01)
KW+BAT	PL	$-1.01^{+0.05}_{-0.06}$	-	-	-	$1.00^{+0.18}_{-0.16}$	225/89 (2.53)
KW+BAT	CPL	$-0.45^{+0.12}_{-0.11}$	-	572^{+122}_{-97}	-	$0.88^{+0.12}_{-0.10}$	98/88 (1.12)
KW+BAT	Band	$-0.45^{+0.12}_{-0.11}$	<-2.08	572^{+122}_{-65}	-	$0.88^{+0.12}_{-0.10}$	98/87 (1.13)
KW+WAM3	PL	$-1.41^{+0.04}_{-0.05}$	-	-	$1.03^{+0.17}_{-0.12}$	-	208/56 (3.72)
KW+WAM3	CPL	$-0.63^{+0.16}_{-0.14}$	-	749^{+108}_{-87}	$0.67^{+0.08}_{-0.07}$	-	62/55 (1.14)
KW+WAM3	Band	$-0.60^{+0.18}_{-0.15}$	<-2.18	712^{+118}_{-103}	$0.66^{+0.08}_{-0.06}$	-	61/54 (1.14)
KW+WAM3+BAT	PL	$-1.28^{+0.04}_{-0.04}$	-	-	$0.80^{+0.12}_{-0.08}$	$0.61^{+0.07}_{-0.07}$	431/114 (3.79)
KW+WAM3+BAT	CPL	$-0.52^{+0.10}_{-0.09}$	-	711^{+81}_{-69}	$0.64^{+0.07}_{-0.06}$	$0.93^{+0.12}_{-0.10}$	125/113 (1.11)
KW+WAM3+BAT	Band	$-0.50^{+0.10}_{-0.10}$	<-2.16	675^{+90}_{-84}	$0.65^{+0.07}_{-0.06}$	$0.93^{+0.12}_{-0.10}$	123/112 (1.10)

* The parameter is not constrained.

Table 33. Spectral parameters: 061007 Reg1

Instrument	Model	α	β	E_{peak} [keV]	C(WAM2)	C(WAM3)	C(BAT)	χ^2/dof
KW	PL	$-1.56^{+0.03}_{-0.03}$	-	-	-	-	-	328/66 (4.98)
KW	CPL	$-0.69^{+0.13}_{-0.12}$	-	284^{+29}_{-24}	-	-	-	71/65 (1.10)
KW	Band	$-0.51^{+0.23}_{-0.18}$	$-2.38^{+0.22}_{-0.39}$	239^{+35}_{-34}	-	-	-	58/64 (0.92)
WAM2	PL	$-2.23^{+0.00}_{-0.12}$	-	-	-	-	-	19/25 (0.77)
WAM2	CPL	$-1.98^{+0.36}_{-0.01}$	-	< 421	-	-	-	16/24 (0.68)
WAM2	Band	$-1.47^{+6.47}_{-1.01}$	< -2.20	< 415	-	-	-	16/23 (0.71)
WAM3	PL	$-2.15^{+0.07}_{-0.07}$	-	-	-	-	-	43/25 (1.76)
WAM3	CPL	$-1.56^{+0.46}_{-0.30}$	-	367^{+83}_{-132}	-	-	-	22/24 (0.92)
WAM3	Band	$-1.15^{+0.95}_{-0.43}$	$-2.75^{+0.32}_{-0.62}$	362^{+47}_{-54}	-	-	-	17/23 (0.78)
BAT	PL	$-1.05^{+0.05}_{-0.05}$	-	-	-	-	-	46/57 (0.82)
BAT	CPL	$-0.88^{+0.20}_{-0.19}$	-	> 235	-	-	-	44/56 (0.79)
BAT	Band	-	-	-	-	-	-	-
BAT+WAM2	PL	$-1.21^{+0.05}_{-0.06}$	-	-	$0.19^{+0.07}_{-0.05}$	-	-	357/83 (4.30)
BAT+WAM2	CPL	$-0.88^{+0.07}_{-0.07}$	-	388^{+76}_{-56}	$0.97^{+0.18}_{-0.16}$	-	-	72/82 (0.88)
BAT+WAM2	Band	$-0.81^{+0.12}_{-0.09}$	$-2.45^{+0.22}_{-0.38}$	300^{+78}_{-75}	$1.13^{+0.27}_{-0.20}$	-	-	61/81 (0.76)
BAT+WAM3	PL	$-1.51^{+0.04}_{-0.05}$	-	-	-	$0.80^{+0.18}_{-0.11}$	-	620/83 (7.48)
BAT+WAM3	CPL	$-0.88^{+0.07}_{-0.06}$	-	384^{+43}_{-36}	-	$0.98^{+0.12}_{-0.11}$	-	71/82 (0.88)
BAT+WAM3	Band	$-0.86^{+0.07}_{-0.07}$	$-2.71^{+0.28}_{-0.51}$	356^{+45}_{-45}	-	$1.02^{+0.13}_{-0.12}$	-	62/81 (0.77)
KW+BAT	PL	$-1.46^{+0.02}_{-0.02}$	-	-	-	-	$0.86^{+0.04}_{-0.05}$	603/124 (4.87)
KW+BAT	CPL	$-0.78^{+0.07}_{-0.07}$	-	298^{+27}_{-24}	-	-	$0.93^{+0.04}_{-0.04}$	118/123 (0.96)
KW+BAT	Band	$-0.73^{+0.08}_{-0.08}$	$-2.50^{+0.27}_{-0.49}$	273^{+29}_{-28}	-	-	$0.93^{+0.04}_{-0.04}$	110/122 (0.90)
KW+WAM2	PL	$-1.61^{+0.02}_{-0.03}$	-	-	$0.72^{+0.09}_{-0.08}$	-	-	462/92 (5.03)
KW+WAM2	CPL	$-0.82^{+0.11}_{-0.10}$	-	318^{+30}_{-25}	$1.06^{+0.10}_{-0.10}$	-	-	107/91 (1.19)
KW+WAM2	Band	$-0.52^{+0.22}_{-0.18}$	$-2.36^{+0.14}_{-0.20}$	241^{+34}_{-31}	$1.09^{+0.11}_{-0.10}$	-	-	76/90 (0.85)
KW+WAM3	PL	$-1.66^{+0.02}_{-0.03}$	-	-	-	$0.92^{+0.09}_{-0.07}$	-	580/92 (6.31)
KW+WAM3	CPL	$-0.87^{+0.09}_{-0.09}$	-	340^{+26}_{-22}	-	$1.02^{+0.07}_{-0.07}$	-	111/91 (1.22)
KW+WAM3	Band	$-0.66^{+0.20}_{-0.15}$	$-2.42^{+0.16}_{-0.23}$	272^{+37}_{-38}	-	$1.06^{+0.08}_{-0.07}$	-	87/90 (0.98)
KW+2WAM†+BAT	PL	$-1.58^{+0.02}_{-0.03}$	-	-	$0.67^{+0.09}_{-0.06}$	$0.76^{+0.07}_{-0.05}$	$0.73^{+0.03}_{-0.04}$	1092/176 (6.21)
KW+2WAM†+BAT	CPL	$-0.87^{+0.06}_{-0.05}$	-	346^{+22}_{-20}	$1.02^{+0.09}_{-0.09}$	$1.01^{+0.07}_{-0.06}$	$0.94^{+0.05}_{-0.04}$	185/175 (1.06)
KW+2WAM†+BAT	Band	$-0.78^{+0.08}_{-0.07}$	$-2.47^{+0.14}_{-0.19}$	292^{+27}_{-27}	$1.06^{+0.10}_{-0.09}$	$1.06^{+0.07}_{-0.07}$	$0.93^{+0.04}_{-0.04}$	151/174 (0.87)

$\dagger$ The joint fit of two WAM spectra.

Table 34. Spectral parameters: 061007 Reg2

Instrument	Model	α	β	E_{peak} [keV]	C(WAM2)	C(WAM3)	C(BAT)	χ^2/dof
KW	PL	-1.47	-	-	-	-	-	3121/86 (36.30)
KW	CPL	$-0.59^{+0.04}_{-0.04}$	-	504^{+19}_{-18}	-	-	-	117/85 (1.38)
KW	Band	$-0.51^{+0.05}_{-0.05}$	$-2.61^{+0.14}_{-0.21}$	452^{+25}_{-23}	-	-	-	82/84 (0.99)
WAM2	PL	$-2.20^{+0.03}_{-0.03}$	-	-	-	-	-	231/25 (9.25)
WAM2	CPL	$-1.34^{+0.18}_{-0.16}$	-	508^{+38}_{-39}	-	-	-	50/24 (2.11)
WAM2	Band	$-0.76^{+0.41}_{-0.30}$	$-2.76^{+0.13}_{-0.17}$	463^{+33}_{-33}	-	-	-	16/23 (0.70)
WAM3	PL	-2.11	-	-	-	-	-	738/25 (29.52)
WAM3	CPL	$-0.98^{+0.13}_{-0.12}$	-	590^{+24}_{-22}	-	-	-	108/24 (4.51)
WAM3	Band	$-0.53^{+0.23}_{-0.20}$	$-2.81^{+0.11}_{-0.14}$	530^{+25}_{-24}	-	-	-	37/23 (1.62)
BAT	PL	$-0.85^{+0.03}_{-0.03}$	-	-	-	-	-	36/57 (0.64)
BAT	CPL	-	-	-	-	-	-	-
BAT	Band	-	-	-	-	-	-	-
BAT+WAM2	PL	-1.44	-	-	0.86	-	-	3253/83 (39.20)
BAT+WAM2	CPL	$-0.71^{+0.03}_{-0.03}$	-	536^{+27}_{-25}	$1.15^{+0.08}_{-0.08}$	-	-	132/82 (1.62)
BAT+WAM2	Band	$-0.67^{+0.04}_{-0.04}$	$-2.77^{+0.12}_{-0.16}$	470^{+30}_{-28}	$1.27^{+0.10}_{-0.09}$	-	-	72/81 (0.90)
BAT+WAM3	PL	-1.80	-	-	-	4.31	-	4392/83 (52.92)
BAT+WAM3	CPL	$-0.72^{+0.03}_{-0.03}$	-	590^{+21}_{-21}	-	$1.14^{+0.06}_{-0.06}$	-	169/82 (2.07)
BAT+WAM3	Band	$-0.69^{+0.03}_{-0.03}$	$-2.86^{+0.11}_{-0.14}$	542^{+23}_{-22}	-	$1.18^{+0.07}_{-0.06}$	-	91/81 (1.13)
KW+BAT	PL	-1.43	-	-	-	-	0.70	4387/144 (30.47)
KW+BAT	CPL	$-0.64^{+0.03}_{-0.03}$	-	522^{+18}_{-17}	-	-	$0.87^{+0.02}_{-0.02}$	179/143 (1.26)
KW+BAT	Band	$-0.62^{+0.03}_{-0.03}$	$-2.81^{+0.21}_{-0.30}$	496^{+22}_{-22}	-	-	$0.87^{+0.02}_{-0.02}$	157/142 (1.11)
KW+WAM2	PL	-1.52	-	-	0.74	-	-	4924/112 (43.97)
KW+WAM2	CPL	$-0.62^{+0.03}_{-0.03}$	-	518^{+16}_{-15}	$0.97^{+0.03}_{-0.03}$	-	-	205/111 (1.85)
KW+WAM2	Band	$-0.52^{+0.05}_{-0.04}$	$-2.70^{+0.09}_{-0.11}$	456^{+19}_{-18}	$1.00^{+0.03}_{-0.03}$	-	-	101/110 (0.92)
KW+WAM3	PL	-1.60	-	-	-	1.11	-	6611/112 (59.03)
KW+WAM3	CPL	$-0.67^{+0.03}_{-0.03}$	-	553^{+14}_{-14}	-	$1.01^{+0.03}_{-0.02}$	-	263/111 (2.37)
KW+WAM3	Band	$-0.59^{+0.04}_{-0.04}$	$-2.76^{+0.09}_{-0.11}$	498^{+17}_{-17}	-	$1.04^{+0.03}_{-0.03}$	-	137/110 (1.25)
KW+2WAM†+BAT	PL	-1.58	-	-	0.90	1.07	0.57	9911/196 (50.57)
KW+2WAM†+BAT	CPL	$-0.68^{+0.02}_{-0.02}$	-	553^{+12}_{-12}	$0.94^{+0.03}_{-0.03}$	$1.02^{+0.03}_{-0.02}$	$0.87^{+0.02}_{-0.02}$	399/195 (2.05)
KW+2WAM†+BAT	Band	$-0.63^{+0.03}_{-0.03}$	$-2.79^{+0.08}_{-0.09}$	503^{+14}_{-14}	$0.97^{+0.03}_{-0.03}$	$1.05^{+0.03}_{-0.03}$	$0.87^{+0.02}_{-0.02}$	225/194 (1.16)

† The joint fit of two WAM spectra.

Table 35. Spectral parameters: 061007 Reg3

Instrument	Model	α	β	E_{peak} [keV]	C(WAM2)	C(WAM3)	C(BAT)	χ^2/dof
KW	PL	-1.54	-	-	-	-	-	2463/86 (28.64)
KW	CPL	$-0.70^{+0.04}_{-0.04}$	-	389^{+15}_{-14}	-	-	-	108/85 (1.28)
KW	Band	$-0.64^{+0.05}_{-0.05}$	$-2.74^{+0.18}_{-0.26}$	361^{+18}_{-17}	-	-	-	87/84 (1.04)
WAM2	PL	$-2.31^{+0.04}_{-0.04}$	-	-	-	-	-	87/25 (3.51)
WAM2	CPL	$-1.54^{+0.29}_{-0.27}$	-	321^{+59}_{-112}	-	-	-	42/24 (1.77)
WAM2	Band	$-0.83^{+0.91}_{-0.51}$	$-2.75^{+0.14}_{-0.21}$	347^{+30}_{-33}	-	-	-	17/23 (0.78)
WAM3	PL	-2.24	-	-	-	-	-	388/25 (15.56)
WAM3	CPL	$-0.91^{+0.19}_{-0.17}$	-	427^{+20}_{-21}	-	-	-	32/24 (1.37)
WAM3	Band	$-0.74^{+0.26}_{-0.22}$	$-3.25^{+0.24}_{-0.41}$	419^{+20}_{-19}	-	-	-	17/23 (0.77)
BAT	PL	$-1.01^{+0.02}_{-0.02}$	-	-	-	-	-	30/57 (0.54)
BAT	CPL	-	-	-	-	-	-	-
BAT	Band	-	-	-	-	-	-	-
BAT+WAM2	PL	-1.16	-	-	0.15	-	-	1941/83 (23.39)
BAT+WAM2	CPL	$-0.81^{+0.03}_{-0.03}$	-	410^{+26}_{-23}	$1.16^{+0.09}_{-0.09}$	-	-	98/82 (1.20)
BAT+WAM2	Band	$-0.78^{+0.04}_{-0.03}$	$-2.79^{+0.15}_{-0.20}$	364^{+30}_{-27}	$1.27^{+0.11}_{-0.11}$	-	-	62/81 (0.77)
BAT+WAM3	PL	-1.51	-	-	-	0.85	-	4103/83 (49.44)
BAT+WAM3	CPL	$-0.82^{+0.03}_{-0.03}$	-	434^{+18}_{-17}	-	$1.17^{+0.06}_{-0.06}$	-	72/82 (0.88)
BAT+WAM3	Band	$-0.81^{+0.03}_{-0.03}$	$-3.30^{+0.25}_{-0.42}$	422^{+20}_{-19}	-	$1.19^{+0.07}_{-0.07}$	-	57/81 (0.71)
KW+BAT	PL	-1.47	-	-	-	-	0.79	3929/144 (27.29)
KW+BAT	CPL	$-0.77^{+0.03}_{-0.03}$	-	407^{+14}_{-14}	-	-	$0.86^{+0.02}_{-0.02}$	162/143 (1.13)
KW+BAT	Band	$-0.75^{+0.03}_{-0.03}$	$-2.91^{+0.24}_{-0.45}$	392^{+17}_{-16}	-	-	$0.86^{+0.02}_{-0.02}$	150/142 (1.06)
KW+WAM2	PL	-1.57	-	-	0.61	-	-	3416/112 (30.51)
KW+WAM2	CPL	$-0.72^{+0.04}_{-0.04}$	-	396^{+13}_{-12}	$0.97^{+0.04}_{-0.04}$	-	-	171/111 (1.54)
KW+WAM2	Band	$-0.63^{+0.05}_{-0.05}$	$-2.75^{+0.11}_{-0.14}$	358^{+15}_{-14}	$1.00^{+0.04}_{-0.04}$	-	-	105/110 (0.96)
KW+WAM3	PL	-1.62	-	-	-	0.85	-	4677/112 (41.76)
KW+WAM3	CPL	$-0.75^{+0.03}_{-0.03}$	-	412^{+11}_{-11}	-	$1.01^{+0.03}_{-0.03}$	-	153/111 (1.39)
KW+WAM3	Band	$-0.70^{+0.04}_{-0.04}$	$-3.05^{+0.16}_{-0.22}$	391^{+13}_{-13}	-	$1.03^{+0.03}_{-0.03}$	-	118/110 (1.08)
KW+2WAM†+BAT	PL	-1.56	-	-	0.59	0.72	0.71	7535/196 (38.45)
KW+2WAM†+BAT	CPL	$-0.78^{+0.02}_{-0.02}$	-	417^{+10}_{-10}	$0.95^{+0.04}_{-0.04}$	$1.02^{+0.03}_{-0.03}$	$0.86^{+0.02}_{-0.02}$	259/195 (1.33)
KW+2WAM†+BAT	Band	$-0.76^{+0.02}_{-0.02}$	$-3.00^{+0.13}_{-0.16}$	396^{+12}_{-11}	$0.97^{+0.04}_{-0.04}$	$1.04^{+0.03}_{-0.03}$	$0.86^{+0.02}_{-0.02}$	199/194 (1.03)

$\dagger$ The joint fit of two WAM spectra.

Table 36. Spectral parameters: 061007 Reg4

Instrument	Model	α	β	E_{peak} [keV]	C(WAM2)	C(WAM3)	C(BAT)	χ^2/dof
KW	PL	-1.51	-	-	-	-	-	4518/86 (52.54)
KW	CPL	$-0.67^{+0.03}_{-0.03}$	-	436^{+13}_{-12}	-	-	-	152/85 (1.80)
KW	Band	$-0.60^{+0.04}_{-0.04}$	$-2.68^{+0.13}_{-0.17}$	400^{+16}_{-15}	-	-	-	111/84 (1.33)
WAM2	PL	$-2.29^{+0.03}_{-0.03}$	-	-	-	-	-	179/25 (7.19)
WAM2	CPL	$-1.53^{+0.20}_{-0.18}$	-	386^{+49}_{-67}	-	-	-	62/24 (2.59)
WAM2	Band	$-0.80^{+0.57}_{-0.36}$	$-2.74^{+0.11}_{-0.14}$	397^{+28}_{-27}	-	-	-	15/23 (0.69)
WAM3	PL	-2.23	-	-	-	-	-	710/25 (28.41)
WAM3	CPL	$-0.97^{+0.14}_{-0.13}$	-	488^{+19}_{-19}	-	-	-	86/24 (3.62)
WAM3	Band	$-0.63^{+0.22}_{-0.19}$	$-2.99^{+0.12}_{-0.16}$	469^{+18}_{-17}	-	-	-	30/23 (1.32)
BAT	PL	$-0.94^{+0.02}_{-0.02}$	-	-	-	-	-	18/57 (0.33)
BAT	CPL	-	-	-	-	-	-	-
BAT	Band	-	-	-	-	-	-	-
BAT+WAM2	PL	-1.29	-	-	0.32	-	-	3624/83 (43.66)
BAT+WAM2	CPL	$-0.78^{+0.03}_{-0.03}$	-	476^{+24}_{-22}	$1.11^{+0.07}_{-0.07}$	-	-	133/82 (1.63)
BAT+WAM2	Band	$-0.73^{+0.03}_{-0.03}$	$-2.76^{+0.11}_{-0.14}$	412^{+27}_{-25}	$1.25^{+0.10}_{-0.09}$	-	-	60/81 (0.75)
BAT+WAM3	PL	-1.73	-	-	-	2.32	-	6185/83 (74.53)
BAT+WAM3	CPL	$-0.78^{+0.03}_{-0.03}$	-	501^{+16}_{-16}	-	$1.14^{+0.05}_{-0.05}$	-	128/82 (1.56)
BAT+WAM3	Band	$-0.76^{+0.03}_{-0.03}$	$-3.03^{+0.13}_{-0.17}$	473^{+18}_{-17}	-	$1.18^{+0.06}_{-0.06}$	-	69/81 (0.86)
KW+BAT	PL	-1.46	-	-	-	-	0.75	6253/144 (43.43)
KW+BAT	CPL	$-0.71^{+0.02}_{-0.02}$	-	450^{+12}_{-12}	-	-	$0.87^{+0.01}_{-0.01}$	205/143 (1.44)
KW+BAT	Band	$-0.69^{+0.03}_{-0.03}$	$-2.82^{+0.18}_{-0.27}$	429^{+15}_{-15}	-	-	$0.86^{+0.01}_{-0.01}$	178/142 (1.26)
KW+WAM2	PL	-1.54	-	-	0.63	-	-	6428/112 (57.39)
KW+WAM2	CPL	$-0.70^{+0.03}_{-0.03}$	-	449^{+11}_{-11}	$0.97^{+0.03}_{-0.03}$	-	-	259/111 (2.33)
KW+WAM2	Band	$-0.60^{+0.04}_{-0.03}$	$-2.71^{+0.08}_{-0.10}$	400^{+13}_{-12}	$1.01^{+0.03}_{-0.03}$	-	-	128/110 (1.17)
KW+WAM3	PL	-1.59	-	-	-	0.91	-	8944/112 (79.86)
KW+WAM3	CPL	$-0.73^{+0.02}_{-0.02}$	-	469^{+10}_{-10}	-	$1.02^{+0.02}_{-0.02}$	-	275/111 (2.48)
KW+WAM3	Band	$-0.67^{+0.03}_{-0.03}$	$-2.88^{+0.09}_{-0.11}$	434^{+12}_{-12}	-	$1.05^{+0.03}_{-0.02}$	-	164/110 (1.50)
KW+2WAM†+BAT	PL	-1.57	-	-	0.69	0.84	0.66	12997/196 (66.31)
KW+2WAM†+BAT	CPL	$-0.75^{+0.02}_{-0.02}$	-	473^{+9}_{-9}	$0.94^{+0.03}_{-0.03}$	$1.02^{+0.02}_{-0.02}$	$0.87^{+0.01}_{-0.01}$	413/195 (2.12)
KW+2WAM†+BAT	Band	$-0.70^{+0.02}_{-0.02}$	$-2.87^{+0.08}_{-0.09}$	438^{+10}_{-10}	$0.97^{+0.03}_{-0.03}$	$1.05^{+0.02}_{-0.02}$	$0.87^{+0.01}_{-0.01}$	242/194 (1.25)

$\dagger$ The joint fit of two WAM spectra.

Table 37. Spectral parameters: 061007 Reg5

Instrument	Model	α	β	E_{peak} [keV]	C(WAM2)	C(WAM3)	C(BAT)	χ^2/dof
KW	PL	$-1.77^{+0.16}_{-0.19}$	-	-	-	-	-	73/86 (0.85)
KW	CPL	-	-	-	-	-	-	-
KW	Band	-	-	-	-	-	-	-
WAM2	PL	$-2.16^{+0.51}_{-0.82}$	-	-	-	-	-	10/15 (0.72)
WAM2	CPL	-	-	-	-	-	-	-
WAM2	Band	-	-	-	-	-	-	-
WAM3	PL	$-2.37^{+0.43}_{-0.63}$	-	-	-	-	-	8/15 (0.55)
WAM3	CPL	-	-	-	-	-	-	-
WAM3	Band	-	-	-	-	-	-	-
BAT	PL	$-1.62^{+0.07}_{-0.07}$	-	-	-	-	-	55/57 (0.97)
BAT	CPL	-	-	-	-	-	-	-
BAT	Band	-	-	-	-	-	-	-
BAT+WAM2	PL	$-1.64^{+0.07}_{-0.07}$	-	-	$0.83^{+0.50}_{-0.41}$	-	-	68/73 (0.94)
BAT+WAM2	CPL	-	-	-	-	-	-	-
BAT+WAM2	Band	-	-	-	-	-	-	-
BAT+WAM3	PL	$-1.65^{+0.07}_{-0.07}$	-	-	-	$0.80^{+0.34}_{-0.27}$	-	72/73 (1.00)
BAT+WAM3	CPL	$-1.55^{+0.14}_{-0.10}$	-	290^{+636}_{-146}	-	$1.32^{+0.67}_{-0.51}$	-	63/72 (0.88)
BAT+WAM3	Band	-	-	-	-	-	-	-
KW+BAT	PL	$-1.65^{+0.07}_{-0.07}$	-	-	-	-	$0.86^{+0.16}_{-0.12}$	129/144 (0.90)
KW+BAT	CPL	-	-	-	-	-	-	-
KW+BAT	Band	-	-	-	-	-	-	-
KW+WAM2	PL	$-1.81^{+0.16}_{-0.18}$	-	-	$1.04^{+0.73}_{-0.52}$	-	-	85/102 (0.84)
KW+WAM2	CPL	-	-	-	-	-	-	-
KW+WAM2	Band	-	-	-	-	-	-	-
KW+WAM3	PL	$-1.88^{+0.16}_{-0.18}$	-	-	-	$1.02^{+0.55}_{-0.37}$	-	86/102 (0.84)
KW+WAM3	CPL	$-1.65^{+0.38}_{-0.28}$	-	>135	-	$1.08^{+0.50}_{-0.36}$	-	82/101 (0.82)
KW+WAM3	Band	-	-	-	-	-	-	-
KW+2WAM†+BAT	PL	$-1.68^{+0.06}_{-0.07}$	-	-	$0.79^{+0.44}_{-0.38}$	$0.72^{+0.29}_{-0.24}$	$0.83^{+0.15}_{-0.12}$	160/176 (0.91)
KW+2WAM†+BAT	CPL	$-1.57^{+0.11}_{-0.09}$	-	352^{+524}_{-157}	$1.22^{+0.66}_{-0.54}$	$1.01^{+0.40}_{-0.32}$	$0.81^{+0.15}_{-0.11}$	148/175 (0.85)
KW+2WAM†+BAT	Band	$-1.57^{+0.07}_{-0.08}$	<-4.0	352^{+525}_{-134}	$1.22^{+0.64}_{-0.53}$	$1.02^{+0.28}_{-0.31}$	$0.81^{+0.11}_{-0.11}$	148/174 (0.85)

† The joint fit of two WAM spectra.

Table 38. Spectral parameters: 061007 Reg15

Instrument	Model	α	β	E_{peak} [keV]	C(WAM2)	C(WAM3)	C(BAT)	χ^2/dof
KW	PL	-1.50	-	-	-	-	-	2968/86 (34.52)
KW	CPL	$-0.71^{+0.04}_{-0.04}$	-	419^{+15}_{-14}	-	-	-	131/85 (1.55)
KW	Band	$-0.63^{+0.05}_{-0.05}$	$-2.53^{+0.13}_{-0.17}$	377^{+18}_{-17}	-	-	-	92/84 (1.10)
WAM2	PL	$-2.28^{+0.04}_{-0.04}$	-	-	-	-	-	108/25 (4.34)
WAM2	CPL	$-1.62^{+0.22}_{-0.19}$	-	368^{+70}_{-105}	-	-	-	38/24 (1.62)
WAM2	Band	$-0.89^{+0.74}_{-0.43}$	$-2.69^{+0.13}_{-0.18}$	392^{+36}_{-34}	-	-	-	12/23 (0.54)
WAM3	PL	-2.21	-	-	-	-	-	444/25 (17.79)
WAM3	CPL	$-1.07^{+0.16}_{-0.15}$	-	482^{+24}_{-24}	-	-	-	63/24 (2.64)
WAM3	Band	$-0.71^{+0.25}_{-0.22}$	$-2.92^{+0.14}_{-0.20}$	461^{+22}_{-21}	-	-	-	27/23 (1.19)
BAT	PL	$-0.99^{+0.02}_{-0.02}$	-	-	-	-	-	26/57 (0.47)
BAT	CPL	-	-	-	-	-	-	-
BAT	Band	-	-	-	-	-	-	-
BAT+WAM2	PL	-1.23	-	-	0.25	-	-	2431/83 (29.29)
BAT+WAM2	CPL	$-0.83^{+0.03}_{-0.03}$	-	483^{+32}_{-29}	$1.06^{+0.09}_{-0.08}$	-	-	107/82 (1.31)
BAT+WAM2	Band	$-0.79^{+0.03}_{-0.03}$	$-2.72^{+0.13}_{-0.17}$	412^{+35}_{-32}	$1.21^{+0.11}_{-0.10}$	-	-	60/81 (0.74)
BAT+WAM3	PL	-1.62	-	-	-	1.51	-	4555/83 (54.89)
BAT+WAM3	CPL	$-0.83^{+0.03}_{-0.03}$	-	498^{+21}_{-19}	-	$1.10^{+0.06}_{-0.06}$	-	109/82 (1.34)
BAT+WAM3	Band	$-0.81^{+0.03}_{-0.03}$	$-2.96^{+0.15}_{-0.20}$	467^{+22}_{-21}	-	$1.15^{+0.06}_{-0.06}$	-	70/81 (0.87)
KW+BAT	PL	-1.45	-	-	-	-	0.76	4318/144 (29.99)
KW+BAT	CPL	$-0.76^{+0.02}_{-0.02}$	-	436^{+15}_{-14}	-	-	$0.87^{+0.02}_{-0.01}$	186/143 (1.31)
KW+BAT	Band	$-0.73^{+0.03}_{-0.03}$	$-2.65^{+0.16}_{-0.24}$	410^{+17}_{-16}	-	-	$0.87^{+0.02}_{-0.01}$	162/142 (1.14)
KW+WAM2	PL	-1.53	-	-	0.60	-	-	4208/112 (37.58)
KW+WAM2	CPL	$-0.75^{+0.03}_{-0.03}$	-	436^{+14}_{-13}	$0.98^{+0.04}_{-0.04}$	-	-	209/111 (1.89)
KW+WAM2	Band	$-0.64^{+0.04}_{-0.04}$	$-2.62^{+0.09}_{-0.10}$	383^{+15}_{-15}	$1.03^{+0.04}_{-0.04}$	-	-	106/110 (0.97)
KW+WAM3	PL	-1.58	-	-	-	0.85	-	5874/112 (52.45)
KW+WAM3	CPL	$-0.78^{+0.03}_{-0.03}$	-	457^{+12}_{-12}	-	$1.01^{+0.03}_{-0.03}$	-	230/111 (2.07)
KW+WAM3	Band	$-0.71^{+0.04}_{-0.03}$	$-2.78^{+0.10}_{-0.12}$	417^{+14}_{-15}	-	$1.05^{+0.03}_{-0.03}$	-	144/110 (1.31)
KW+2WAM†+BAT	PL	-1.55	-	-	0.63	0.77	0.68	8846/196 (45.14)
KW+2WAM†+BAT	CPL	$-0.80^{+0.02}_{-0.02}$	-	464^{+11}_{-11}	$0.95^{+0.03}_{-0.03}$	$1.01^{+0.03}_{-0.02}$	$0.87^{+0.02}_{-0.01}$	341/195 (1.75)
KW+2WAM†+BAT	Band	$-0.75^{+0.02}_{-0.02}$	$-2.79^{+0.08}_{-0.10}$	427^{+12}_{-12}	$0.98^{+0.03}_{-0.03}$	$1.05^{+0.03}_{-0.03}$	$0.87^{+0.02}_{-0.01}$	215/194 (1.11)

† The joint fit of two WAM spectra.

Table 39. Spectral parameters: 061222A Reg1

Instrument	Model	α	β	$E_{\rm peak}$ [keV]	C(WAM2)	C(WAM3)	C(BAT)	χ^2/dof
KW	PL	$-1.50^{+0.03}_{-0.03}$	-	-	-	-	-	160/60 (2.68)
KW	CPL	$-0.97^{+0.12}_{-0.11}$	-	330^{+58}_{-42}	-	-	-	53/59 (0.91)
KW	Band	$-0.89^{+0.15}_{-0.13}$	$-2.28^{+0.27}_{-0.61}$	285^{+55}_{-47}	-	-	-	48/58 (0.84)
WAM2	PL	$-1.92^{+0.07}_{-0.07}$	-	-	-	-	-	37/14 (2.71)
WAM2	CPL	$-1.00^{+0.37}_{-0.32}$	-	467^{+71}_{-50}	-	-	-	7/13 (0.57)
WAM2	Band	$-0.96^{+0.53}_{-0.35}$	< -2.41	459^{+76}_{-73}	-	-	-	7/12 (0.60)
WAM3	PL	$-1.97^{+0.14}_{-0.16}$	-	-	-	-	-	12/14 (0.87)
WAM3	CPL	-	-	-	-	-	-	-
WAM3	Band	-	-	-	-	-	-	-
BAT	PL	$-1.17^{+0.03}_{-0.03}$	-	-	-	-	-	47/57 (0.84)
BAT	CPL	$-0.95^{+0.13}_{-0.13}$	-	300^{+311}_{-88}	-	-	-	39/56 (0.70)
BAT	Band	-	-	-	-	-	-	-
BAT+WAM2	PL	$-1.34^{+0.02}_{-0.03}$	-	-	$0.93^{+0.09}_{-0.06}$	-	-	426/72 (5.92)
BAT+WAM2	CPL	$-1.04^{+0.04}_{-0.04}$	-	464^{+59}_{-50}	$1.21^{+0.09}_{-0.08}$	-	-	47/71 (0.67)
BAT+WAM2	Band	$-1.04^{+0.04}_{-0.04}$	< -2.40	459^{+62}_{-56}	$1.22^{+0.09}_{-0.08}$	-	-	47/70 (0.68)
BAT+WAM3	PL	$-1.22^{+0.03}_{-0.03}$	-	-	-	$0.57^{+0.07}_{-0.06}$	-	166/72 (2.31)
BAT+WAM3	CPL	$-1.03^{+0.06}_{-0.05}$	-	427^{+129}_{-93}	-	$1.06^{+0.15}_{-0.13}$	-	58/71 (0.82)
BAT+WAM3	Band	$-0.91^{+0.11}_{-0.10}$	$-2.02^{+0.18}_{-0.32}$	262^{+108}_{-59}	-	$1.23^{+0.19}_{-0.17}$	-	52/70 (0.75)
KW+BAT	PL	$-1.34^{+0.02}_{-0.02}$	-	-	-	-	$0.98^{+0.05}_{-0.05}$	371/118 (3.15)
KW+BAT	CPL	$-0.97^{+0.05}_{-0.05}$	-	329^{+45}_{-37}	-	-	$0.83^{+0.04}_{-0.04}$	92/117 (0.79)
KW+BAT	Band	$-0.94^{+0.06}_{-0.06}$	$-2.28^{+0.26}_{-0.69}$	294^{+48}_{-39}	-	-	$0.83^{+0.04}_{-0.03}$	88/116 (0.76)
KW+WAM2	PL	$-1.59^{+0.03}_{-0.03}$	-	-	$1.25^{+0.09}_{-0.07}$	-	-	294/75 (3.92)
KW+WAM2	CPL	$-1.09^{+0.08}_{-0.07}$	-	423^{+48}_{-40}	$1.13^{+0.07}_{-0.06}$	-	-	69/74 (0.94)
KW+WAM2	Band	$-1.06^{+0.11}_{-0.10}$	< -2.18	392^{+69}_{-65}	$1.13^{+0.07}_{-0.06}$	-	-	68/73 (0.94)
KW+WAM3	PL	$-1.53^{+0.03}_{-0.03}$	-	-	-	$0.96^{+0.09}_{-0.08}$	-	205/75 (2.74)
KW+WAM3	CPL	$-1.04^{+0.10}_{-0.09}$	-	365^{+60}_{-46}	-	$0.97^{+0.09}_{-0.08}$	-	74/74 (1.00)
KW+WAM3	Band	$-0.87^{+0.16}_{-0.13}$	$-2.14^{+0.17}_{-0.26}$	271^{+54}_{-46}	-	$0.99^{+0.09}_{-0.09}$	-	62/73 (0.86)
KW+2WAM†+BAT	PL	$-1.42^{+0.02}_{-0.02}$	-	-	$1.01^{+0.06}_{-0.05}$	$0.84^{+0.08}_{-0.07}$	$0.87^{+0.04}_{-0.04}$	693/148 (4.69)
KW+2WAM†+BAT	CPL	$-1.04^{+0.04}_{-0.04}$	-	411^{+37}_{-33}	$1.11^{+0.06}_{-0.06}$	$0.94^{+0.08}_{-0.08}$	$0.86^{+0.04}_{-0.04}$	129/147 (0.88)
KW+2WAM†+BAT	Band	$-1.00^{+0.06}_{-0.05}$	$-2.32^{+0.22}_{-0.64}$	353^{+58}_{-51}	$1.13^{+0.07}_{-0.06}$	$0.95^{+0.08}_{-0.08}$	$0.85^{+0.04}_{-0.04}$	124/146 (0.86)

† The joint fit of two WAM spectra.

Table 40. Spectral parameters: 070328 Reg1

Instrument	Model	α	β	E_{peak} [keV]	C(WAM1)	C(BAT)	χ^2/dof
KW	PL	$-1.38^{+0.03}_{-0.03}$	-	-	-	-	157/76 (2.07)
KW	CPL	$-1.12^{+0.09}_{-0.08}$	-	1205^{+475}_{-317}	-	-	91/75 (1.23)
KW	Band	$-0.95^{+0.15}_{-0.13}$	$-1.81^{+0.15}_{-0.29}$	615^{+306}_{-178}	-	-	82/74 (1.12)
WAM1	PL	$-1.67^{+0.04}_{-0.04}$	-	-	-	-	84/25 (3.38)
WAM1	CPL	$-1.25^{+0.12}_{-0.12}$	-	1905^{+435}_{-296}	-	-	37/24 (1.54)
WAM1	Band	$-0.90^{+0.48}_{-0.28}$	$-2.02^{+0.14}_{-0.24}$	1001^{+485}_{-311}	-	-	30/23 (1.34)
BAT	PL	$-1.12^{+0.04}_{-0.04}$	-	-	-	-	62/57 (1.09)
BAT	CPL	-	-	-	-	-	-
BAT	Band	-	-	-	-	-	-
BAT+WAM1	PL	$-1.44^{+0.02}_{-0.03}$	-	-	$1.25^{+0.16}_{-0.11}$	-	397/83 (4.79)
BAT+WAM1	CPL	$-1.10^{+0.04}_{-0.04}$	-	1680^{+239}_{-206}	$0.92^{+0.09}_{-0.08}$	-	103/82 (1.26)
BAT+WAM1	Band	$-1.06^{+0.05}_{-0.05}$	$-2.06^{+0.16}_{-0.27}$	1184^{+277}_{-216}	$0.96^{+0.09}_{-0.09}$	-	93/81 (1.15)
KW+BAT	PL	$-1.31^{+0.02}_{-0.02}$	-	-	-	$0.90^{+0.05}_{-0.05}$	293/134 (2.19)
KW+BAT	CPL	$-1.08^{+0.05}_{-0.05}$	-	1080^{+300}_{-228}	-	$0.91^{+0.05}_{-0.05}$	154/133 (1.16)
KW+BAT	Band	$-1.02^{+0.06}_{-0.06}$	$-1.83^{+0.17}_{-0.33}$	713^{+253}_{-178}	-	$0.89^{+0.05}_{-0.05}$	145/132 (1.10)
KW+WAM1	PL	$-1.49^{+0.02}_{-0.03}$	-	-	$1.07^{+0.09}_{-0.07}$	-	338/102 (3.32)
KW+WAM1	CPL	$-1.19^{+0.05}_{-0.05}$	-	1711^{+266}_{-219}	$0.94^{+0.06}_{-0.06}$	-	133/101 (1.32)
KW+WAM1	Band	$-1.08^{+0.08}_{-0.07}$	$-1.99^{+0.13}_{-0.19}$	1044^{+276}_{-213}	$0.94^{+0.06}_{-0.06}$	-	121/100 (1.21)
KW+WAM1+BAT	PL	$-1.41^{+0.02}_{-0.02}$	-	-	$0.89^{+0.07}_{-0.05}$	$0.78^{+0.04}_{-0.04}$	560/160 (3.50)
KW+WAM1+BAT	CPL	$-1.13^{+0.04}_{-0.03}$	-	1577^{+210}_{-189}	$0.91^{+0.06}_{-0.05}$	$0.92^{+0.05}_{-0.05}$	201/159 (1.27)
KW+WAM1+BAT	Band	$-1.06^{+0.05}_{-0.04}$	$-1.98^{+0.12}_{-0.18}$	1017^{+206}_{-173}	$0.93^{+0.06}_{-0.05}$	$0.91^{+0.05}_{-0.05}$	183/158 (1.16)

Table 41. Spectral parameters: 070328 Reg2

Instrument	Model	α	β	E_{peak} [keV]	C(WAM1)	C(BAT)	χ^2/dof
KW	PL	$-1.42^{+0.02}_{-0.02}$	-	-	-	-	248/76 (3.27)
KW	CPL	$-1.02^{+0.08}_{-0.08}$	-	686^{+155}_{-110}	-	-	94/75 (1.27)
KW	Band	$-0.87^{+0.13}_{-0.11}$	$-1.92^{+0.13}_{-0.21}$	449^{+116}_{-88}	-	-	77/74 (1.05)
WAM1	PL	$-1.82^{+0.04}_{-0.04}$	-	-	-	-	130/25 (5.24)
WAM1	CPL	$-1.19^{+0.16}_{-0.14}$	-	1143^{+180}_{-153}	-	-	31/24 (1.33)
WAM1	Band	$-0.74^{+0.41}_{-0.31}$	$-2.36^{+0.17}_{-0.30}$	762^{+185}_{-130}	-	-	23/23 (1.01)
BAT	PL	$-1.17^{+0.03}_{-0.03}$	-	-	-	-	51/57 (0.91)
BAT	CPL	-	-	-	-	-	-
BAT	Band	-	-	-	-	-	-
BAT+WAM1	PL	$-1.46^{+0.02}_{-0.03}$	-	-	$1.04^{+0.13}_{-0.07}$	-	670/83 (8.08)
BAT+WAM1	CPL	$-1.12^{+0.04}_{-0.04}$	-	1100^{+142}_{-126}	$0.95^{+0.08}_{-0.07}$	-	83/82 (1.02)
BAT+WAM1	Band	$-1.10^{+0.04}_{-0.04}$	$-2.51^{+0.26}_{-0.63}$	943^{+165}_{-134}	$0.98^{+0.08}_{-0.08}$	-	78/81 (0.96)
KW+BAT	PL	$-1.35^{+0.02}_{-0.02}$	-	-	-	$0.91^{+0.04}_{-0.04}$	413/134 (3.09)
KW+BAT	CPL	$-1.08^{+0.04}_{-0.04}$	-	759^{+137}_{-110}	-	$0.89^{+0.04}_{-0.03}$	147/133 (1.11)
KW+BAT	Band	$-1.04^{+0.05}_{-0.05}$	$-1.97^{+0.17}_{-0.37}$	596^{+144}_{-105}	-	$0.88^{+0.04}_{-0.03}$	137/132 (1.04)
KW+WAM1	PL	$-1.53^{+0.02}_{-0.02}$	-	-	$0.97^{+0.08}_{-0.06}$	-	623/102 (6.11)
KW+WAM1	CPL	$-1.13^{+0.05}_{-0.05}$	-	995^{+130}_{-107}	$0.91^{+0.05}_{-0.05}$	-	137/101 (1.36)
KW+WAM1	Band	$-1.05^{+0.06}_{-0.06}$	$-2.30^{+0.15}_{-0.23}$	766^{+112}_{-96}	$0.92^{+0.05}_{-0.05}$	-	120/100 (1.20)
KW+WAM+BAT	PL	$-1.44^{+0.01}_{-0.02}$	-	-	$0.77^{+0.06}_{-0.04}$	$0.81^{+0.03}_{-0.03}$	926/160 (5.79)
KW+WAM+BAT	CPL	$-1.12^{+0.03}_{-0.03}$	-	974^{+115}_{-92}	$0.90^{+0.05}_{-0.05}$	$0.91^{+0.04}_{-0.03}$	189/159 (1.19)
KW+WAM+BAT	Band	$-1.08^{+0.04}_{-0.03}$	$-2.33^{+0.16}_{-0.26}$	804^{+104}_{-88}	$0.93^{+0.05}_{-0.05}$	$0.90^{+0.04}_{-0.03}$	172/158 (1.09)

Table 42. Spectral parameters: 070328 Reg3

Instrument	Model	α	β	E_{peak} [keV]	C(WAM1)	C(BAT)	χ^2/dof
KW	PL	$-1.56^{+0.15}_{-0.16}$	-	-	-	-	63/60 (1.06)
KW	CPL	$-0.92^{+0.82}_{-0.58}$	-	219^{+806}_{-84}	-	-	59/59 (1.00)
KW	Band	$0.13^{+1.52}_{-4.72}$	$-1.93^{+0.31}_{-0.29}$	105^{+211}_{-14}	-	-	56/58 (0.98)
WAM1	PL	$-1.99^{+0.28}_{-0.37}$	-	-	-	-	21/15 (1.41)
WAM1	CPL	-	-	-	-	-	-
WAM1	Band	-	-	-	-	-	-
BAT	PL	$-1.34^{+0.09}_{-0.09}$	-	-	-	-	37/57 (0.65)
BAT	CPL	$-1.03^{+0.36}_{-0.36}$	-	>110	-	-	35/56 (0.63)
BAT	Band	-	-	-	-	-	-
BAT+WAM1	PL	$-1.41^{+0.08}_{-0.09}$	-	-	$0.54^{+0.24}_{-0.18}$	-	73/73 (1.00)
BAT+WAM1	CPL	$-1.25^{+0.14}_{-0.12}$	-	498^{+752}_{-233}	$0.93^{+0.40}_{-0.29}$	-	55/72 (0.77)
BAT+WAM1	Band	-	-	-	-	-	-
KW+BAT	PL	$-1.40^{+0.08}_{-0.08}$	-	-	-	$1.07^{+0.25}_{-0.19}$	105/118 (0.89)
KW+BAT	CPL	$-1.12^{+0.25}_{-0.19}$	-	240^{+368}_{-93}	-	$0.88^{+0.20}_{-0.14}$	95/117 (0.81)
KW+BAT	Band	$-1.01^{+0.37}_{-0.27}$	<-1.57	175^{+279}_{-68}	-	$0.87^{+0.19}_{-0.14}$	94/116 (0.81)
KW+WAM1	PL	$-1.67^{+0.13}_{-0.14}$	-	-	$0.94^{+0.45}_{-0.30}$	-	89/76 (1.18)
KW+WAM1	CPL	$-1.27^{+0.38}_{-0.29}$	-	436^{+710}_{-178}	$0.94^{+0.36}_{-0.26}$	-	79/75 (1.07)
KW+WAM1	Band	$+0.02^{+4.98}_{-1.46}$	<-1.72	112^{+584}_{-69}	$1.08^{+0.46}_{-0.34}$	-	78/74 (1.06)
KW+WAM1+BAT	PL	$-1.45^{+0.07}_{-0.08}$	-	-	$0.61^{+0.23}_{-0.18}$	$1.00^{+0.22}_{-0.17}$	138/134 (1.04)
KW+WAM1+BAT	CPL	$-1.22^{+0.14}_{-0.13}$	-	391^{+408}_{-144}	$0.94^{+0.33}_{-0.26}$	$0.93^{+0.21}_{-0.14}$	116/133 (0.87)
KW+WAM1+BAT	Band	$-1.02^{+0.36}_{-0.39}$	<-1.73	181^{+659}_{-69}	$1.07^{+0.42}_{-0.31}$	$0.87^{+0.21}_{-0.13}$	115/132 (0.87)

Table 43. Spectral parameters: 070328 Reg13

Instrument	Model	α	β	E_{peak} [keV]	C(WAM1)	C(BAT)	χ^2/dof
KW	PL	$-1.43^{+0.03}_{-0.03}$	-	-	-	-	190/76 (2.51)
KW	CPL	$-1.04^{+0.10}_{-0.09}$	-	622^{+163}_{-112}	-	-	84/75 (1.13)
KW	Band	$-0.88^{+0.15}_{-0.13}$	$-1.91^{+0.15}_{-0.23}$	407^{+119}_{-90}	-	-	71/74 (0.96)
WAM1	PL	$-1.85^{+0.04}_{-0.05}$	-	-	-	-	105/25 (4.22)
WAM1	CPL	$-1.21^{+0.18}_{-0.16}$	-	1115^{+203}_{-160}	-	-	31/24 (1.31)
WAM1	Band	$-0.65^{+0.55}_{-0.44}$	$-2.33^{+0.17}_{-0.37}$	706^{+242}_{-126}	-	-	25/23 (1.11)
BAT	PL	$-1.19^{+0.03}_{-0.03}$	-	-	-	-	38/57 (0.68)
BAT	CPL	-	-	-	-	-	-
BAT	Band	-	-	-	-	-	-
BAT+WAM1	PL	$-1.43^{+0.02}_{-0.03}$	-	-	$0.86^{+0.12}_{-0.07}$	-	550/83 (6.63)
BAT+WAM1	CPL	$-1.14^{+0.04}_{-0.04}$	-	1083^{+165}_{-141}	$0.94^{+0.08}_{-0.08}$	-	69/82 (0.85)
BAT+WAM1	Band	$-1.13^{+0.04}_{-0.04}$	$-2.56^{+0.33}_{-1.31}$	936^{+203}_{-166}	$0.98^{+0.10}_{-0.09}$	-	66/81 (0.82)
KW+BAT	PL	$-1.35^{+0.02}_{-0.02}$	-	-	-	$0.94^{+0.04}_{-0.04}$	323/134 (2.41)
KW+BAT	CPL	$-1.10^{+0.04}_{-0.04}$	-	690^{+148}_{-111}	-	$0.89^{+0.04}_{-0.04}$	123/133 (0.93)
KW+BAT	Band	$-1.06^{+0.05}_{-0.05}$	$-1.94^{+0.17}_{-0.42}$	539^{+152}_{-106}	-	$0.88^{+0.04}_{-0.04}$	116/132 (0.88)
KW+WAM1	PL	$-1.55^{+0.02}_{-0.03}$	-	-	$0.96^{+0.09}_{-0.07}$	-	480/102 (4.71)
KW+WAM1	CPL	$-1.16^{+0.06}_{-0.06}$	-	965^{+156}_{-117}	$0.92^{+0.06}_{-0.06}$	-	126/101 (1.25)
KW+WAM1	Band	$-1.08^{+0.08}_{-0.07}$	$-2.30^{+0.17}_{-0.30}$	732^{+139}_{-109}	$0.94^{+0.06}_{-0.06}$	-	114/100 (1.15)
KW+WAM1+BAT	PL	$-1.43^{+0.02}_{-0.02}$	-	-	$0.72^{+0.06}_{-0.04}$	$0.83^{+0.03}_{-0.04}$	741/160 (4.63)
KW+WAM1+BAT	CPL	$-1.14^{+0.03}_{-0.03}$	-	947^{+123}_{-112}	$0.91^{+0.06}_{-0.05}$	$0.91^{+0.04}_{-0.04}$	164/159 (1.04)
KW+WAM1+BAT	Band	$-1.11^{+0.04}_{-0.04}$	$-2.33^{+0.18}_{-0.32}$	767^{+124}_{-100}	$0.94^{+0.06}_{-0.06}$	$0.90^{+0.04}_{-0.04}$	152/158 (0.97)

Table 44. Fluxes: 051008 Reg1

Instrument	Energy range	Flux (PL)	Flux (CPL)	Flux (Band)	Inst fixed to 1
	[keV]	$[10^{-7} \mathrm{\ erg\ cm^{-2}\ s^{-1}}]$	$[10^{-7} \mathrm{\ erg\ cm^{-2}\ s^{-1}}]$	$[10^{-7} \mathrm{\ erg\ cm^{-2}\ s^{-1}}]$	-
KW	20-1000	$14.9^{+0.6}_{-0.6}$	$17.3^{+0.7}_{-0.4}$	$16.8^{+0.9}_{-1.0}$	-
WAM0	120-1000	$12.0^{+0.3}_{-0.3}$	$13.7^{+0.4}_{-0.4}$	$13.6^{+0.5}_{-0.5}$	-
WAM3	120-1000	$11.9^{+0.4}_{-0.4}$	$13.4^{+0.2}_{-0.5}$	$13.3^{+0.5}_{-0.5}$	-
BAT	15-150	$3.4^{+0.1}_{-0.1}$	$3.3^{+0.1}_{-0.1}$	-	-
BAT+WAM0	15-1000	$9.5^{+0.5}_{-0.5}$	$16.3^{+1.2}_{-1.1}$	$16.2^{+1.2}_{-1.1}$	BAT
BAT+WAM3	15-1000	$8.9^{+0.5}_{-0.5}$	$15.1^{+1.1}_{-1.0}$	$14.9^{+1.1}_{-1.1}$	BAT
KW+BAT	15-1000	$15.4^{+0.6}_{-0.6}$	$17.4^{+0.7}_{-0.7}$	$16.9^{+0.9}_{-0.9}$	KW
KW+WAM0	20-1000	$13.8^{+0.6}_{-0.6}$	$17.2^{+0.7}_{-0.7}$	$17.2^{+0.7}_{-0.7}$	KW
KW+WAM3	20-1000	$13.6^{+0.6}_{-0.6}$	$16.9^{+0.7}_{-0.7}$	$16.7^{+0.8}_{-0.7}$	KW
KW+2WAM+BAT	15-1000	$14.1^{+0.6}_{-0.6}$	$17.2^{+0.7}_{-0.6}$	$17.0^{+0.7}_{-0.7}$	KW

Table 45. Fluxes: 051008 Reg2

Instrument	Energy range	Flux (PL)	Flux (CPL)	Flux (Band)	Inst fixed to 1
	[keV]	$[10^{-7} \mathrm{\ erg\ cm^{-2}\ s^{-1}}]$	$[10^{-7} \mathrm{\ erg\ cm^{-2}\ s^{-1}}]$	$[10^{-7} \mathrm{\ erg\ cm^{-2}\ s^{-1}}]$	-
KW	20-1000	$1.9^{+0.3}_{-0.3}$	$1.7^{+0.3}_{-0.3}$	$1.7^{+0.2}_{-0.3}$	-
WAM0	120-1000	$1.8^{+0.2}_{-0.2}$	$1.9^{+0.2}_{-0.2}$	$1.9^{+0.2}_{-0.2}$	-
WAM3	120-1000	$1.9^{+0.2}_{-0.2}$	$1.9^{+0.2}_{-0.2}$	$1.9^{+0.2}_{-0.2}$	-
KW-WAM0	20-1000	$1.8^{+0.3}_{-0.3}$	$1.9^{+0.3}_{-0.3}$	$2.0^{+0.2}_{-0.1}$	KW
KW-WAM3	20-1000	$1.8^{+0.3}_{-0.3}$	$1.9^{+0.3}_{-0.3}$	$1.9^{+0.3}_{-0.2}$	KW
KW-2WAM	20-1000	$1.8^{+0.3}_{-0.2}$	$2.0^{+0.3}_{-0.1}$	$1.9^{+0.3}_{-0.3}$	KW

Table 46. Fluxes: 051008 Reg12

Instrument	Energy range	Flux (PL)	Flux (CPL)	Flux (Band)	Inst fixed to 1
	[keV]	$[10^{-7} \mathrm{\ erg\ cm^{-2}\ s^{-1}}]$	$[10^{-7} \mathrm{\ erg\ cm^{-2}\ s^{-1}}]$	$[10^{-7} \mathrm{\ erg\ cm^{-2}\ s^{-1}}]$	-
KW	20-1000	$4.4^{+0.2}_{-0.2}$	$4.6^{+0.3}_{-0.3}$	$4.4^{+0.4}_{-0.3}$	-
WAM0	120-1000	$3.6^{+0.1}_{-0.1}$	$4.0^{+0.2}_{-0.2}$	$3.9^{+0.2}_{-0.2}$	-
WAM3	120-1000	$3.6^{+0.1}_{-0.1}$	$4.0^{+0.2}_{-0.2}$	$4.0^{+0.2}_{-0.2}$	-
KW-WAM0	20-1000	$4.1^{+0.2}_{-0.2}$	$4.8^{+0.3}_{-0.2}$	$4.7^{+0.3}_{-0.3}$	KW
KW-WAM3	20-1000	$4.1^{+0.2}_{-0.2}$	$4.7^{+0.3}_{-0.3}$	$4.5^{+0.3}_{-0.3}$	KW
KW-2WAM	20-1000	$4.0^{+0.2}_{-0.2}$	$4.7^{+0.2}_{-0.2}$	$4.7^{+0.3}_{-0.3}$	KW

Table 47. Fluxes: 051221A Reg1

Instrument	Energy range	Flux (PL)	Flux (CPL)	Flux (Band)	Inst fixed to 1
	[keV]	$[10^{-7}$ erg cm^{-2} s$^{-1}]$	$[10^{-7}$ erg cm^{-2} s$^{-1}]$	$[10^{-7}$ erg cm^{-2} s$^{-1}]$	-
KW	20-1000	$100.2^{+7.6}_{-7.6}$	$100.9^{+9.2}_{-9.5}$	$97.7^{+8.3}_{-8.4}$	-
WAM0	120-1000	$14.1^{+3.5}_{-3.6}$	$14.3^{+3.6}_{-3.7}$	$14.2^{+3.7}_{-3.9}$	-
WAM1	120-1000	$13.9^{+1.5}_{-1.5}$	$13.9^{+1.5}_{-1.5}$	$13.9^{+1.1}_{-1.1}$	-
BAT	15-150	$29.0^{+1.0}_{-1.0}$	$28.8^{+1.0}_{-1.0}$	-	-
BAT-WAM0	15-1000	$224.0^{+26.4}_{-23.7}$	$111.1^{+74.9}_{-38.7}$	$117.6^{+51.8}_{-32.5}$	BAT
BAT-WAM1	15-1000	$174.4^{+20.0}_{-18.0}$	$90.6^{+17.7}_{-14.6}$	$86.1^{+14.0}_{-11.8}$	BAT
KW-BAT	15-1000	$108.9^{+7.6}_{-7.6}$	$98.2^{+10.2}_{-10.2}$	$99.1^{+8.3}_{-8.4}$	KW
KW-WAM0	20-1000	$100.1^{+7.6}_{-7.6}$	$101.8^{+9.0}_{-4.6}$	$98.3^{+8.1}_{-8.1}$	KW
KW-WAM1	20-1000	$95.3^{+7.7}_{-7.7}$	$98.1^{+8.6}_{-8.5}$	$95.4^{+7.9}_{-7.8}$	KW
KW-2WAM-BAT	15-1000	$109.8^{+7.4}_{-7.4}$	$98.5^{+9.0}_{-8.8}$	$97.9^{+7.7}_{-7.6}$	KW

Table 48. Fluxes: 060105 Reg1

Instrument	Energy range	Flux (PL)	Flux (CPL)	Flux (Band)	Inst fixed to 1
	[keV]	$[10^{-7}$ erg cm^{-2} s$^{-1}]$	$[10^{-7}$ erg cm^{-2} s$^{-1}]$	$[10^{-7}$ erg cm^{-2} s$^{-1}]$	-
KW	20-1000	$19.0^{+0.4}_{-0.4}$	$21.8^{+0.5}_{-0.5}$	$21.9^{+0.4}_{-0.6}$	-
WAM0	120-1000	$13.4^{+1.3}_{-1.3}$	$15.3^{+0.8}_{-1.7}$	$15.2^{+1.6}_{-1.8}$	-
WAM3	120-1000	$34.4^{+2.0}_{-2.0}$	$36.4^{+2.2}_{-1.1}$	$35.8^{+2.6}_{-1.2}$	-
BAT	15-150	$3.8^{+0.1}_{-0.1}$	-	-	-
BAT-WAM0	15-1000	$28.0^{+2.4}_{-2.2}$	$20.2^{+2.4}_{-2.3}$	$20.4^{+1.5}_{-0.4}$	BAT
BAT-WAM3	15-1000	$23.5^{+2.2}_{-1.9}$	$13.7^{+1.3}_{-1.2}$	$14.2^{-2.5}_{-1.2}$	BAT
KW-BAT	15-1000	$19.6^{+0.4}_{-0.4}$	$21.9^{+0.5}_{-0.5}$	$22.2^{+0.3}_{-0.8}$	KW
KW-WAM0	20-1000	$19.0^{+0.4}_{-0.4}$	$21.9^{+0.5}_{-0.5}$	$21.9^{+0.4}_{-0.6}$	KW
KW-WAM3	20-1000	$18.9^{+0.4}_{-0.4}$	$21.5^{+0.5}_{-0.5}$	$21.6^{+0.4}_{-0.4}$	KW
KW-2WAM-BAT	15-1000	$19.5^{+0.4}_{-0.4}$	$21.6^{+0.5}_{-0.5}$	$21.8^{+0.4}_{-0.6}$	KW

Table 49. Fluxes: 060105 Reg2

Instrument	Energy range	Flux (PL)	Flux (CPL)	Flux (Band)	Inst fixed to 1
	[keV]	$[10^{-7}$ erg cm^{-2} s$^{-1}]$	$[10^{-7}$ erg cm^{-2} s$^{-1}]$	$[10^{-7}$ erg cm^{-2} s$^{-1}]$	-
KW	20-1000	$11.7^{+0.3}_{-0.3}$	$10.2^{+0.4}_{-0.4}$	$10.4^{+0.4}_{-0.4}$	-
WAM0	120-1000	$6.3^{+1.3}_{-1.3}$	$6.4^{+1.4}_{-1.8}$	$6.3^{+1.1}_{-1.4}$	-
WAM3	120-1000	$16.9^{+1.9}_{-1.9}$	$16.8^{+2.2}_{-2.2}$	$16.8^{+2.0}_{-2.1}$	-
BAT	15-150	$3.82^{+0.07}_{-0.07}$	$3.80^{+0.08}_{-0.08}$	-	-
BAT-WAM0	15-1000	$22.7^{+1.6}_{-1.5}$	$10.4^{+2.6}_{-1.9}$	$10.5^{+2.4}_{-1.5}$	BAT
BAT-WAM3	15-1000	$21.9^{+1.5}_{-1.4}$	$8.9^{+1.2}_{-1.0}$	$8.8^{+1.2}_{-1.0}$	BAT
KW-BAT	15-1000	$12.73^{+0.3}_{-0.3}$	$10.6^{+0.4}_{-0.4}$	$10.6^{+0.4}_{-0.4}$	KW
KW-WAM0	20-1000	$11.7^{+0.3}_{-0.3}$	$10.2^{+0.4}_{-0.4}$	$10.4^{+0.4}_{-0.4}$	KW
KW-WAM3	20-1000	$11.6^{+0.3}_{-0.3}$	$10.2^{+0.4}_{-0.4}$	$10.3^{+0.4}_{-0.4}$	KW
KW-2WAM-BAT	15-1000	$12.7^{+0.3}_{-0.3}$	$10.5^{+0.4}_{-0.4}$	$10.6^{+0.4}_{-0.4}$	KW

Table 50. Fluxes: 060105 Reg12

Instrument	Energy range [keV]	Flux (PL) $[10^{-7}$ erg cm^{-2} s$^{-1}]$	Flux (CPL) $[10^{-7}$ erg cm^{-2} s$^{-1}]$	Flux (Band) $[10^{-7}$ erg cm^{-2} s$^{-1}]$	Inst fixed to 1 -
KW	20-1000	$15.7^{+0.3}_{-0.3}$	$16.1^{+0.4}_{-0.4}$	$15.8^{+0.4}_{-0.4}$	-
WAM0	120-1000	$10.1^{+1.0}_{-1.0}$	$10.8^{+1.2}_{-1.1}$	$10.6^{+1.2}_{-1.2}$	-
WAM3	120-1000	$25.7^{+1.4}_{-1.4}$	$26.8^{+1.5}_{-1.5}$	$26.3^{+1.9}_{-1.5}$	-
BAT	15-150	$3.82^{+0.06}_{-0.06}$	-	-	-
BAT-WAM0	15-1000	$25.1^{+1.5}_{-1.4}$	$16.6^{+2.0}_{-1.9}$	$16.3^{+2.0}_{-2.3}$	BAT
BAT-WAM3	15-1000	$22.5^{+1.4}_{-1.3}$	$11.5^{+1.0}_{-0.9}$	$11.1^{+0.9}_{-0.8}$	BAT
KW-BAT	15-1000	$16.4^{+0.3}_{-0.3}$	$16.3^{+0.4}_{-0.4}$	$16.1^{+0.5}_{-0.4}$	KW
KW-WAM0	20-1000	$15.7^{+0.3}_{-0.3}$	$16.1^{+0.4}_{-0.4}$	$15.8^{+0.4}_{-0.4}$	KW
KW-WAM3	20-1000	$15.6^{+0.3}_{-0.3}$	$15.8^{+0.4}_{-0.4}$	$15.6^{+0.4}_{-0.3}$	KW
KW-2WAM-BAT	15-1000	$16.3^{+0.3}_{-0.3}$	$16.1^{+0.3}_{-0.3}$	$15.9^{+0.4}_{-0.4}$	KW

Table 51. Fluxes: 060117 Reg1

Instrument	Energy range [keV]	Flux (PL) $[10^{-7}$ erg cm^{-2} s$^{-1}]$	Flux (CPL) $[10^{-7}$ erg cm^{-2} s$^{-1}]$	Flux (Band) $[10^{-7}$ erg cm^{-2} s$^{-1}]$	Inst fixed to 1 -
KW	20-1000	$12.0^{+0.5}_{-0.5}$	$10.2^{+0.6}_{-0.5}$	$10.2^{+0.5}_{-0.6}$	-
WAM0	120-1000	$5.2^{+0.4}_{-0.4}$	$5.2^{+0.4}_{-0.4}$	$5.1^{+0.2}_{+0.2}$	-
WAM1	120-1000	$4.9^{+0.3}_{-0.3}$	$4.8^{+0.3}_{-0.4}$	$5.6^{-0.7}_{-0.4}$	-
BAT	15-150	$7.1^{+0.2}_{-0.2}$	$7.0^{+0.2}_{-0.2}$	$6.9^{+0.2}_{-0.2}$	-
BAT-WAM0	15-1000	$14.3^{+0.7}_{-0.7}$	$11.1^{+1.0}_{-0.8}$	$10.8^{+0.8}_{-0.7}$	BAT
BAT-WAM1	15-1000	$14.0^{+0.7}_{-0.6}$	$11.6^{+0.8}_{-0.7}$	$11.1^{+0.7}_{-0.6}$	BAT
KW-BAT	15-1000	$13.5^{+0.5}_{-0.5}$	$10.8^{+0.6}_{-0.5}$	$11.2^{+0.7}_{-0.6}$	KW
KW-WAM0	20-1000	$11.8^{+0.5}_{-0.5}$	$10.5^{+0.5}_{-0.5}$	$10.8^{+0.5}_{-0.5}$	KW
KW-WAM1	20-1000	$11.7^{+0.5}_{-0.5}$	$10.8^{+0.5}_{-0.5}$	$11.0^{+0.5}_{-0.5}$	KW
KW-2WAM-BAT	15-1000	$13.2^{+0.4}_{-0.4}$	$11.6^{+0.5}_{-0.5}$	$11.6^{+0.6}_{-0.4}$	KW

Table 52. Fluxes: 060117 Reg2

Instrument	Energy range [keV]	Flux (PL) $[10^{-7}$ erg cm^{-2} s$^{-1}]$	Flux (CPL) $[10^{-7}$ erg cm^{-2} s$^{-1}]$	Flux (Band) $[10^{-7}$ erg cm^{-2} s$^{-1}]$	Inst fixed to 1 -
KW	20-1000	$31.9^{+0.8}_{-0.8}$	$26.6^{+0.9}_{-0.8}$	$27.5^{+1.0}_{-1.0}$	-
WAM0	120-1000	$12.2^{+0.6}_{-0.6}$	$12.1^{+0.5}_{-0.5}$	$12.6^{-0.3}_{-0.2}$	-
WAM1	120-1000	$11.8^{+0.4}_{-0.4}$	$11.2^{+0.6}_{-0.6}$	$11.3^{+0.5}_{-0.5}$	-
BAT	15-150	$18.8^{+0.3}_{-0.3}$	$18.5^{+0.4}_{-0.4}$	$18.5^{+0.3}_{-0.3}$	-
BAT-WAM0	15-1000	$38.1^{+1.4}_{-1.4}$	$27.8^{+1.2}_{-1.1}$	$27.5^{+1.2}_{-1.1}$	BAT
BAT-WAM1	15-1000	$36.5^{+1.3}_{-1.3}$	$29.3^{+1.1}_{-1.0}$	$29.5^{+1.1}_{-1.0}$	BAT
KW-BAT	15-1000	$35.8^{+0.8}_{-0.8}$	$28.0^{+0.9}_{-0.8}$	$29.0^{+1.1}_{-1.0}$	KW
KW-WAM0	20-1000	$30.5^{+0.8}_{-0.8}$	$26.9^{+0.7}_{-0.7}$	$27.8^{+0.8}_{-0.8}$	KW
KW-WAM1	20-1000	$30.1^{+0.8}_{-0.8}$	$27.6^{+0.7}_{-0.7}$	$28.3^{+0.8}_{-0.8}$	KW
KW-2WAM-BAT	15-1000	$33.7^{+0.8}_{-0.8}$	$29.1^{+0.7}_{-0.7}$	$29.6^{+0.7}_{-0.7}$	KW

Table 53. Fluxes: 060117 Reg3

Instrument	Energy range	Flux (PL)	Flux (CPL)	Flux (Band)	Inst fixed to 1
	[keV]	$[10^{-7}$ erg cm^{-2} s$^{-1}]$	$[10^{-7}$ erg cm^{-2} s$^{-1}]$	$[10^{-7}$ erg cm^{-2} s$^{-1}]$	-
KW	20-1000	$8.0^{+0.4}_{-0.4}$	$6.7^{+0.4}_{-0.4}$	$6.8^{+0.5}_{-0.4}$	-
WAM0	120-1000	$2.7^{+0.4}_{-0.3}$	-	-	-
WAM1	120-1000	$2.2^{+0.3}_{-0.3}$	-	-	-
BAT	15-150	$6.0^{+0.2}_{-0.2}$	$5.9^{+0.2}_{-0.2}$	$5.8^{+0.2}_{-0.2}$	-
BAT-WAM0	15-1000	$9.7^{+0.4}_{-0.4}$	$7.2^{+0.5}_{-0.4}$	$7.3^{+0.5}_{-0.4}$	BAT
BAT-WAM1	15-1000	$9.7^{+0.4}_{-0.4}$	$7.5^{+0.5}_{-0.4}$	$7.9^{+0.6}_{-0.7}$	BAT
KW-BAT	15-1000	$9.5^{+0.4}_{-0.4}$	$7.4^{+0.4}_{-0.3}$	$7.5^{+0.5}_{-0.4}$	KW
KW-WAM0	20-1000	$7.8^{+0.4}_{-0.4}$	$6.8^{+0.4}_{-0.3}$	$7.0^{+0.4}_{-0.4}$	KW
KW-WAM1	20-1000	$7.8^{+0.4}_{-0.4}$	$7.0^{+0.4}_{-0.3}$	$7.1^{+0.4}_{-0.4}$	KW
KW-2WAM-BAT	15-1000	$9.4^{+0.4}_{-0.4}$	$7.8^{+0.3}_{-0.3}$	$7.9^{+0.4}_{-0.3}$	KW

Table 54. Fluxes: 060117 Reg13

Instrument	Energy range	Flux (PL)	Flux (CPL)	Flux (Band)	Inst fixed to 1
	[keV]	$[10^{-7}$ erg cm^{-2} s$^{-1}]$	$[10^{-7}$ erg cm^{-2} s$^{-1}]$	$[10^{-7}$ erg cm^{-2} s$^{-1}]$	-
KW	20-1000	$15.3^{+0.3}_{-0.3}$	$12.7^{+0.4}_{-0.3}$	$13.1^{+0.4}_{-0.4}$	-
WAM0	120-1000	$5.9^{+0.3}_{-0.3}$	-	-	-
WAM1	120-1000	$5.5^{+0.2}_{-0.2}$	-	-	-
BAT	15-150	$9.4^{+0.1}_{-0.1}$	$9.2^{+0.2}_{-0.2}$	$9.1^{+0.2}_{-0.2}$	-
BAT-WAM0	15-1000	$17.5^{+0.5}_{-0.5}$	$13.5^{+0.5}_{-0.5}$	$13.4^{+0.5}_{-0.5}$	BAT
BAT-WAM1	15-1000	$17.2^{+0.5}_{-0.5}$	$14.2^{+0.5}_{-0.4}$	$14.1^{+0.6}_{-0.5}$	BAT
KW-BAT	15-1000	$17.0^{+0.3}_{-0.3}$	$13.6^{+0.4}_{-0.4}$	$14.1^{+0.4}_{-0.4}$	KW
KW-WAM0	20-1000	$14.8^{+0.3}_{-0.3}$	$12.9^{+0.3}_{-0.3}$	$13.3^{+0.3}_{-0.3}$	KW
KW-WAM1	20-1000	$14.7^{+0.3}_{-0.3}$	$13.3^{+0.3}_{-0.3}$	$13.6^{+0.3}_{-0.3}$	KW
KW-2WAM-BAT	15-1000	$16.4^{+0.3}_{-0.3}$	$14.2^{+0.3}_{-0.3}$	$14.4^{+0.3}_{-0.3}$	KW

Table 55. Fluxes: 060124 Reg1

Instrument	Energy range	Flux (PL)	Flux (CPL)	Flux (Band)	Inst fixed to 1
	[keV]	$[10^{-7}$ erg cm^{-2} s$^{-1}]$	$[10^{-7}$ erg cm^{-2} s$^{-1}]$	$[10^{-7}$ erg cm^{-2} s$^{-1}]$	-
KW	20-1000	$3.4^{+0.4}_{-0.4}$	$2.8^{+0.5}_{-0.4}$	$2.8^{+0.5}_{-0.3}$	-
WAM2	120-1000	$1.6^{+0.5}_{-0.5}$	-	-	-
WAM3	120-1000	$1.6^{+0.4}_{-0.3}$	-	-	-
KW-WAM2	20-1000	$3.3^{+0.4}_{-0.4}$	$2.9^{+0.5}_{-0.4}$	$2.9^{+0.4}_{-0.3}$	KW
KW-WAM3	20-1000	$3.3^{+0.4}_{-0.4}$	$3.0^{+0.5}_{-0.4}$	$3.0^{+0.5}_{-0.3}$	KW
KW-2WAM	20-1000	$3.3^{+0.4}_{-0.4}$	$3.0^{+0.4}_{-0.4}$	$3.1^{+0.4}_{-0.3}$	KW

Table 56. Fluxes: 060124 Reg2

Instrument	Energy range	Flux (PL)	Flux (CPL)	Flux (Band)	Inst fixed to 1
	[keV]	$[10^{-7}$ erg cm^{-2} s$^{-1}]$	$[10^{-7}$ erg cm^{-2} s$^{-1}]$	$[10^{-7}$ erg cm^{-2} s$^{-1}]$	-
KW	20-1000	$11.1^{+0.5}_{-0.5}$	$10.4^{+0.7}_{-0.7}$	$10.4^{+0.6}_{-0.6}$	-
WAM2	120-1000	$5.0^{+0.6}_{-0.6}$	$5.0^{+0.7}_{-0.7}$	$4.8^{+0.6}_{-0.6}$	-
WAM3	120-1000	$4.6^{+0.4}_{-0.4}$	$4.5^{+0.5}_{-0.5}$	$4.5^{+0.5}_{-0.2}$	-
KW-WAM2	20-1000	$10.9^{+0.5}_{-0.5}$	$10.5^{+0.7}_{-0.6}$	$10.4^{+0.6}_{-0.6}$	KW
KW-WAM3	20-1000	$10.7^{+0.5}_{-0.5}$	$10.3^{+0.6}_{-0.6}$	$10.2^{+0.6}_{-0.6}$	KW
KW-2WAM	20-1000	$10.6^{+0.5}_{-0.5}$	$10.3^{+0.6}_{-0.6}$	$10.3^{+0.5}_{-0.5}$	KW

Table 57. Fluxes: 060124 Reg3

Instrument	Energy range	Flux (PL)	Flux (CPL)	Flux (Band)	Inst fixed to 1
	[keV]	$[10^{-7}$ erg cm^{-2} s$^{-1}]$	$[10^{-7}$ erg cm^{-2} s$^{-1}]$	$[10^{-7}$ erg cm^{-2} s$^{-1}]$	-
KW	20-1000	$1.9^{+0.3}_{-0.3}$	$1.5^{+0.3}_{-0.2}$	$1.5^{+0.2}_{-0.3}$	-
WAM2	120-1000	$0.8^{+0.4}_{-0.3}$	$0.7^{+0.3}_{-0.2}$	-	-
WAM3	120-1000	$0.9^{+0.3}_{-0.3}$	-	-	-
KW-WAM2	20-1000	$1.8^{+0.3}_{-0.3}$	$1.5^{+0.3}_{-0.2}$	$1.5^{+0.3}_{-0.2}$	KW
KW-WAM3	20-1000	$1.8^{+0.3}_{-0.3}$	$1.5^{+0.3}_{-0.2}$	$1.6^{+0.3}_{-0.3}$	KW
KW-2WAM	20-1000	$1.8^{+0.3}_{-0.3}$	$1.6^{+0.3}_{-0.2}$	$1.6^{+0.3}_{-0.2}$	KW

Table 58. Fluxes: 060124 Reg13

Instrument	Energy range	Flux (PL)	Flux (CPL)	Flux (Band)	Inst fixed to 1
	[keV]	$[10^{-7}$ erg cm^{-2} s$^{-1}]$	$[10^{-7}$ erg cm^{-2} s$^{-1}]$	$[10^{-7}$ erg cm^{-2} s$^{-1}]$	-
KW	20-1000	$4.6^{+0.2}_{-0.2}$	$4.1^{+0.3}_{-0.3}$	$4.1^{+0.3}_{-0.3}$	-
WAM2	120-1000	$2.0^{+0.3}_{-0.3}$	$1.8^{+0.4}_{-0.3}$	$1.9^{+0.3}_{-0.3}$	-
WAM3	120-1000	$2.0^{+0.2}_{-0.2}$	$2.0^{+0.2}_{-0.2}$	-	-
KW-WAM2	20-1000	$4.6^{+0.23}_{-0.22}$	$4.1^{+0.3}_{-0.3}$	$4.1^{+0.3}_{-0.3}$	KW
KW-WAM3	20-1000	$4.5^{+0.22}_{-0.22}$	$4.2^{+0.3}_{-0.3}$	$4.2^{+0.2}_{-0.2}$	KW
KW-2WAM	20-1000	$4.5^{+0.22}_{-0.22}$	$4.2^{+0.3}_{-0.2}$	$4.2^{+0.2}_{-0.2}$	KW

Table 59. Fluxes: 060502A Reg1

Instrument	Energy range	Flux (PL)	Flux (CPL)	Flux (Band)	Inst fixed to 1
	[keV]	$[10^{-7}$ erg cm^{-2} s$^{-1}]$	$[10^{-7}$ erg cm^{-2} s$^{-1}]$	$[10^{-7}$ erg cm^{-2} s$^{-1}]$	-
KW	20-1000	$2.7^{+0.5}_{-0.4}$	$2.2^{+0.5}_{-0.4}$	$2.4^{+0.5}_{-0.6}$	-
WAM3	120-1000	$1.1^{+0.4}_{-0.3}$	-	-	-
BAT	15-150	$1.21^{+0.06}_{-0.06}$	$1.18^{+0.07}_{-0.07}$	-	-
BAT-WAM3	15-1000	$5.1^{+0.8}_{-0.7}$	$1.9^{+0.7}_{-0.4}$	$2.0^{+0.6}_{-0.4}$	BAT
KW-BAT	15-1000	$3.4^{+0.4}_{-0.4}$	$2.1^{+0.4}_{-0.3}$	$2.5^{+0.5}_{-0.5}$	KW
KW-WAM3	20-1000	$2.5^{+0.5}_{-0.4}$	$2.1^{+0.4}_{-0.4}$	$2.2^{+0.4}_{-0.4}$	KW
KW-WAM-BAT	15-1000	$3.3^{+0.4}_{-0.4}$	$2.1^{+0.4}_{-0.3}$	$2.3^{+0.4}_{-0.4}$	KW

Table 60. Fluxes: 060813 Reg1

Instrument	Energy range	Flux (PL)	Flux (CPL)	Flux (Band)	Inst fixed to 1
	[keV]	$[10^{-7}$ erg cm^{-2} s$^{-1}]$	$[10^{-7}$ erg cm^{-2} s$^{-1}]$	$[10^{-7}$ erg cm^{-2} s$^{-1}]$	-
KW	20-1000	$19.7^{+0.7}_{-0.7}$	$16.3^{+0.8}_{-0.8}$	$17.1^{+0.9}_{-0.9}$	-
WAM0	120-1000	$13.4^{+0.5}_{-0.5}$	$12.8^{+0.6}_{-0.6}$	-	-
WAM3	120-1000	$11.6^{+0.5}_{-0.5}$	$11.2^{+0.6}_{-0.7}$	$11.1^{+0.5}_{-0.6}$	-
BAT	15-150	$6.8^{+0.1}_{-0.1}$	$6.7^{+0.2}_{-0.2}$	-	-
BAT-WAM0	15-1000	$19.8^{+1.1}_{-1.1}$	$16.7^{+1.0}_{-0.9}$	$16.7^{+1.0}_{-0.9}$	BAT
BAT-WAM3	15-1000	$22.0^{+1.3}_{-1.2}$	$16.4^{+1.1}_{-1.0}$	$16.5^{+1.0}_{-1.0}$	BAT
KW-BAT	15-1000	$21.8^{+0.7}_{-0.7}$	$16.9^{+0.8}_{-0.8}$	$17.5^{+0.8}_{-0.9}$	KW
KW-WAM0	20-1000	$17.4^{+0.7}_{-0.7}$	$17.2^{+0.7}_{-0.6}$	$17.7^{+0.7}_{-0.6}$	KW
KW-WAM3	20-1000	$17.9^{+0.7}_{-0.7}$	$17.0^{+0.7}_{-0.7}$	$17.7^{+0.7}_{-0.7}$	KW
KW-2WAM-BAT	15-1000	$19.4^{+0.7}_{-0.7}$	$17.6^{+0.6}_{-0.6}$	$17.9^{+0.6}_{-0.6}$	KW

Table 61. Fluxes: 060814 Reg1

Instrument	Energy range	Flux (PL)	Flux (CPL)	Flux (Band)	Inst fixed to 1
	[keV]	$[10^{-7}$ erg cm^{-2} s$^{-1}]$	$[10^{-7}$ erg cm^{-2} s$^{-1}]$	$[10^{-7}$ erg cm^{-2} s$^{-1}]$	-
KW	20-1000	$7.1^{+0.4}_{-0.4}$	$6.3^{+0.5}_{-0.5}$	$6.4^{+0.5}_{-0.5}$	-
WAM0	120-1000	$3.5^{+0.4}_{-0.5}$	-	-	-
WAM1	120-1000	$4.0^{+0.2}_{-0.2}$	-	-	-
BAT	15-150	$2.36^{+0.05}_{-0.05}$	$2.34^{+0.05}_{-0.05}$	-	-
BAT-WAM0	15-1000	$7.9^{+0.5}_{-0.5}$	$6.0^{+0.5}_{-1.0}$	$5.6^{+0.9}_{-0.7}$	BAT
BAT-WAM1	15-1000	$7.3^{+0.4}_{-0.4}$	$6.4^{+0.5}_{-0.5}$	$6.2^{+0.5}_{-0.5}$	BAT
KW-BAT	15-1000	$7.7^{+0.4}_{-0.4}$	$6.5^{+0.5}_{-0.5}$	$6.6^{+0.5}_{-0.5}$	KW
KW-WAM0	20-1000	$7.0^{+0.4}_{-0.4}$	$6.4^{+0.5}_{-0.5}$	$6.4^{+0.4}_{-0.4}$	KW
KW-WAM1	20-1000	$6.8^{+0.4}_{-0.4}$	$6.7^{+0.4}_{-0.4}$	$6.6^{+0.4}_{-0.4}$	KW
KW-2WAM-BAT	15-1000	$7.5^{+0.4}_{-0.4}$	$6.9^{+0.4}_{-0.4}$	$6.7^{+0.4}_{-0.4}$	KW

Table 62. Fluxes: 060814 Reg2

Instrument	Energy range	Flux (PL)	Flux (CPL)	Flux (Band)	Inst fixed to 1
	[keV]	$[10^{-7}$ erg cm^{-2} s$^{-1}]$	$[10^{-7}$ erg cm^{-2} s$^{-1}]$	$[10^{-7}$ erg cm^{-2} s$^{-1}]$	-
KW	20-1000	$3.4^{+0.3}_{-0.3}$	$3.0^{+0.4}_{-0.4}$	$3.1^{+0.4}_{-0.4}$	-
WAM0	120-1000	$2.4^{+0.3}_{-0.4}$	-	-	-
WAM1	120-1000	$2.5^{+0.2}_{-0.2}$	-	-	-
BAT	15-150	$1.36^{+0.03}_{-0.03}$	-	-	-
BAT-WAM0	15-1000	$4.2^{+0.3}_{-0.3}$	-	-	BAT
BAT-WAM1	15-1000	$4.0^{+0.2}_{-0.2}$	$3.7^{+0.2}_{-0.3}$	$3.5^{+0.5}_{-0.3}$	BAT
KW-BAT	15-1000	$3.9^{+0.3}_{-0.3}$	$3.2^{+0.4}_{-0.3}$	$3.2^{+0.4}_{-0.3}$	KW
KW-WAM0	20-1000	$3.5^{+0.3}_{-0.3}$	$3.4^{+0.3}_{-0.4}$	$3.3^{+0.3}_{-0.3}$	KW
KW-WAM1	20-1000	$3.4^{+0.3}_{-0.3}$	$3.4^{+0.3}_{-0.3}$	$3.4^{+0.3}_{-0.3}$	KW
KW-2WAM-BAT	15-1000	$3.9^{+0.3}_{-0.3}$	$3.7^{+0.3}_{-0.3}$	$3.6^{+0.3}_{-0.3}$	KW

Table 63. Fluxes: 060814 Reg12

Instrument	Energy range	Flux (PL)	Flux (CPL)	Flux (Band)	Inst fixed to 1
	[keV]	$[10^{-7} \text{ erg cm}^{-2} \text{ s}^{-1}]$	$[10^{-7} \text{ erg cm}^{-2} \text{ s}^{-1}]$	$[10^{-7} \text{ erg cm}^{-2} \text{ s}^{-1}]$	-
KW	20-1000	$3.1^{+0.2}_{-0.2}$	$2.8^{+0.3}_{-0.3}$	$2.8^{+0.3}_{-0.3}$	-
WAM0	120-1000	$1.8^{+0.2}_{-0.2}$	-	-	-
WAM1	120-1000	$1.9^{+0.1}_{-0.1}$	-	-	-
BAT	15-150	$1.10^{+0.02}_{-0.02}$	-	-	-
BAT-WAM0	15-1000	$3.3^{+0.2}_{-0.2}$	$3.1^{+0.4}_{-0.4}$	$2.8^{+0.4}_{-0.4}$	BAT
BAT-WAM1	15-1000	$3.2^{+0.2}_{-0.2}$	$3.0^{+0.2}_{-0.2}$	$2.8^{+0.3}_{-0.2}$	BAT
KW-BAT	15-1000	$3.4^{+0.2}_{-0.2}$	$2.9^{+0.3}_{-0.3}$	$2.9^{+0.3}_{-0.3}$	KW
KW-WAM0	20-1000	$3.0^{+0.2}_{-0.2}$	$3.0^{+0.2}_{-0.3}$	$2.9^{+0.2}_{-0.2}$	KW
KW-WAM1	20-1000	$3.0^{+0.2}_{-0.2}$	$3.0^{+0.2}_{-0.2}$	$3.0^{+0.2}_{-0.2}$	KW
KW-2WAM-BAT	15-1000	$3.3^{+0.2}_{-0.2}$	$3.1^{+0.2}_{-0.2}$	$3.0^{+0.2}_{-0.2}$	KW

Table 64. Fluxes: 060904A Reg1

Instrument	Energy range	Flux (PL)	Flux (CPL)	Flux (Band)	Inst fixed to 1
	[keV]	$[10^{-7} \text{ erg cm}^{-2} \text{ s}^{-1}]$	$[10^{-7} \text{ erg cm}^{-2} \text{ s}^{-1}]$	$[10^{-7} \text{ erg cm}^{-2} \text{ s}^{-1}]$	-
KW	20-1000	$8.2^{+0.5}_{-0.5}$	$6.7^{+0.5}_{-0.5}$	$6.8^{+0.6}_{-0.6}$	-
WAM0	120-1000	$4.3^{+0.5}_{-0.5}$	$4.3^{+0.6}_{-0.6}$	$4.4^{+0.5}_{-0.6}$	-
WAM3	120-1000	$4.9^{+0.3}_{-0.3}$	$4.9^{+0.3}_{-0.3}$	$4.8^{+0.3}_{-0.4}$	-
BAT	15-150	$3.02^{+0.06}_{-0.06}$	-	-	-
BAT-WAM0	15-1000	$12.4^{+0.8}_{-0.8}$	$8.2^{+1.2}_{-1.0}$	$8.2^{+1.0}_{-0.4}$	BAT
BAT-WAM3	15-1000	$10.0^{+0.6}_{-0.6}$	$7.5^{+0.6}_{-0.5}$	$7.4^{+0.6}_{-0.5}$	BAT
KW-BAT	15-1000	$9.6^{+0.5}_{-0.5}$	$7.2^{+0.5}_{-0.5}$	$7.2^{+0.6}_{-0.5}$	KW
KW-WAM0	20-1000	$8.0^{+0.5}_{-0.5}$	$7.0^{+0.5}_{-0.5}$	$7.1^{+0.5}_{-0.5}$	KW
KW-WAM3	20-1000	$7.4^{+0.5}_{-0.5}$	$7.4^{+0.4}_{-0.4}$	$7.5^{+0.4}_{-0.4}$	KW
KW-2WAM-BAT	15-1000	$9.2^{+0.5}_{-0.5}$	$7.7^{+0.4}_{-0.4}$	$7.8^{+0.4}_{-0.4}$	KW

Table 65. Fluxes: 060904A Reg2

Instrument	Energy range	Flux (PL)	Flux (CPL)	Flux (Band)	Inst fixed to 1
	[keV]	$[10^{-7} \text{ erg cm}^{-2} \text{ s}^{-1}]$	$[10^{-7} \text{ erg cm}^{-2} \text{ s}^{-1}]$	$[10^{-7} \text{ erg cm}^{-2} \text{ s}^{-1}]$	-
KW	20-1000	$2.5^{+0.4}_{-0.4}$	$1.8^{+0.3}_{-0.3}$	$1.9^{+0.5}_{-0.4}$	-
WAM0	120-1000	$1.1^{+0.5}_{-0.5}$	-	-	-
WAM3	120-1000	$1.0^{+0.2}_{-0.2}$	-	-	-
BAT	15-150	$0.98^{+0.04}_{-0.04}$	$0.94^{+0.05}_{-0.05}$	$0.94^{+0.05}_{-0.05}$	-
BAT-WAM0	15-1000	$2.8^{+0.3}_{-0.3}$	$1.4^{+0.9}_{-0.3}$	$2.0^{+0.3}_{-0.6}$	BAT
BAT-WAM3	15-1000	$2.6^{+0.3}_{-0.3}$	$1.6^{+0.4}_{-0.3}$	$1.6^{+0.4}_{-0.3}$	BAT
KW-BAT	15-1000	$2.8^{+0.4}_{-0.4}$	$1.8^{+0.4}_{-0.3}$	$1.9^{+0.6}_{-0.1}$	KW
KW-WAM0	20-1000	$2.5^{+0.4}_{-0.4}$	$1.9^{+0.3}_{-0.3}$	$2.1^{+0.4}_{-0.2}$	KW
KW-WAM3	20-1000	$2.3^{+0.4}_{-0.4}$	$2.0^{+0.3}_{-0.3}$	$2.1^{+0.4}_{-0.3}$	KW
KW-2WAM-BAT	15-1000	$2.8^{+0.4}_{-0.4}$	$2.1^{+0.4}_{-0.3}$	$2.1^{+0.4}_{-0.3}$	KW

Table 66. Fluxes: 060904A Reg12

Instrument	Energy range	Flux (PL)	Flux (CPL)	Flux (Band)	Inst fixed to 1
	[keV]	$[10^{-7} \text{ erg cm}^{-2} \text{ s}^{-1}]$	$[10^{-7} \text{ erg cm}^{-2} \text{ s}^{-1}]$	$[10^{-7} \text{ erg cm}^{-2} \text{ s}^{-1}]$	-
KW	20-1000	$5.5^{+0.3}_{-0.3}$	$4.3^{+0.3}_{-0.3}$	$4.4^{+0.4}_{-0.4}$	-
WAM0	120-1000	$2.8^{+0.4}_{-0.4}$	$2.7^{+0.5}_{-0.5}$	$2.7^{+0.5}_{-0.4}$	-
WAM3	120-1000	$3.0^{+0.2}_{-0.2}$	$2.9^{+0.2}_{-0.1}$	$3.0^{+0.2}_{-0.1}$	-
BAT	15-150	$2.01^{+0.04}_{-0.04}$	-	-	-
BAT-WAM0	15-1000	$7.4^{+0.5}_{-0.4}$	$5.2^{+0.8}_{-0.7}$	$5.2^{+0.7}_{-0.7}$	BAT
BAT-WAM3	15-1000	$6.3^{+0.4}_{-0.3}$	$4.6^{+0.4}_{-0.3}$	$4.6^{+0.4}_{-0.3}$	BAT
KW-BAT	15-1000	$6.3^{+0.3}_{-0.3}$	$4.6^{+0.4}_{-0.3}$	$4.7^{+0.4}_{-0.4}$	KW
KW-WAM0	20-1000	$5.4^{+0.3}_{-0.3}$	$4.5^{+0.4}_{-0.3}$	$4.7^{+0.4}_{-0.4}$	KW
KW-WAM3	20-1000	$5.0^{+0.3}_{-0.3}$	$4.8^{+0.3}_{-0.3}$	$4.9^{+0.3}_{-0.3}$	KW
KW-2WAM-BAT	15-1000	$6.1^{+0.3}_{-0.3}$	$5.1^{+0.3}_{-0.3}$	$5.1^{+0.3}_{-0.3}$	KW

Table 67. Fluxes: 060912 Reg1

Instrument	Energy range	Flux (PL)	Flux (CPL)	Flux (Band)	Inst fixed to 1
	[keV]	$[10^{-7} \text{ erg cm}^{-2} \text{ s}^{-1}]$	$[10^{-7} \text{ erg cm}^{-2} \text{ s}^{-1}]$	$[10^{-7} \text{ erg cm}^{-2} \text{ s}^{-1}]$	-
KW	20-1000	$3.1^{+0.5}_{-0.5}$	-	-	-
WAM2	120-1000	$1.6^{+0.5}_{-0.5}$	-	-	-
BAT	15-150	$1.27^{+0.07}_{-0.07}$	-	-	-
BAT-WAM2	15-1000	$2.8^{+0.5}_{-0.4}$	-	-	BAT
KW-BAT	15-1000	$3.4^{+0.5}_{-0.5}$	-	-	KW
KW-WAM2	20-1000	$3.1^{+0.5}_{-0.5}$	-	-	KW
KW-WAM-BAT	15-1000	$3.4^{+0.5}_{-0.5}$	-	-	KW

Table 68. Fluxes: 061006 Reg1

Instrument	Energy range	Flux (PL)	Flux (CPL)	Flux (Band)	Inst fixed to 1
	[keV]	$[10^{-7} \text{ erg cm}^{-2} \text{ s}^{-1}]$	$[10^{-7} \text{ erg cm}^{-2} \text{ s}^{-1}]$	$[10^{-7} \text{ erg cm}^{-2} \text{ s}^{-1}]$	-
KW	20-1000	$76.8^{+7.0}_{-7.0}$	$77.6^{+9.1}_{-9.4}$	$74.9^{+7.6}_{-7.7}$	-
WAM3	120-1000	$40.3^{+2.0}_{-2.0}$	$46.0^{+1.3}_{-2.5}$	$45.4^{+2.7}_{-2.8}$	-
BAT	15-150	$10.8^{+0.6}_{-0.6}$	-	-	-
BAT-WAM3	15-1000	$30.9^{+4.2}_{-3.7}$	$79.6^{+11.4}_{-10.1}$	$77.9^{+11.5}_{-10.2}$	BAT
KW-BAT	15-1000	$81.5^{+6.7}_{-6.7}$	$77.1^{+9.4}_{-9.4}$	$75.4^{+7.7}_{-7.9}$	KW
KW-WAM3	20-1000	$51.8^{+6.3}_{-6.1}$	$79.1^{+7.4}_{-7.2}$	$78.5^{+7.4}_{-7.3}$	KW
KW-WAM-BAT	15-1000	$64.9^{+6.4}_{-6.3}$	$81.3^{+7.1}_{-6.9}$	$79.6^{+7.4}_{-7.1}$	KW

Table 69. Fluxes: 061007 Reg1

Instrument	Energy range	Flux (PL)	Flux (CPL)	Flux (Band)	Inst fixed to 1
	[keV]	$[10^{-7}$ erg cm^{-2} s$^{-1}]$	$[10^{-7}$ erg cm^{-2} s$^{-1}]$	$[10^{-7}$ erg cm^{-2} s$^{-1}]$	-
KW	20-1000	$12.3^{+0.4}_{-0.4}$	$10.9^{+0.6}_{-0.8}$	$11.2^{+0.5}_{-0.5}$	-
WAM2	120-1000	$9.2^{+0.7}_{-0.7}$	$9.3^{+0.7}_{-0.7}$	$9.2^{+0.8}_{-0.7}$	-
WAM3	120-1000	$9.1^{+0.5}_{-0.5}$	$9.2^{+0.4}_{-0.5}$	$9.2^{+0.5}_{-0.5}$	-
BAT	15-150	$3.7^{+0.1}_{-0.1}$	$3.7^{+0.1}_{-0.1}$	-	-
BAT-WAM2	15-1000	$17.9^{+2.1}_{-1.8}$	$12.2^{+1.5}_{-1.3}$	$10.9^{+1.5}_{-1.4}$	BAT
BAT-WAM3	15-1000	$10.2^{+0.9}_{-0.8}$	$12.1^{+1.0}_{-0.9}$	$11.8^{+1.0}_{-0.9}$	BAT
KW-BAT	15-1000	$13.1^{+0.4}_{-0.4}$	$11.3^{+0.6}_{-0.5}$	$11.5^{+0.5}_{-0.5}$	KW
KW-WAM2	20-1000	$11.9^{+0.4}_{-0.4}$	$11.5^{+0.5}_{-0.5}$	$11.3^{+0.5}_{-0.4}$	KW
KW-WAM3	20-1000	$11.4^{+0.4}_{-0.4}$	$11.8^{+0.5}_{-0.5}$	$11.5^{+0.4}_{-0.4}$	KW
KW-2WAM-BAT	15-1000	$12.4^{+0.4}_{-0.4}$	$12.0^{+0.4}_{-0.4}$	$11.7^{+0.4}_{-0.4}$	KW

Table 70. Fluxes: 061007 Reg2

Instrument	Energy range	Flux (PL)	Flux (CPL)	Flux (Band)	Inst fixed to 1
	[keV]	$[10^{-7}$ erg cm^{-2} s$^{-1}]$	$[10^{-7}$ erg cm^{-2} s$^{-1}]$	$[10^{-7}$ erg cm^{-2} s$^{-1}]$	-
KW	20-1000	39.6	$51.1^{+0.8}_{-0.8}$	$49.6^{+0.9}_{-0.9}$	-
WAM2	120-1000	$45.7^{+1.3}_{-1.3}$	$44.0^{+1.3}_{-1.3}$	$42.9^{+1.4}_{-1.4}$	-
WAM3	120-1000	47.8	$45.2^{+0.9}_{-0.9}$	$44.0^{+1.0}_{-1.0}$	-
BAT	15-150	$9.2^{+0.1}_{-0.1}$	-	-	-
BAT-WAM2	15-1000	26.7	$43.4^{+2.0}_{-1.9}$	$40.5^{+2.0}_{-1.9}$	BAT
BAT-WAM3	15-1000	14.3	$45.9^{+1.9}_{-1.8}$	$44.5^{+1.8}_{-1.8}$	BAT
KW-BAT	15-1000	41.0	$51.5^{+0.8}_{-0.8}$	$50.5^{+0.9}_{-0.9}$	KW
KW-WAM2	20-1000	38.3	$51.3^{+0.8}_{-0.8}$	$49.6^{+0.8}_{-0.8}$	KW
KW-WAM3	20-1000	35.8	$51.9^{+0.7}_{-0.7}$	$50.7^{+0.8}_{-0.8}$	KW
KW-2WAM-BAT	15-1000	37.2	$52.0^{+0.7}_{-0.7}$	$50.7^{+0.7}_{-0.7}$	KW

Table 71. Fluxes: 061007 Reg3

Instrument	Energy range	Flux (PL)	Flux (CPL)	Flux (Band)	Inst fixed to 1
	[keV]	$[10^{-7}$ erg cm^{-2} s$^{-1}]$	$[10^{-7}$ erg cm^{-2} s$^{-1}]$	$[10^{-7}$ erg cm^{-2} s$^{-1}]$	-
KW	20-1000	27.6	$30.1^{+0.5}_{-0.5}$	$29.7^{+0.5}_{-0.5}$	-
WAM2	120-1000	$25.4^{+1.0}_{-0.9}$	$24.6^{+1.0}_{-1.0}$	$23.9^{+1.0}_{-1.0}$	-
WAM3	120-1000	26.8	$24.9^{+0.7}_{-0.7}$	$24.6^{+0.7}_{-0.7}$	-
BAT	15-150	$7.10^{+0.08}_{-0.08}$	-	-	-
BAT-WAM2	15-1000	39.1	$25.7^{+1.1}_{-1.1}$	$24.2^{+1.2}_{-1.1}$	BAT
BAT-WAM3	15-1000	21.1	$26.6^{+0.9}_{-0.9}$	$26.2^{+0.9}_{-0.9}$	BAT
KW-BAT	15-1000	29.0	$30.6^{+0.5}_{-0.5}$	$30.3^{+0.5}_{-0.5}$	KW
KW-WAM2	20-1000	27.0	$30.3^{+0.5}_{-0.5}$	$29.6^{+0.5}_{-0.5}$	KW
KW-WAM3	20-1000	26.0	$30.6^{+0.5}_{-0.5}$	$30.2^{+0.5}_{-0.5}$	KW
KW-2WAM-BAT	15-1000	27.9	$30.8^{+0.4}_{-0.4}$	$30.3^{+0.5}_{-0.4}$	KW

Table 72. Fluxes: 061007 Reg4

Instrument	Energy range	Flux (PL)	Flux (CPL)	Flux (Band)	Inst fixed to 1
	[keV]	$[10^{-7}$ erg cm^{-2} s$^{-1}]$	$[10^{-7}$ erg cm^{-2} s$^{-1}]$	$[10^{-7}$ erg cm^{-2} s$^{-1}]$	-
KW	20-1000	31.7	$36.3^{+0.5}_{-0.5}$	$35.6^{+0.5}_{-0.5}$	-
WAM2	120-1000	$33.0^{+0.9}_{-0.9}$	$30.8^{+1.0}_{-1.0}$	$29.7^{+1.1}_{-1.1}$	-
WAM3	120-1000	35.2	$31.2^{+0.7}_{-0.7}$	$30.4^{+0.7}_{-0.7}$	-
BAT	15-150	$7.69^{+0.09}_{-0.09}$	-	-	-
BAT-WAM2	15-1000	33.3	$31.8^{+1.2}_{-1.2}$	$29.5^{+1.3}_{-1.2}$	BAT
BAT-WAM3	15-1000	15.3	$32.8^{+1.0}_{-1.0}$	$31.9^{+1.0}_{-1.0}$	BAT
KW-BAT	15-1000	32.9	$36.8^{+0.5}_{-0.5}$	$36.2^{+0.5}_{-0.5}$	KW
KW-WAM2	20-1000	31.0	$36.6^{+0.4}_{-0.4}$	$35.6^{+0.4}_{-0.4}$	KW
KW-WAM3	20-1000	29.6	$37.0^{+0.4}_{-0.4}$	$36.2^{+0.4}_{-0.4}$	KW
KW-2WAM-BAT	15-1000	31.1	$37.2^{+0.4}_{-0.4}$	$36.4^{+0.4}_{-0.4}$	KW

Table 73. Fluxes: 061007 Reg5

Instrument	Energy range	Flux (PL)	Flux (CPL)	Flux (Band)	Inst fixed to 1
	[keV]	$[10^{-7}$ erg cm^{-2} s$^{-1}]$	$[10^{-7}$ erg cm^{-2} s$^{-1}]$	$[10^{-7}$ erg cm^{-2} s$^{-1}]$	-
KW	20-1000	$1.9^{+0.3}_{-0.3}$	-	-	-
WAM2	120-1000	$1.3^{+0.6}_{-0.6}$	-	-	-
WAM3	120-1000	$1.0^{+0.3}_{-0.3}$	-	-	-
BAT	15-150	$0.66^{+0.03}_{-0.03}$	-	-	-
BAT-WAM2	15-1000	$1.8^{+0.2}_{-0.2}$	-	-	BAT
BAT-WAM3	15-1000	$1.8^{+0.2}_{-0.2}$	$1.4^{+0.3}_{-0.3}$	-	BAT
KW-BAT	15-1000	$2.1^{+0.3}_{-0.3}$	-	-	KW
KW-WAM2	20-1000	$1.8^{+0.3}_{-0.3}$	-	-	KW
KW-WAM3	20-1000	$1.7^{+0.3}_{-0.3}$	$1.7^{+0.4}_{-0.2}$	-	KW
KW-2WAM-BAT	15-1000	$2.0^{+0.3}_{-0.3}$	$1.8^{+0.3}_{-0.3}$	$1.8^{+0.3}_{-0.3}$	KW

Table 74. Fluxes: 061007 Reg15

Instrument	Energy range	Flux (PL)	Flux (CPL)	Flux (Band)	Inst fixed to 1
	[keV]	$[10^{-7}$ erg cm^{-2} s$^{-1}]$	$[10^{-7}$ erg cm^{-2} s$^{-1}]$	$[10^{-7}$ erg cm^{-2} s$^{-1}]$	-
KW	20-1000	20.6	$21.9^{+0.3}_{-0.3}$	$21.5^{+0.3}_{-0.3}$	-
WAM2	120-1000	$19.8^{+0.7}_{-0.7}$	$18.6^{+0.7}_{-0.7}$	$17.9^{+0.8}_{-0.8}$	-
WAM3	120-1000	20.7	$18.5^{+0.5}_{-0.5}$	$18.1^{+0.5}_{-0.5}$	-
BAT	15-150	$4.94^{+0.06}_{-0.03}$	-	-	-
BAT-WAM2	15-1000	23.7	$19.9^{+0.9}_{-0.8}$	$18.4^{+0.9}_{-0.9}$	BAT
BAT-WAM3	15-1000	12.0	$20.3^{+0.7}_{-0.7}$	$19.7^{+0.7}_{-0.7}$	BAT
KW-BAT	15-1000	21.5	$22.2^{+0.3}_{-0.3}$	$21.9^{+0.3}_{-0.3}$	KW
KW-WAM2	20-1000	20.2	$22.1^{+0.3}_{-0.3}$	$21.5^{+0.3}_{-0.3}$	KW
KW-WAM3	20-1000	19.5	$22.4^{+0.3}_{-0.3}$	$21.9^{+0.3}_{-0.3}$	KW
KW-2WAM-BAT	15-1000	20.5	$22.6^{+0.3}_{-0.3}$	$22.1^{+0.3}_{-0.3}$	KW

Table 75. Fluxes: 061222A Reg1

Instrument	Energy range	Flux (PL)	Flux (CPL)	Flux (Band)	Inst fixed to 1
	[keV]	$[10^{-7}$ erg cm^{-2} s$^{-1}]$	$[10^{-7}$ erg cm^{-2} s$^{-1}]$	$[10^{-7}$ erg cm^{-2} s$^{-1}]$	-
KW	20-1000	$11.3^{+0.5}_{-0.5}$	$10.0^{+0.6}_{-0.6}$	$10.1^{+0.6}_{-0.6}$	-
WAM2	120-1000	$9.2^{+0.4}_{-0.4}$	$9.4^{+0.4}_{-0.2}$	$9.3^{+0.5}_{-0.5}$	-
WAM3	120-1000	$7.5^{+0.6}_{-0.6}$	-	-	-
BAT	15-150	$2.98^{+0.05}_{-0.05}$	$2.96^{+0.05}_{-0.05}$	-	-
BAT-WAM2	15-1000	$12.2^{+0.6}_{-0.6}$	$10.1^{+0.6}_{-0.6}$	$10.0^{+0.7}_{-0.6}$	BAT
BAT-WAM3	15-1000	$15.1^{+0.9}_{-0.8}$	$9.7^{+1.2}_{-1.2}$	$8.6^{+1.0}_{-0.9}$	BAT
KW-BAT	15-1000	$12.5^{+0.4}_{-0.4}$	$10.2^{+0.6}_{-0.6}$	$10.3^{+0.5}_{-0.6}$	KW
KW-WAM2	20-1000	$10.5^{+0.5}_{-0.5}$	$10.7^{+0.5}_{-0.5}$	$10.6^{+0.5}_{-0.5}$	KW
KW-WAM3	20-1000	$11.1^{+0.5}_{-0.5}$	$10.3^{+0.6}_{-0.6}$	$10.2^{+0.5}_{-0.5}$	KW
KW-2WAM-BAT	15-1000	$12.1^{+0.4}_{-0.4}$	$10.9^{+0.5}_{-0.5}$	$10.7^{+0.5}_{-0.4}$	KW

Table 76. Fluxes: 070328 Reg1

Instrument	Energy range	Flux (PL)	Flux (CPL)	Flux (Band)	Inst fixed to 1
	[keV]	$[10^{-7}$ erg cm^{-2} s$^{-1}]$	$[10^{-7}$ erg cm^{-2} s$^{-1}]$	$[10^{-7}$ erg cm^{-2} s$^{-1}]$	-
KW	20-1000	$14.1^{+0.6}_{-0.6}$	$15.8^{+0.7}_{-0.7}$	$15.0^{+0.8}_{-0.7}$	-
WAM1	120-1000	$11.8^{+0.5}_{-0.5}$	$12.2^{+0.5}_{-0.5}$	$12.2^{+0.5}_{-0.5}$	-
BAT	15-150	$3.14^{+0.08}_{-0.08}$	-	-	-
BAT-WAM1	15-1000	$10.5^{+0.6}_{-0.6}$	$15.6^{+1.1}_{-1.0}$	$15.2^{+1.1}_{-1.0}$	BAT
KW-BAT	15-1000	$14.7^{+0.6}_{-0.6}$	$16.0^{+0.7}_{-0.7}$	$15.2^{+0.9}_{-0.8}$	KW
KW-WAM1	20-1000	$13.0^{+0.6}_{-0.6}$	$15.6^{+0.7}_{-0.7}$	$15.7^{+0.7}_{-0.7}$	KW
KW-WAM-BAT	15-1000	$14.1^{+0.6}_{-0.6}$	$16.2^{+0.6}_{-0.6}$	$15.9^{+0.7}_{-0.7}$	KW

Table 77. Fluxes: 070328 Reg2

Instrument	Energy range	Flux (PL)	Flux (CPL)	Flux (Band)	Inst fixed to 1
	[keV]	$[10^{-7}$ erg cm^{-2} s$^{-1}]$	$[10^{-7}$ erg cm^{-2} s$^{-1}]$	$[10^{-7}$ erg cm^{-2} s$^{-1}]$	-
KW	20-1000	$11.0^{+0.3}_{-0.3}$	$11.9^{+0.4}_{-0.5}$	$11.2^{+0.4}_{-0.4}$	-
WAM1	120-1000	$8.9^{+0.3}_{-0.3}$	$9.0^{+0.3}_{-0.3}$	$8.9^{+0.4}_{-0.4}$	-
BAT	15-150	$2.59^{+0.05}_{-0.05}$	-	-	-
BAT-WAM1	15-1000	$8.5^{+0.4}_{-0.4}$	$11.5^{+0.6}_{-0.6}$	$11.3^{+0.6}_{-0.6}$	BAT
KW-BAT	15-1000	$11.5^{+0.3}_{-0.3}$	$12.0^{+0.3}_{-0.4}$	$11.5^{+0.5}_{-0.4}$	KW
KW-WAM1	20-1000	$10.0^{+0.3}_{-0.3}$	$12.1^{+0.4}_{-0.4}$	$12.0^{+0.4}_{-0.4}$	KW
KW-WAM-BAT	15-1000	$11.0^{+0.3}_{-0.3}$	$12.3^{+0.4}_{-0.4}$	$12.1^{+0.4}_{-0.4}$	KW

Table 78. Fluxes: 070328 Reg3

Instrument	Energy range	Flux (PL)	Flux (CPL)	Flux (Band)	Inst fixed to 1
	[keV]	$[10^{-7}$ erg cm^{-2} s$^{-1}]$	$[10^{-7}$ erg cm^{-2} s$^{-1}]$	$[10^{-7}$ erg cm^{-2} s$^{-1}]$	-
KW	20-1000	$1.8^{+0.4}_{-0.4}$	$1.4^{+0.6}_{-0.4}$	$1.6^{+0.4}_{-0.5}$	-
WAM1	120-1000	$1.1^{+0.3}_{-0.3}$	-	-	-
BAT	15-150	$0.58^{+0.03}_{-0.03}$	$0.57^{+0.03}_{-0.03}$	-	-
BAT-WAM1	15-1000	$2.1^{+0.4}_{-0.3}$	$1.7^{+0.5}_{-0.4}$	-	BAT
KW-BAT	15-1000	$2.0^{+0.3}_{-0.3}$	$1.4^{+0.5}_{-0.4}$	$1.6^{+0.4}_{-0.4}$	KW
KW-WAM1	20-1000	$1.7^{+0.4}_{-0.3}$	$1.7^{+0.3}_{-0.4}$	$1.6^{+0.3}_{-0.3}$	KW
KW-WAM-BAT	15-1000	$2.0^{+0.3}_{-0.3}$	$1.7^{+0.4}_{-0.4}$	$1.6^{+0.3}_{-0.3}$	KW

Table 79. Fluxes: 070328 Reg13

Instrument	Energy range	Flux (PL)	Flux (CPL)	Flux (Band)	Inst fixed to 1
	[keV]	$[10^{-7}$ erg cm^{-2} s$^{-1}]$	$[10^{-7}$ erg cm^{-2} s$^{-1}]$	$[10^{-7}$ erg cm^{-2} s$^{-1}]$	-
KW	20-1000	$7.4^{+0.3}_{-0.3}$	$7.8^{+0.4}_{-0.4}$	$7.4^{+0.3}_{-0.3}$	-
WAM1	120-1000	$6.0^{+0.3}_{-0.3}$	$5.9^{+0.3}_{-0.3}$	$5.8^{+0.3}_{-0.3}$	-
BAT	15-150	$1.79^{+0.03}_{-0.03}$	-	-	-
BAT-WAM1	15-1000	$6.2^{+0.3}_{-0.3}$	$7.7^{+0.4}_{-0.4}$	$7.5^{+0.5}_{-0.5}$	BAT
KW-BAT	15-1000	$7.8^{+0.3}_{-0.3}$	$7.9^{+0.3}_{-0.4}$	$7.6^{+0.4}_{-0.3}$	KW
KW-WAM1	20-1000	$6.75^{+0.3}_{-0.3}$	$8.0^{+0.3}_{-0.3}$	$7.9^{+0.3}_{-0.3}$	KW
KW-WAM-BAT	15-1000	$7.6^{+0.3}_{-0.3}$	$8.2^{+0.3}_{-0.3}$	$8.0^{+0.3}_{-0.3}$	KW